CECW-EG Engineer Manual 1110-2-1902	Department of the Army U.S. Army Corps of Engineers Washington, DC 20314-1000	EM 1110-2-1902 1 April 1970
	Engineering and Design Stability of Earth and Rock-Fill Dams (Inclusive of Change 1)	
	Distribution Restriction Statement Approved for public release; distribution is unlimited.	

<u>Foreword</u>

This manual was prepared in the U. S. Army Waterways Experiment Station under direction from the Office, Chief of Engineers. General supervision and technical guidance was provided by W. E. Johnson, Chief, Engineering Division, G. E. Bertram, Chief, Soil Mechanics Branch until 1968, and R. A. Barron, Branch Chief from 1968 to date.

The manual was prepared by W. E. Strohm, Jr., assisted by C. C. Trahan, Yu-Shih Jeng, and D. P. Hammer under the immediate direction of S. J. Johnson and J. R. Compton, of the staff at the U. S. Army Waterways Experiment Station.

A draft of the manual was reviewed by the Corps Advisory Board for Soil Mechanics. The Board consists of R. A. Barron, Chairman; A. Casagrande, Harvard University; R. B. Peck, University of Illinois; G. E. Bertram, Consulting Engineer; S. D. Wilson, Shannon & Wilson, Inc; J. Lowe, III, Tippetts-Abbett-McCarthy-Stratton; and S. J. Johnson, Waterways Experiment Station.

ENGCW-ES

DEPARTMENT OF THE ARMY
Office of the Chief of Engineers
Washington, D. C. 20314

EM 1110-2-1902

Manual
No. 1110-2-1902

1 April 1970

ENGINEERING AND DESIGN
Stability of Earth and Rock-Fill Dams

Table of Contents

APPENDIX VII
Wedge Analysis

PLATES

APPENDIX VIII
Evaluation of Embankment Stability
During Construction

PLATES

DEPARTMENT OF THE ARMY
Office of the Chief of Engineers
Washington, D. C. 20314

ENGCW-ES

Manual
No. 1110-2-1902

ENGINEERING AND DESIGN
Stability of Earth and Rock-Fill Dams

1. Purpose. This manual establishes procedures for analyzing the stability of earth and rock-fill dams.

2. Scope. Criteria are presented for (a) types of strength tests to be used, (b) conditions requiring analysis, and (c) minimum acceptable safety factors. Methods for computing embankment stability are described and illustrated by examples in the appendixes. The methods of this manual are approved methods, but this does not prohibit the use of the Swedish slide method (method of slices, Case (c)) given in Appendix D of WES Technical Report No. 3-777 (ref 1) if the factors of safety given in table I, page 25, are used. Minimum requirements are given, but special tests or design analyses that may be required are not included.

3. Applicability. This manual is applicable to all Corps of Engineers Divisions and Districts having civil works functions. It is applicable to stability analyses for dikes, levees, and highway fills, as well as for earth and rock-fill dams.

4. References. a. EM 1110-2-2300. Types of earth and rock-fill dams, factors influencing selection of cross section, zoning, and material utilization, and general design criteria that must be satisfied to provide stability during all phases of construction and reservoir operation are described in EM 1110-2-2300, Earth and Rock-Fill Dams, General Design and Construction Considerations (issued in draft form September 1969).

b. Other Engineer Manuals. The following manuals also relate to use and design of earth and rock-fill dams and should be referred to for criteria other than stability:

EM 1110-1-1801 Geological Investigations (November 1960)

This manual rescinds EM 1110-2-1805, 21 July 1964, and EM 1110-2-1902, 27 Dec 1960.

EM 1110-2-1802	Geophysical Explorations (September 1948)
EM 1110-2-1803	Subsurface Investigations--Soils (March 1954)
EM 1110-2-1901	Seepage Control (February 1952)
EM 1110-2-1904	Settlement Analysis (January 1953)
EM 1110-2-1906	Laboratory Soils Testing (10 May 1965)
EM 1110-2-2902	Conduits, Culverts and Pipes (3 March 1969)

Where the above-listed references and this manual do not agree, the provision of this manual shall govern.

c. Selected References. Selected references are cited herein and are designated by superscript numbers; these numbers correspond to similarly numbered references in Appendix I.

5. Notation. Symbols used in this manual are listed and defined in Appendix II. The majority of them correspond to those recommended by the Committee on Glossary of Terms and Definitions of the Soil Mechanics and Foundations Division, American Society of Civil Engineers.[2]

6. Basic Design Considerations. a. The stability of an embankment must be evaluated for construction and operating conditions utilizing expected in situ engineering properties of the foundation and embankment materials and pertinent geologic information. When determining and selecting engineering properties of proposed embankment materials, consideration must be given to (1) possible variation in borrow materials, (2) natural water contents of borrow materials, (3) variations in placement rate and methods, (4) climatic conditions, and (5) inevitable variations in placement water contents and compacted densities that must be expected with normal construction control. The decrease in friction angle of granular embankment and foundation materials under high confining stresses must be considered for high dams.[3]

b. Other factors that must be accounted for in establishing design values, but which can be evaluated only through exercise of engineering judgment, include (1) the effect of differential settlements where embankments are located on compressible foundations or in narrow, deep valleys, and (2) compatibility of strain characteristics within the embankment and of

the embankment with the foundation. The stability analyses presented in this manual assume that design strengths are mobilized simultaneously in all materials along assumed sliding surfaces.

c. Geologic information that should be considered includes (1) groundwater and seepage conditions; (2) lithology, stratigraphy, and geologic details disclosed by borings and geologic interpretation; (3) maximum past overburden at site as deduced from geological evidence; (4) structure, including bedding, folding (amount, open, closed, etc.), and faulting; (5) alteration of materials by faulting; (6) joints and joint systems; (7) weathering; (8) slickensides; and (9) field evidence relating to slides, earthquake activity, movement along existing faults, and tension jointing.

d. The results of stability analyses afford a means for comparing relative merits of trial cross sections during design and for evaluating the effects of changes in assumed embankment and foundation material properties during and after construction. The value of stability analyses depends on the validity of assumed design shear strengths, and results should be reviewed for compatibility with analyses for similar structures where construction and operating experiences are known.

e. The design procedures described herein utilize effective stresses where pore water pressures can be satisfactorily predicted, and total stresses for all other cases. In general, effective normal stresses are used to evaluate (1) partial pool and steady seepage conditions, (2) stability during and after construction where piezometer observations are available, and (3) the stability of existing dams when foundation and embankment have become fully consolidated and no excess pore pressures exist. Total normal stresses are used in designing for construction and, in a general sense, for rapid drawdown and earthquake conditions.

7. Causes of Unsatisfactory Embankment Performance.

a. Shear Failure. A failure in which a portion of an embankment or of an embankment and foundation moves by sliding or rotation relative to the remainder of the mass is designated as a shear failure. A shear failure is

conventionally represented as occurring along a surface and is so assumed in stability analyses, although shearing may occur in a zone of substantial thickness. The failure surface in relatively homogeneous embankments and in soil foundations consisting of thick, fine-grained deposits may be approximately represented by a circular arc. Where zoned embankments or thin foundation layers overlying bedrock are involved or where a weak stratum exists within a thick, fine-grained deposit, the failure surface may more nearly approximate a combination of interconnected arcs and planes or several interconnected plane surfaces.

b. Excessive Deformation. Some cohesive soils, especially those compacted on the wet side of optimum water content, require relatively large strains to develop given levels of shear resistance. Even when compacted slightly dry of optimum water content and to densities equal to or slightly greater than standard maximum, relatively large strains may develop in such materials. As a consequence, when these soils are placed in an embankment they may deform excessively and create high pore water pressures as additional fill is placed. During the design study, particular attention should be given to the shape of the stress-strain curves for soils to be used in an embankment and existing in the foundation. When Q and R strength tests show peak shear strengths at high strains or have not peaked at 15 percent strain, it may be necessary to (1) limit average placement water contents to slightly on the dry side of optimum, or (2) use conservative values for design shear strengths. However, excessive settlement may occur if the soil is compacted too dry and then becomes saturated. Excessive embankment deformation may also result from consolidation of the foundation, especially where large differential settlements will occur. Shear deformations in the foundation may be high under these conditions and also where the peak strengths in the foundation are mobilized at large strains Surface movement indicators and piezometers should be installed to detect excessive deformation and excessive pore water pressure so that the rate of placement of fill can be controlled.

c. Liquefaction. The phenomenon of liquefaction of loose, saturated sands, sensitive silts, and quick clays is of major concern, and may occur when such materials are subjected to shear deformations or earthquake shocks. The possibility of liquefaction must presently be evaluated on the basis of empirical knowledge[4] supplemented by special laboratory tests[5] and engineering judgment. Sands having a relative density equal to or greater than 70 percent are believed to be not susceptible to liquefaction. However, for cohesionless materials in embankment fills and drainage zones, an average relative density of 85 percent is required to minimize embankment settlement, or the danger of piping, and to provide adequate shear strength.

8. Special Problems. Certain soil types and potential failure conditions present unusual problems requiring more comprehensive stability investigations than those described in this manual. Some of these problems are briefly discussed below.

a. Progressive Failure. (1) Because of nonuniform stress distribution in potential failure zones, relatively large strains may develop in some areas and peak strengths may be reached progressively, so that the total shear resistance will be less than if the peak strength is mobilized simultaneously along the entire failure surface. Where the stress-strain curve for a soil exhibits a significant drop in shear stress after peak stresses are reached, the possibility of progressive failure is increased, and the use of peak shear strengths in stability analyses would be unconservative. Possible solutions are to increase the safety factor or to use shear strengths that are less than peak strengths. In certain soils, it may even be necessary to use ultimate shear strengths.

(2) Where embankments are constructed on foundations consisting of brittle, highly plastic, or heavily overconsolidated clays, or clay shales having stress-strain characteristics significantly different from those of the embankment, consideration should be given to (a) increasing the safety factor over the minimums required in table I (page 25), (b) using shear strengths for the embankment at strains comparable to those in the foundation, or

(c) using ultimate shear strengths of the foundation soils.

(3) Progressive failure also may start along tension cracks resulting from longitudinal or transverse differential settlements occurring during or subsequent to construction or from shrinkage caused by drying. The maximum depth of cracking, assuming an infinite slope, can be estimated from the equation $\frac{2c}{\gamma}$ tan $(45 + \frac{\phi}{2})$ with the limitation that the maximum depth assumed does not exceed 0.5 times the slope height. Shear resistance along the crack should be ignored and the crack assumed to be filled with water in all stability analyses for embankments where this condition is expected.

b. Problem Shales. (1) Shales may be divided into two broad groups: (a) clay shales (compaction shales) that have been consolidated by the weight of overlying sediments and lack significant strength from cementation and (b) cemented shales that have substantial strength produced by calcareous, siliceous, or other types of deposits, or in which particle bonding has occurred because of heat and pressure. Clay shales usually slake rapidly into noncohering fine particles when subjected to a few cycles of wetting and drying, whereas cemented shales are usually either unaffected or reduced to small pieces.

(2) Foundation problems have been encountered more frequently in clay shales than in cemented shales. Clay shales, particularly those containing montmorillonite, are highly susceptible to expansion and consequent loss of strength upon unloading and/or exposure to weathering. The shear strength and deformation modulus of clay shales may be quite low, even under unaltered in situ conditions, and high pore water pressures may develop under increase in load with soil properties approaching those of clays. The presence of slickensides in clay shales is usually an indication of low shear strengths. Prediction of the field behavior of clay shales should not be based solely on results of conventional laboratory tests, since they may be misleading, and large-scale field tests may be required. Existence of problem clay shales can be determined by (a) observation of slide areas through aerial or ground reconnaissance, (b) presence of slickensides, (c) presence

of bentonite layers, (d) comparison of Atterberg liquid and plastic limits with natural water contents, and (e) clay mineralogical tests.

(3) All types of shales may present foundation problems where they contain joints, slickensides, faults, seams filled with soft material, and weak layers. Such defects and excess pore water pressures may control the overall strength of the mass. A detailed geologic investigation is essential wherever shales are encountered. In addition, special laboratory tests may be required to determine physical properties such as shear strength and pore water pressure.

c. Rate of Fill Placement. (1) Foundations. Construction of embankments on silt, clay, or clay shale foundations may create excessive pore water pressures and significant deformations. Instruments should be installed to measure horizontal and vertical movements and pore water pressures occurring during construction. Analyses of such observations, judgment, and past experience are used to control the rate of fill placement (Appendix VIII).

(2) Embankments. Excessive pore water pressures and deformations may also occur in embankments where impervious soils are placed at water contents greater than optimum. Some soils may develop high pore water pressures and deform excessively even when placed at water contents slightly dry of optimum. Observations of horizontal and vertical movements and of pore water pressures during construction can provide data that may be used to control the rate of fill placement. In some cases except on weak, plastic foundations it may be necessary to limit placement water contents of semipervious material in the outer shells of embankments to the dry side of optimum while placing the core material slightly wet of optimum water content.

9. Design Shear Strengths. a. Laboratory Tests. (1) Shear strength values used in stability analyses are generally determined from laboratory tests performed under three conditions of test specimen drainage. Tests corresponding to these drainage conditions are (a) Q tests in which the water

content is kept constant during the test, (b) R tests in which consolidation or swelling is allowed under initial stress conditions but the water content is kept constant during application of shearing stresses, and (c) S tests in which full consolidation or swelling is permitted under the initial stress conditions and also for each increment of load during shear. Q, R, and S tests will be conducted on each representative soil for which design shear strengths are needed. However, Q tests are generally not required for relatively free-draining soils unless they occur in the foundation in a very loose condition. The test conditions designated by the letters Q, R, and S provide limiting shear strength values corresponding to various prototype loading and drainage conditions.

(2) Normally, all strength tests will be made with triaxial compression apparatus except for S tests on fine-grained soils, which usually are tested with direct shear apparatus. Where impervious soils contain significant quantities of gravel sizes, S tests should be performed in triaxial compression apparatus using large-diameter specimens.

(3) Molding water contents used in preparing strength test specimens of cohesive soils should correspond to standard optimum water content and to expected maximum and minimum field placement water contents. The compaction effort applied should result in the estimated minimum allowable placement density (such as 95 or 97 percent of standard maximum density). Test specimens should also be prepared at optimum water content and compacted to 100 percent standard maximum dry density. These minimum requirements, which are illustrated graphically in figure 1, are intended to determine the variation in shear strength for expected placement conditions. However, it may be necessary to test additional specimens within the zone of expected placement conditions as shown in figure 1. For dams having narrow central cores and shells of gravel or rock, the shear strength of the impervious core materials is less important in the stability analysis. Shear tests at the maximum estimated placement water content are considered sufficient.

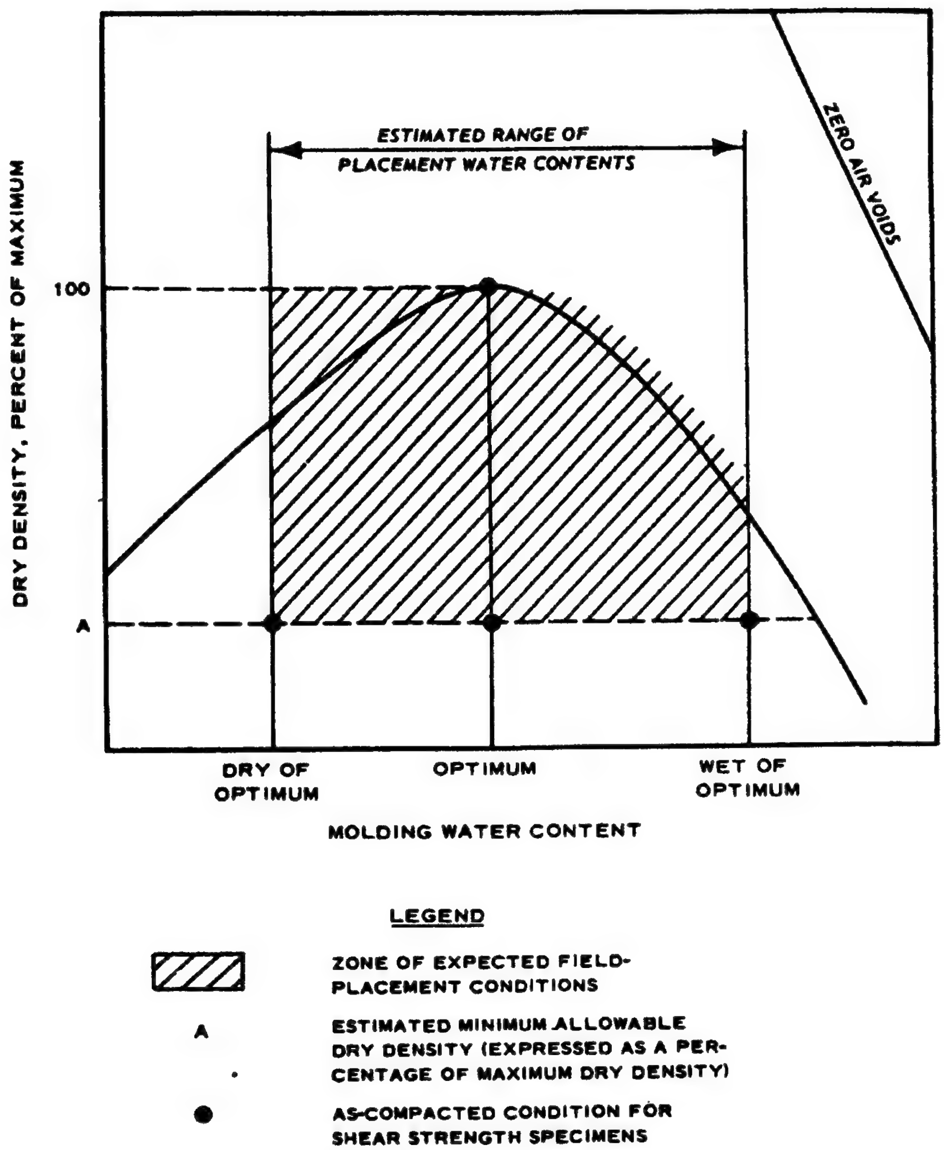

Figure 1. Compaction of shear test specimens of cohesive soils

(4) Strength test specimens of free-draining pervious soils should be compacted to densities corresponding to a relative density of 85 percent, which is the average acceptable relative density for field compaction.

(5) All representative soil types in the borrow areas or from other sources should be tested. Composite samples of different soil types should not be used in test programs unless it can be demonstrated that the same proportion of the individual soils making up the test composites will be placed in the embankment in similar proportions, and should not be used where individual samples are more representative.

(6) The maximum minor principal stress used in triaxial compression tests and the normal stress used in direct shear tests should result in normal stresses on failure planes comparable to those expected in the proposed embankment and/or foundation to obviate extrapolation of shear data in design analysis.

(7) When results of triaxial compression tests are plotted in the form of Mohr circles, the strength envelope customarily is drawn tangent to the circles. This procedure is correct when effective stresses are plotted, but is slightly in error if total stresses for Q and R tests are plotted, as the strength envelope should pass through the points on Mohr circles corresponding to the normal stresses on failure planes. The error is considered unimportant for undisturbed soils because of the compensating effect of disturbance caused by sampling and testing. Therefore, for undisturbed soils the strength envelope should be drawn tangent to the Mohr circles. However, for compacted specimens, which are presumed to have negligible disturbance before testing, the strength envelopes should be drawn through points on the Mohr envelopes representing stresses on the failure plane, as illustrated in figure 2.

(a) Q test. The shear strength resulting from a Q test corresponds to a constant water content condition. This means that water content change is not permitted either prior to or during shear. However, a volume decrease occurs in partially saturated samples as a result of compression of gas (air)

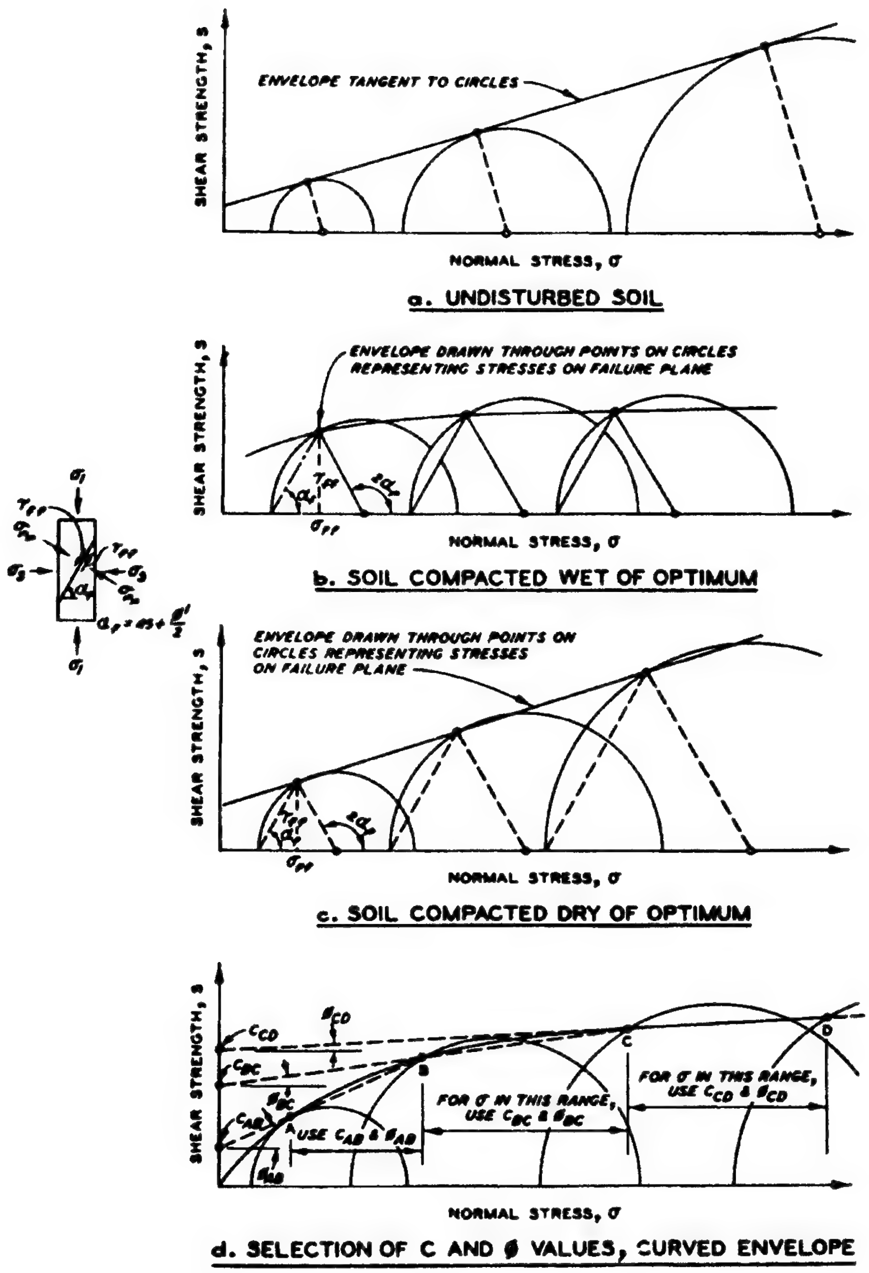

Figure 2. Construction of failure envelopes

in the voids and from increased solution of gas in the pore water under test pressure. While strength envelopes for Q tests of fully saturated soils are generally represented by horizontal lines parallel to the abscissa of the strength diagram, envelopes for partially saturated soils have a curved portion in the low stress range. This curved portion of the envelope should be used, including the cohesion intercept, when the embankment stresses are in this low range. For purposes of design, the curved envelope may be replaced with a series of straight lines approximately parallel to the curved envelope so that the cohesion intercept and friction angle can be determined for the various normal ranges (illustrated in fig. 2d). Q test conditions approximate end-of-construction shear strengths of embankments consisting of impervious soils, or of impervious zones of zoned embankments. This test is also applicable to impervious foundation layers in which the consolidation rate is slow compared to the fill placement rate. In cases where a foundation soil exists that is unsaturated but will become saturated during construction, it is advisable to saturate undisturbed specimens prior to axial loading in the Q test.

(b) R test. The shear strength resulting from an R test is obtained by inducing complete saturation in specimens using back-pressure methods, consolidating these specimens under confining stresses that bracket estimated field conditions, and then shearing the specimens at constant water content. The pore pressures developed in the R test are only those due to shearing; pore pressures due to reservoir water must be also considered in the stability analysis. The test applies to conditions in which impervious or semipervious soils that have been fully consolidated under one set of stresses are subject to a stress change without time for consolidation to take place. This test approximates the behavior, during sudden drawdown, of impervious embankment zones and of impervious foundation layers that have consolidated fully during the embankment construction period and swell under high reservoir conditions prior to sudden drawdown. This test is also used in analyzing upstream slopes during a partial pool condition and

downstream slopes during steady seepage.

(c) S test. The shear strength resulting from an S test is obtained by consolidating a sample under an initial confining stress and applying shearing stresses slowly enough to permit excess pore water pressures to dissipate under each loading increment. Results of S tests are applicable to (1) free-draining soils in which pore pressures do not develop, (2) evaluating shear strengths of embankment or foundation materials that tend to increase in volume during shear and in which excess pore water pressures due to incomplete consolidation have been measured or can be estimated, as discussed in Appendix VIII, and (3) evaluating field shear strengths where pore water pressures have been measured and slope failures have occurred or are impending.

b. Selection of Design Shear Strengths. (1) When selecting design shear strengths the shape of the stress-strain curves for individual soil tests should be considered. Where undisturbed foundation soils and compacted soils do not show a significant drop in shear or deviator stress after peak stresses are reached, the design shear strength can be chosen as (a) the peak shear stress in S direct shear tests, (b) the peak deviator stress, or (c) the deviator stress at 15 percent strain where the shear resistance in creases with increased strain. However, for sensitive foundation soils, the design strength should be intermediate between the peak undisturbed and remolded strengths. While design shear strengths will generally correspond to either Q or R or S test conditions, intermediate strength values may be selected where appropriate.

(2) For each embankment zone and foundation layer, design shear strengths should be selected such that two-thirds of the test values exceed the design values. In most cases, the design shear strength for the various zones and layers should always be greater than the lowest test value for the zones and layers being considered. However, design shear strengths lower than laboratory test values should be used when it is shown by field tests or other means that laboratory results are not conservative.

(3) The shear strength can be estimated by interpolating between the envelopes on the basis of the estimated degree of consolidation as illustrated in figure 3, where the degree of consolidation is expected to be intermediate between that in the Q and R tests. Care must be used in estimating the degree of consolidation, since an overestimate may result in unconservative design strength values. A careful consolidation testing program will be required to assist in estimating the probable degree of consolidation. Where this procedure is used, provisions must be made to measure and evaluate during construction the rate of consolidation, magnitude and dissipation of excess pore pressures, and field shear strengths.

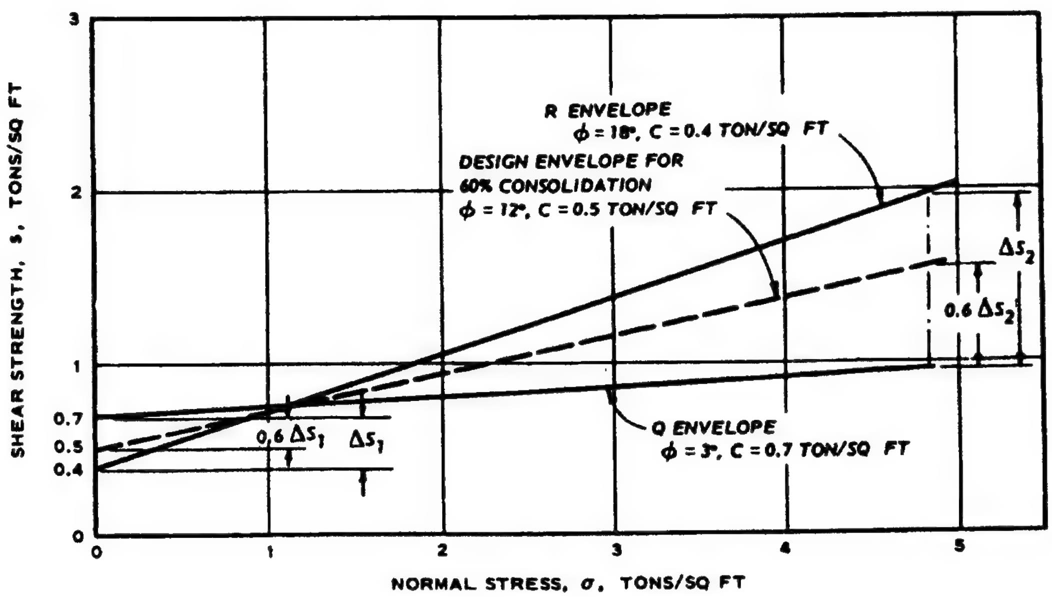

Figure 3. Estimation of strength values intermediate between Q and R strength values

10. <u>Methods of Stability Analysis.</u> The methods of analyzing the stability of earth and rock-fill embankments that are outlined in the appendixes are simple adaptations of the circular arc and sliding wedge methods. The circular arc method is generally more applicable for analyzing essentially

homogeneous earth dams and dams on thick deposits of fine-grained materials, whereas the wedge method is generally more applicable to rock-fill dams on firm foundations and to earth dams on foundations containing one or more weak layers. In addition, the infinite slope method is used to some extent to supplement the circular arc or wedge method. These methods provide a uniform basis for evaluating alternative designs and may be supplemented by other methods or alternative procedures at the discretion of the designer. The use of the modified Swedish method given in Appendix VI is optional. If desired, the forces on the vertical sides of slices may be ignored.

11. Design Conditions for Analysis. An embankment and its foundation are subjected to shear stresses imposed by the weight of the embankment and by pool fluctuations, seepage, or earthquake forces. The cases for which stability analyses shall be performed are designated (I) end of construction, (II) sudden drawdown from maximum pool, (III) sudden drawdown from spillway crest elevation, (IV) partial pool, (V) steady seepage with maximum storage pool, (VI) steady seepage with surcharge pool, and where applicable (VII) earthquake. Cases I and VII apply to both upstream and downstream slopes; Cases II, III, and IV apply to upstream slopes only; and Cases V and VI apply to downstream slopes.

a. Case I: End of Construction. In an embankment composed partially or entirely of impervious soils placed at water contents higher than those corresponding to ultimate water contents after complete consolidation under the imposed loading, pore pressure will be induced because the soil cannot consolidate readily during the construction period. Where this is indicated, applicable shear strengths are determined from Q tests on specimens compacted to anticipated field placement water contents and densities. The Q shear strength is also applicable to impervious foundation layers that are too thick to consolidate significantly during construction. The use of Q shear strengths implies that pore water pressures occurring in laboratory tests satisfactorily approximate field pore water pressures. Except for

thick, impervious foundation strata, the use of Q shear strength is usually conservative, since some consolidation will occur during construction. For overconsolidated soils, the average strength based on Q tests may be higher than that based on R tests. Therefore, swelling may reduce the shear strength, which should be considered in selecting design values. Where consolidation during construction is significant, its effect can be estimated by performing stability analyses using strength values intermediate between Q and R as described in paragraph 9b. When an embankment is to be constructed on clays having low Q strengths, evaluation of the time rate of consolidation characteristics may show that stage construction would result in a significant gain in foundation strengths during the construction period and permit a more economical embankment design. For stage construction where excess pore water pressures are expected to develop in the foundation or embankment, piezometer observations should be used to reevaluate stability during construction (Appendix VIII). Further, at the completion of each stage, foundation samples must be tested to determine the actual change in shear strength due to consolidation caused by stage fill.

b. Cases II and III: Sudden Drawdown. Embankments may become saturated by seepage during prolonged high reservoir stages. If subsequently the reservoir pool is drawn down faster than pore water can escape, excess pore water pressures and unbalanced seepage forces result. Shear strengths to be used in Cases II and III shall be based on the minimum of the combined R and S envelopes (fig. 4). In general, analyses for these cases are based on the conservative assumptions that (1) pore pressure dissipation does not occur during drawdown and (2) the water surface is lowered instantaneously from maximum pool (Case II) or spillway crest elevation (Case III) to the minimum pool elevation. For embankments composed of impervious materials, the resisting friction forces should be determined using saturated or moist weights above the line of seepage at full pool and submerged weights below this level; driving forces should be determined using saturated weights above the lowered pool elevation, saturated weights

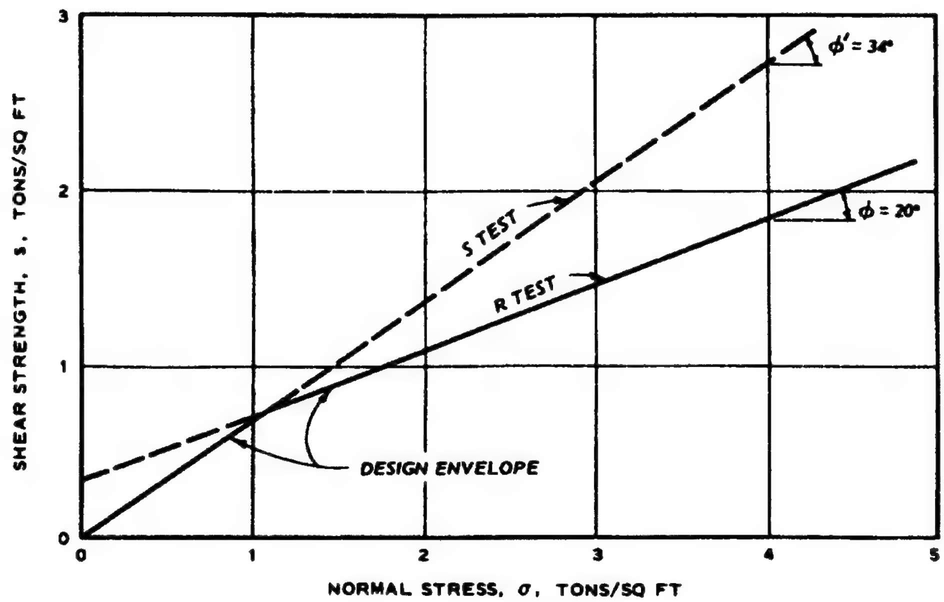

Figure 4. Design envelope for Cases II and III

within the drawdown zone, and submerged weights below the drawdown zone (assuming a horizontal extension of the minimum pool level). Shear strengths of free-draining shell materials, which are defined as those in which drainage of pore water can proceed concurrently with lowering of the pool or with only a minor time lag, are represented by S test conditions. Where sudden drawdown analyses control the design of the upstream slope and where this drawdown assumption appears to be excessively conservative, considering possible drawdown rates and the permeabilities of proposed embankment materials, analyses for relatively incompressible materials may be performed for expected drawdown rates and seepage forces determined from a flow net to evaluate effective normal stresses. Approximate criteria, given in Appendix III, for the lowering of the line of seepage may be used as a basis for constructing flow nets and determining seepage effects. The shear strength envelopes for these analyses should be the same as for sudden drawdown analyses.

c. Case IV: Partial Pool. Analyses of the upstream slope for intermediate reservoir stages should assume that a condition oı steady seepage has developed at these intermediate stages. The design shear strength of impervious soils should correspond to a strength envelope midway between the R and S test envelopes where the S strength is greater than the R strength and to the S envelope where the S strength is less than the R strength (fig. 5). The design shear strength of freely draining cohesionless soils should be the S test envelope. The demarcation between moist and submerged soils may be approximated by a horizontal line from the pool to the downstream limit of the impervious zone, thus eliminating the need for flow net construction. Stability analyses should be performed for several pool elevations, and the factors of safety plotted as a function of reservoir stage to determine the minimum safety factor. The analysis must account for reduction in effective normal stresses where pore water pressures

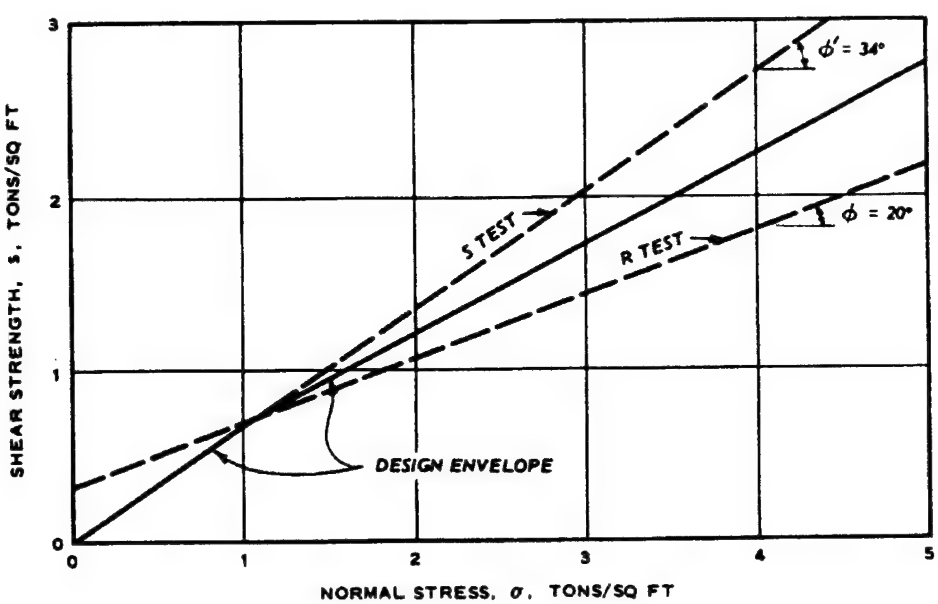

Figure 5. Design envelope for Cases IV, V, and VI

developed during construction are not dissipated before a partial pool condition can develop.

d. Case V: Steady Seepage with Maximum Storage Pool. A condition of steady seepage from the maximum water storage level that can be maintained sufficiently long to produce a condition of steady seepage throughout an embankment may be critical for downstream slope stability. A flow net should be constructed to determine the phreatic line and seepage forces when the assumption of a horizontal phreatic line in the impervious zone is overly conservative. Shear strengths used in Case V should be based on the same shear strength envelope used in Case IV, except for large downstream zones consisting of cohesionless materials that may be analyzed by the infinite slope method using the S strength envelope. The stability of upstream slopes need not be examined for this case. Where downstream slopes composed mainly of cohesionless soils rest on weak foundations, analyses by the infinite slope method should be supplemented with analyses by the circular arc or wedge methods to determine if a failure plane through the foundation is more critical.

e. Case VI: Steady Seepage with Surcharge Pool. The case where a steady seepage condition exists in an embankment and an additional horizontal thrust is imposed by a surcharge pool should also be examined for downstream slope stability. This condition is especially critical for rockfill dams with narrow central cores. Shear strengths used should be the same as those used in Case V, and analyses should be by the wedge or circular arc method. The surcharge pool should be considered as a temporary condition causing no saturation of impervious materials above the steady seepage saturation line.

f. Case VII: Earthquake. Much research is in progress on the behavior of earth dams subjected to earthquake shocks, and new analytical methods for evaluating seismic effects are being developed. However, at present, the traditional approach is still recommended. This assumes that the earthquake imparts an additional horizontal force F_h acting in the

direction of potential failure. The arc or set of planes found to be critical without earthquake loading is used with this added driving force to determine the factor of safety for Case VI. It is not necessary to study effects of earthquake loading in sudden drawdown stability analyses. The horizontal seismic force is equal to the mass involved times the horizontal acceleration, i.e.

$$F_h = \frac{W}{g} a_h = \psi W$$

The total weight of the sliding soil mass W should be based on saturated unit weights below the saturation line and moist unit weights above the line. Selection of the seismic coefficient ψ should be based on the degree of seismic activity in the region in which the dam is to be built. * The seismic coefficients for the various geographical areas are shown on figures 6 through 6c. In areas where earthquakes are likely, or for locations near active faults, the safety of dams should be increased by utilization of defensive design features regardless of the method or results of the earthquake analyses. The defensive design features may include: (a) ample freeboard to allow for the loss of crest elevation due to subsidence, slumping or fault displacement; (b) wide transition sections of filter materials which are less vulnerable to cracking; (c) vertical or near-vertical drainage zones in the central portion of the embankment; (d) filter materials of rounded to subrounded gravels and sands; (e) increased hydraulic conductivity of filter layers and vertical drainage zones or the inclusion of additional properly designed filter zones of higher conductivity; (f) wide impervious cores of plastic clay materials or of suitable, well-graded materials to help insure self-healing in the event cracking should occur; (g) stabilization of reservoir rim slopes to provide for dam safety against effects caused by slides into the reservoir; (h) crest details that will minimize erosion in the event of overtopping; (i) removal of foundation material that may be adversely affected by ground motion; (j) flaring embankment sections at abutment contacts; and (k) zoning of embankments to minimize saturation of materials. In some cases, stock-piling of filter material may be desirable for use in emergency repairs. *

g. At-Rest Earth Pressure Analyses. (1) An at-rest earth pressure (K_0) analysis is sometimes made as an independent check of the stability of an embankment.[6] This analysis is particularly applicable to earth and rockfill dams with narrow central cores, and is performed to check analyses of Case I (end of construction) and Case V (steady seepage) conditions.

(2) For Case I and assuming that construction pore water pressures are negligible or have dissipated; the horizontal earth force acting on a

vertical plane through the crest is compared with the shear resistance along the downstream base of the embankment to determine the factor of safety using an equation similar to the following.

$$F.S. = \frac{cL + W_p \tan \phi}{\frac{1}{2} H^2 \gamma_m K_o}$$

The strengths would be the same as those used for other Case I analyses. The shear resistance terms in the equation above should be modified if a lower shear resistance is obtained by shifting the sliding plane from the foundation into the embankment and/or by using the S strength at low normal stresses. If pore water pressures are expected to exist at the end of construction, they should be estimated using methods such as those described in Appendix VIII, and included in the computation of the horizontal force. This force should be based on a horizontal pressure diagram developed from the following equation.

$$p_h = (z\gamma_m - u) K_o + u$$

The value for K_o is often taken as 0.5, although values greater than 0.5 may be required for normally consolidated clays with an overconsolidation ratio of 1 (OCR = 1) with a high plasticity index (PI).[7] A relationship of K_o and PI for overconsolidation ratios of 1 and 2 is shown in figure 7. An example for case I is given in figure 8.

(3) For Case V, the water force from the maximum pool and submerged soil weights are used in computing the horizontal force and checking the factor of safety using an equation similar to the following.

$$F.S. = \frac{cL + W_p \tan \phi}{\frac{1}{2}\left(\gamma_w h_w^2 + \gamma' H^2 K_o\right)}$$

The strengths shown in table I are used for Case V, and it is assumed that

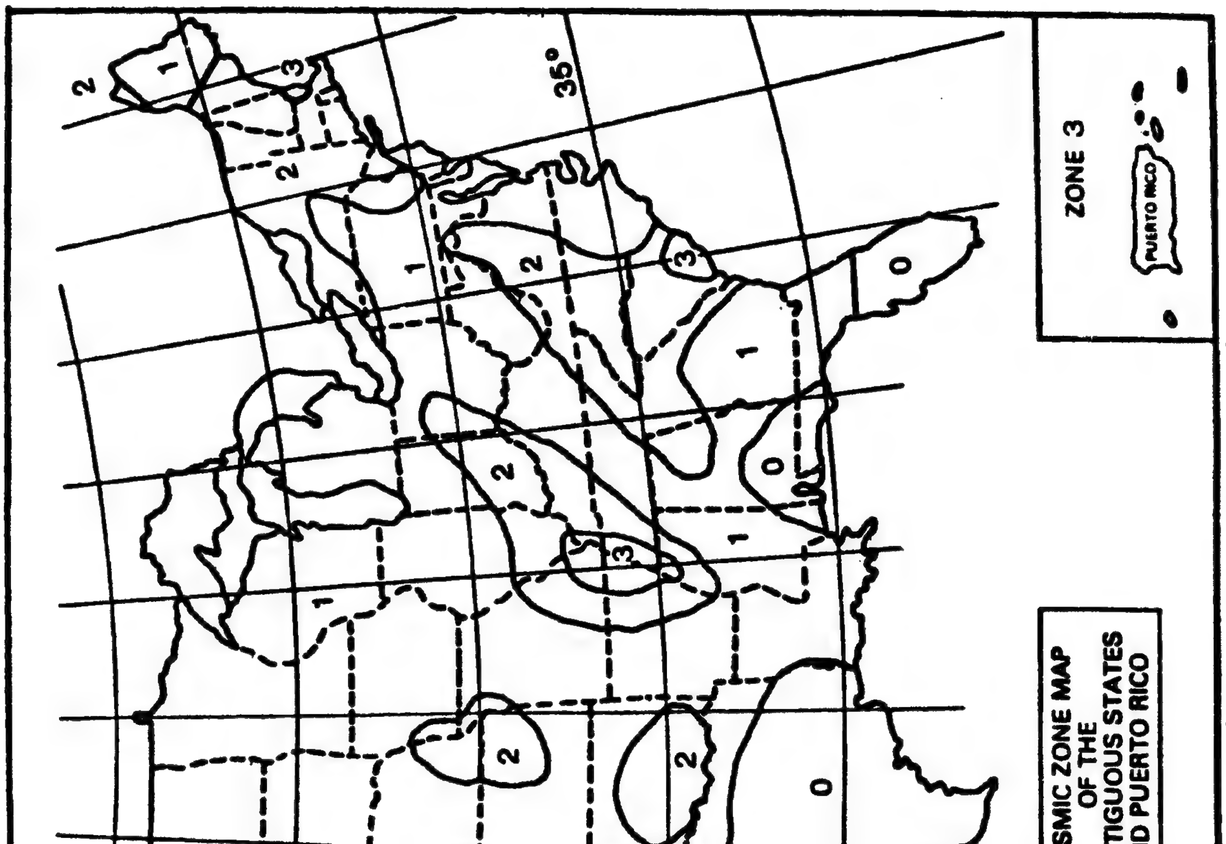

* Figure 6. Seismic Zone Map of Contiguous States and Puerto Rico *

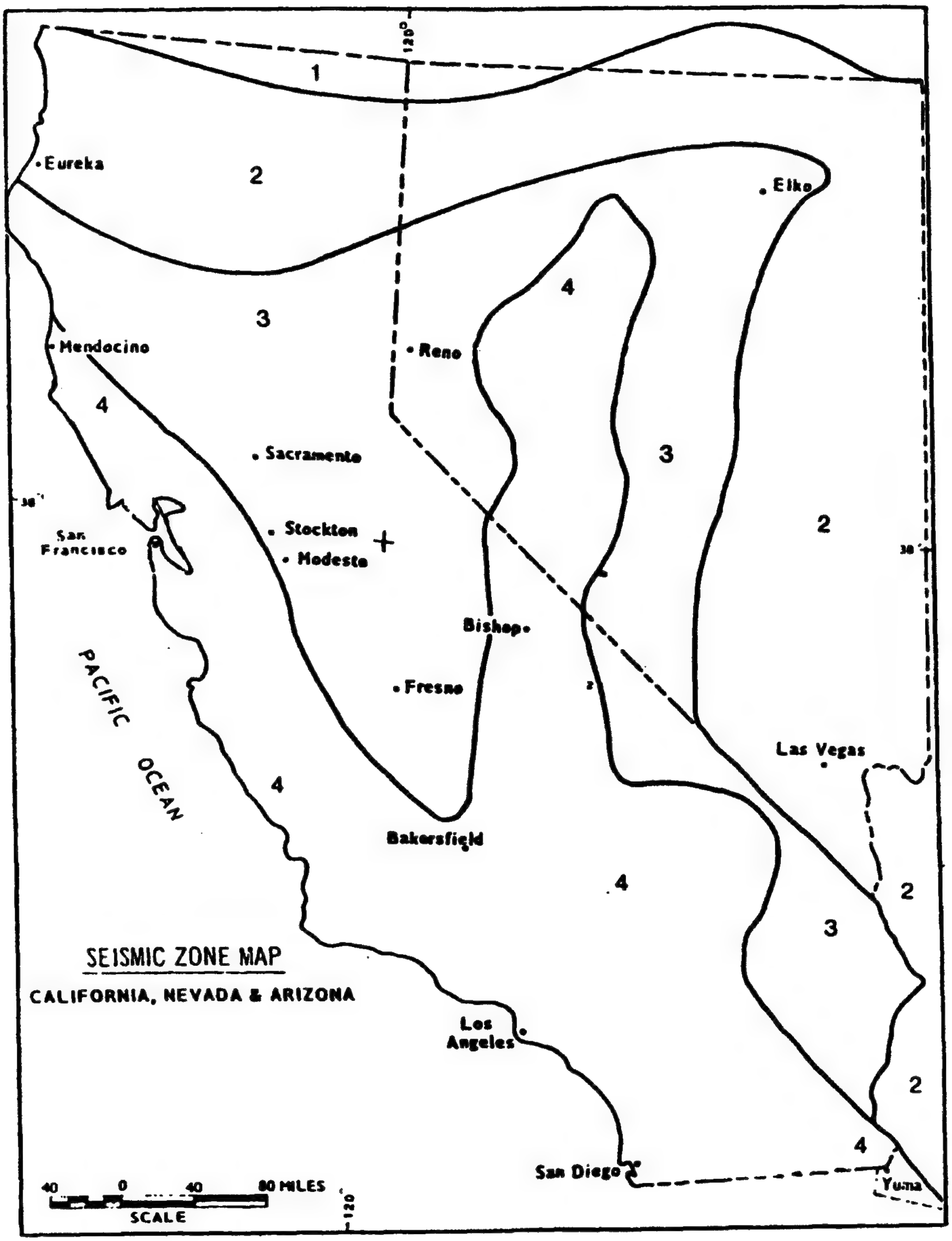

* Figure 6a. Seismic Zone Map of California, Nevada and Arizona *

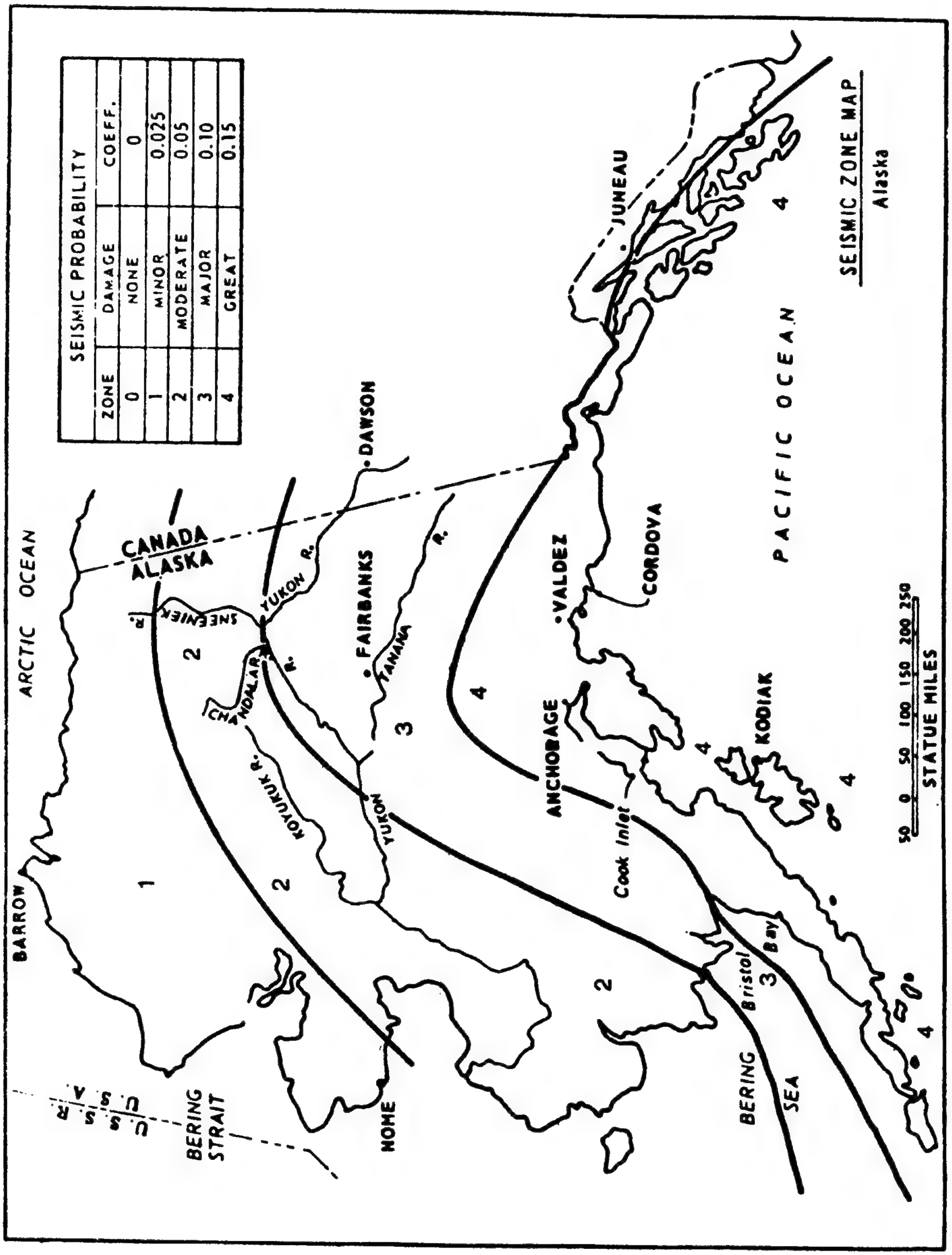

SEISMIC PROBABILITY

ZONE	DAMAGE	COEFF.
0	NONE	0
1	MINOR	0.025
2	MODERATE	0.05
3	MAJOR	0.10
4	GREAT	0.15

* Figure 6b. Seismic Zone Map of Alaska *

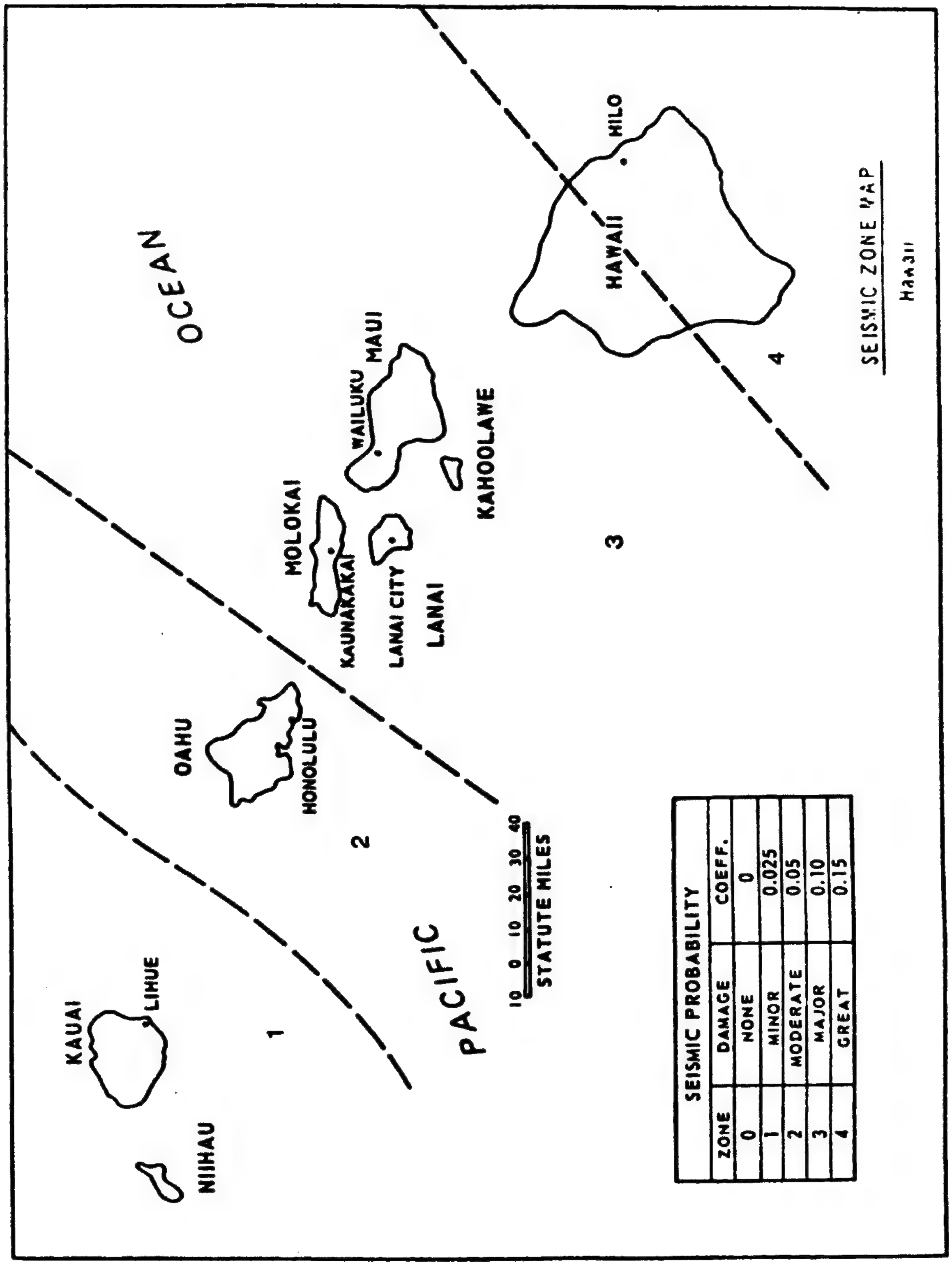

ZONE	SEISMIC PROBABILITY	
	DAMAGE	COEFF.
0	NONE	0
1	MINOR	0.025
2	MODERATE	0.05
3	MAJOR	0.10
4	GREAT	0.15

* Figure 6c. Seismic Zone Map of Hawaii *

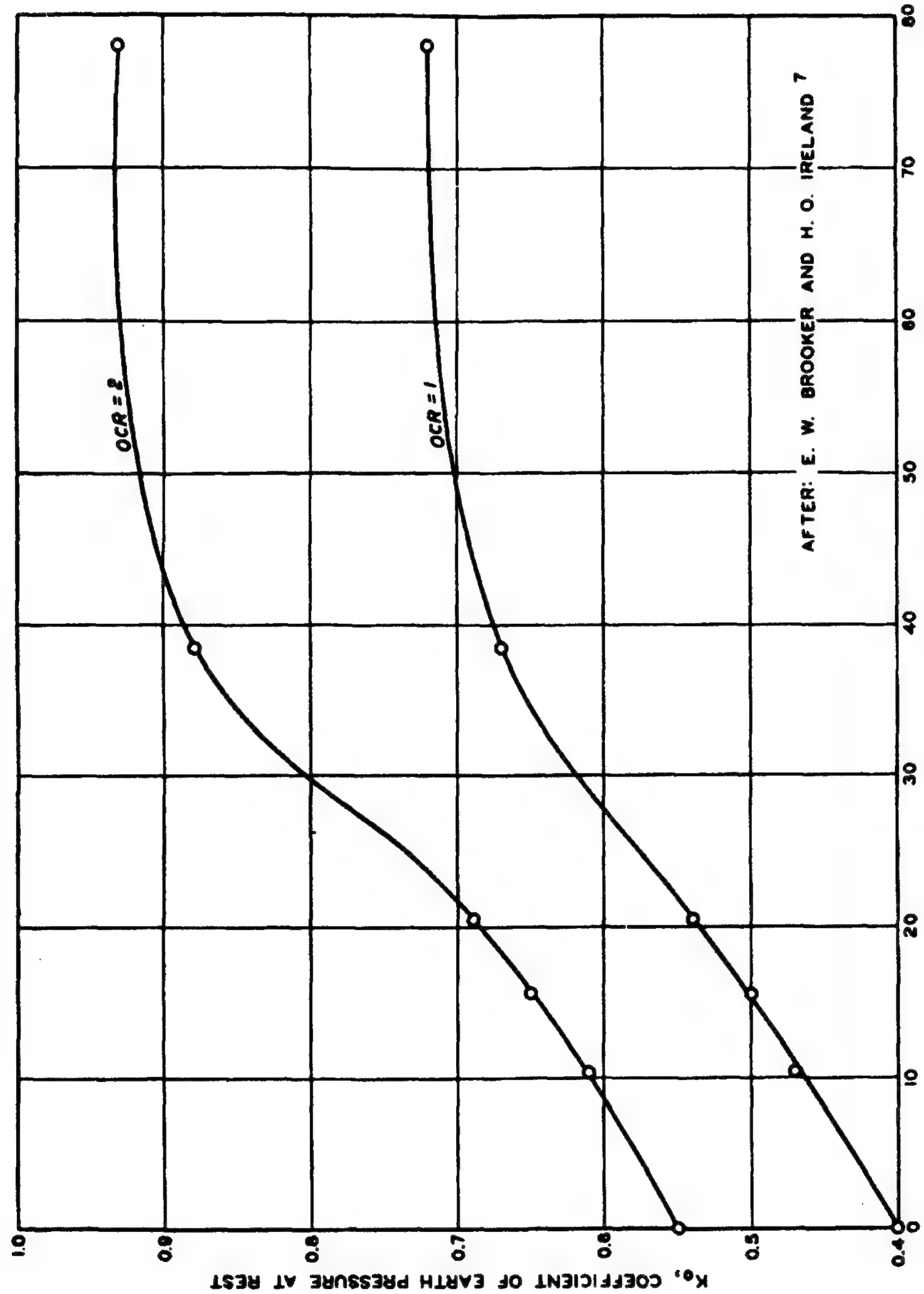

Figure 7. K versus PI and overconsolidation ratio (Brooker and Ireland)[7]

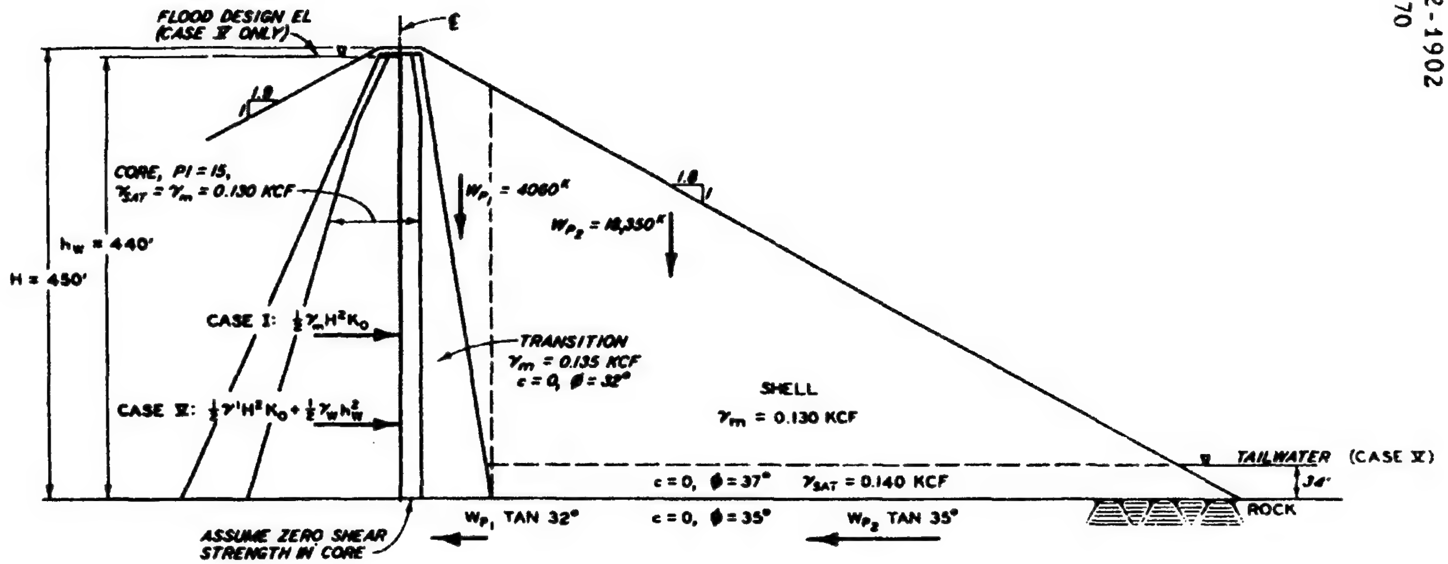

CASE I, END OF CONSTRUCTION: $F.S. = \dfrac{4060 \tan 32° + 20{,}230 \tan 35°}{\frac{1}{2}(0.130)(450)^2(0.5)} = \dfrac{2540 + 14{,}180}{6560} = 2.55$

$K_o = 0.5$ FROM
FIGURE 7 FOR PI = 15
AND OCR = 1.

CASE V, STEADY SEEPAGE: $F.S. = \dfrac{4060 \tan 32° + 18{,}350 \tan 35°}{\frac{1}{2}(0.0624)(440)^2 + \frac{1}{2}(0.0678)(450)^2(0.65)} = \dfrac{15{,}390}{6050 + 4450} = 1.47$

$K_o = 0.65$ FROM
FIGURE 7 FOR PI = 15
AND OCR = 2.

Figure 8. Examples of at-rest earth pressure analyses, Cases I and V

Table I
Minimum Factors of Safety†

Case No.	Design Condition	Minimum Factor of Safety	Shear Strength	Remarks
I	End of construction	1.3††	Q or S‡	Upstream and downstream slopes
II	Sudden drawdown from maximum pool	1.0‡‡	R, S	Upstream slope only. Use composite envelope. See fig. 4
III	Sudden drawdown from spillway crest or top of gates	1.2‡‡	R, S	Upstream slope only. Use composite envelope. See fig. 4
IV	Partial pool with steady seepage	1.5	$\frac{R+S}{2}$ for $R < S$, S for $R > S$	Upstream slope only. Use intermediate envelope. See fig. 5
V	Steady seepage with maximum storage pool	1.5	$\frac{R+S}{2}$ for $R < S$, S for $R > S$	Downstream slope only. Use intermediate envelope. See fig. 5
VI	Steady seepage with surcharge pool	1.4		
VII	Earthquake (Cases I, IV, and V with seismic loading)	1.0	§	Upstream and downstream slopes

† Not applicable to embankments on clay shale foundations.
†† For embankments over 50 ft high on relatively weak foundations use minimum factor of safety of 1.4.
‡ In zones where no excess pore water pressures are anticipated, use S strength.
‡‡ The safety factor should not be less than 1.5 when drawdown rate and pore water pressures developed from flow nets (Appendix III) are used in stability analyses.
§ Use shear strength for case analyzed without earthquake except that it is not necessary to analyze sudden dravdown for earthquake effects.

the core has an overconsolidation ratio of 2 (since weights have changed from moist to submerged values) in selecting a value for K_o from figure 7. An example for Case V is given in figure 8.

12. Factors of Safety. Appropriate values of computed safety factors depend on the (a) design condition being analyzed, (b) estimated reliability of shear strength design values, (c) embankment height, (d) presence of structures within the embankment, (e) thoroughness of investigations, (f) stress-strain characteristics and compatibility of embankment and foundation materials, (g) probable quality of construction control, and (h) judgment based on past experience with earth and rock-fill dams. In the final analysis, the consequences of a failure with respect to human life, property damage, and impairment of functions are important considerations in establishing acceptable factors of safety for specific projects. Table I lists minimum safety factors required for the various design conditions, the portions of the dam for which analyses are required, and applicable types of shear tests. Methods of stability analyses described in the appendixes are the modified Swedish (normally considering circular arc surfaces) method with several alternative procedures, the wedge method, and the infinite slope method. The factor of safety is based on developed shear strength s_D where

$$s_D = \frac{c}{F.S.} + \sigma \frac{\tan \phi}{F.S.}$$

Trial factors of safety are tried until a condition of limiting equilibrium is reached. In the infinite slope method, the factor of safety is related directly to the frictional shearing resistance and slope inclination. Due to differences in basic assumptions, comparisons of relative factors of safety should be made with caution. For example, factors of safety determined by the circular arc method for plastic soils are not directly comparable in degree of safety to those determined by infinite slope computations for granular materials.

13. Presentation in Design Memoranda. Uniformity in presenting results

of stability analyses and supporting data facilitates review of design memoranda. Analyses should generally conform in scope to those given in the appendixes. Each analysis should include the following data:

a. A cross section of the embankment and foundation being analyzed showing the assumed failure surface for the lowest factor of safety obtained for the condition analyzed, applicable flow net construction or lines of saturation, zones or strata corresponding to the shear strength values used, and graphical delineation of all forces and reactions. Separate cross sections should be included as necessary to indicate thoroughness of analyses. All centers of circles with factors of safety and circle radii should be shown on these sections. The locations of the trial failure surfaces analyzed, either circular arc or wedge, and the safety factors found in addition to those for the critical surface will be presented in sufficient number to demonstrate the extent of the stability analyses performed.

b. A tabulation of shear strength values, together with unit weights for each of the materials comprising the embankment and foundation. Correlations of foundation shear strength with Atterberg limits, graphical summaries of shear strength envelopes, presentations of foundation and borrow material Atterberg limits on plasticity charts, and similar correlations are valuable aids to reviews and should be presented.

c. A tabulation of the computations for the critical arc or wedge.

d. A brief discussion of the rate of reservoir rise, the duration of full pool, and rate of drawdown as a basis for sudden drawdown computations or for a slow rate of drawdown that may apply to an ungated flood control embankment.

e. Presentation of design shear strength data and composite or intermediate S and R strength envelopes, as shown in figures 3 and 4. Presentation of shear strength test data for representative samples is required to support the selection of these design shear strengths.

f. Proposed instrumentation to be installed. Complete information on instrumentation should be included in accordance with guidance contained in

Civil Works Engineer Letter 65-7 (ref 9).

14. Use of Electronic Computers. The use of electronic computers is recommended to (a) reduce computational effort, (b) evaluate effects of possible variations in material properties, and (c) investigate alternative embankment sections and zoning. To obtain valid solutions, the computer program used must be capable of evaluating all significant boundary conditions. Computer solutions must be reviewed to establish that the critical circle or set of planes found have not been limited by the computer program employed. Under some conditions, computer programs may search out the critical circle or set of planes in only one of two or more potential failure areas. The analyses presented in the design memoranda should include the location, radius, and safety factor for a sufficient number of trial surfaces to verify that the critical circle or set of planes has been obtained. Computer solutions must also be verified to ensure that computer programs used are compatible with design procedures and criteria presented herein. Consequently, an analysis by manual procedures must be made to check the critical circle or set of planes found by the computer for each design condition. The manual computations must be presented in the design memoranda so that an independent check can be made, if desired, of all critical circles or sets of planes.

FOR THE CHIEF OF ENGINEERS:

RICHARD F. McADOO
Colonel, Corps of Engineers
Executive

8 Appendixes

Appendix I	- References
Appendix II	- Notation
Appendix III	- Estimating Seepage During Reservoir Drawdown
Appendix IV	- Procedures for Determination of Embankment Slopes
Appendix V	- Infinite Slope Analysis for Cohesionless Soils
Appendix VI	- Modified Swedish Method of Analysis Using Slice Procedure
Appendix VII	- Wedge Analysis
Appendix VIII	- Evaluation of Embankment Stability During Construction

APPENDIX I

References

1. U. S. Army Engineer Waterways Experiment Station, CE, "Soil Mechanics Design, Stability of Slopes and Foundations," Technical Report No. 3-777, Appendix D, Feb 1952 (reprinted Apr 1967), Vicksburg, Miss.

2. "Progress Report on Glossary of Terms and Definitions in Soil Mechanics," ASCE, Soil Mechanics and Foundations Division, Journal, Vol 84, Paper 1826, No. SM4, Oct 1958.

3. Banks, D. C. and MacIver, B. N., "Variation in Angle of Internal Friction with Confining Pressure," Miscellaneous Paper S-69-12, Apr 1969, U. S. Army Engineer Waterways Experiment Station, CE, Vicksburg, Miss.

4. Banks, D. C. and Strohm, W. E., Jr., "Methods of Preventing Flow Slides," Potamology Investigations Report 12-16, Oct 1965, U. S. Army Engineer Waterways Experiment Station, CE, Vicksburg, Miss.

5. Seed, H. B. and Lee, K. L., "Liquefaction of Saturated Sands During Cyclic Loading," ASCE, Soil Mechanics and Foundations Division, Journal, Vol 92, Paper 4972, No. SM6, Nov 1966, pp 105-134.

6. Robeson, F. A. and Crisp, R. L., Jr., "Rockfill Design - Carters Dam," ASCE, Construction Division, Journal, Vol 92, Paper 4906, No. C03, Sept 1966, p 51.

7. Brooker, E. W. and Ireland, H. O., "Earth Pressures at Rest Related to Stress History," Canadian Geotechnical Journal, Vol 2, No. 1, Feb 1965, pp 1-15.

8. Algermissen, S. T., "Seismic Risk Studies in the United States," Proceedings, Fourth World Conference on Earthquake Engineering, Santiago, Chile, 14 Jan 1969.

9. Office, Chief of Engineers, "Inclusion of Proposed Instrumentation in Embankment and Foundation Design Memoranda," Civil Works Engineer Letter 65-7, 2 Mar 1965, Washington, D. C.

10. Schnitter, G. and Zeller, J., "Sickerströmungen als Folge von Stauspiegelschwankungen in Erddämmen (Seepage Flow Resulting from Fluctuation or Level in Earth Dams)," Schweizerische Bauzeitung, 75 Jahrgang, Nr. 52, 28 Dec 1957, pp 808-814.

11. Terzaghi, K. and Peck, R. B., Soil Mechanics in Engineering Practice, 2d ed., Wiley, New York, 1967, p 138.

12. Janbu, N., "Stability Analysis of Slopes with Dimensionless Parameters," Soil Mechanics Series No. 46, Jan 1954 (reprinted May 1959), Harvard University, Cambridge, Mass.

13. Scott, R. F., Principles of Soil Mechanics, Addison-Wesley, Reading, Mass., 1963.

14. Jumikis, A. R., "Active and Passive Earth Pressure Coefficient Tables," Engineering Research Publication No. 43, 1962, Rutgers University, College of Engineering Research, New Brunswick, N. Y.

15. Clough, G. W. and Snyder, J. W., "Embankment Pore Pressures During Construction," Technical Report No. 3-722, May 1966, U. S. Army Engineer Waterways Experiment Station, CE, Vicksburg, Miss.

16. Hilf, J. W., "Estimating Construction Pore Pressures in Rolled Earth Dams," Proceedings, Second International Conference on Soil Mechanics and Foundation Engineering, Rotterdam, Vol 3, 1948, p 234.

17. Bruggeman, J. R., Zanger, C. N., and Brahtz. J. H. A., "Notes on Analytic Soil Mechanics," Technical Memorandum No. 592, p 124, June 1939, U. S. Bureau of Reclamation, Denver, Colo.

18. Bishop, A. W., "Some Factors Controlling the Pore Pressure Set Up During the Construction of Earth Dams," Proceedings, Fourth International Conference on Soil Mechanics and Foundation Engineering, London, Vol 2, 1957, pp 294-300.

19. Moran, Proctor, Mueser & Rutledge, Consulting Engineers, New York, "Study of Deep Soil Stabilization by Vertical Sand Drains," NOy88812, June 1958, Bureau of Yards and Docks, Department of the Navy, Washington, D. C.

20. Skempton, A. W., "The Pore-Pressure Coefficients A and B," Geotechnique, Institution of Civil Engineers, London, Vol 4, 1954, pp 143-147.

21. Snyder, J. W., "Pore Pressures in Embankment Foundations," Technical Report S-68-2, July 1968, U. S. Army Engineer Waterways Experiment Station, CE, Vicksburg, Miss.

22. Gould, J. P., "Analysis of Pore Pressure and Settlement Observations at Logan International Airport," Soil Mechanics Series No. 34,

Dec 1949, Harvard University, Cambridge, Mass.

23. Lowe III, J. and Karafiath, L., "Effect of Anisotropic Consolidation on the Undrained Shear Strength of Compacted Clays," ASCE Research Conference on Shear Strength of Cohesive Soils, University of Colorado, Boulder, Colo., June 1960, pp 837-858.

APPENDIX II

Notation

1. The symbols that follow are used throughout this manual and correspond wherever possible to those recommended by the American Society of Civil Engineers.

Symbol	Term
A, B	Skempton's experimentally determined pore pressure coefficients
a_h	Horizontal seismic acceleration
b	Cot β = cotangent of the embankment slope angle with the horizontal
C_A	Developed cohesion force of active wedge
C_{CB}	Developed cohesion force of central block
C_D	Developed cohesion force
C_P	Developed cohesion force of passive wedge
c	Cohesion per unit area
c_D	Developed cohesion per unit area (cohesion required for equilibrium)
D	Depth of foundation layer
E	Earth force on side of slice
E_A	Resultant force of active wedge
E_{CB}	Resultant force of central block
E_P	Resultant force of passive wedge
ΔE_H	Force required to close force polygon in wedge analysis
ΔE	Resultant of earth forces on left and right sides of slice (modified Swedish method: Finite Slice Procedure)
$\Delta E'$	Resultant of earth forces acting on left and right sides of the unit width slice in units of γ_{base} (modified Swedish method: Graphical Integration Procedure)
F_A	Resultant of normal and frictional forces of active wedges
F_{CB}	Resultant of normal and frictional forces of central block
F_D	Resultant of developed normal and frictional forces

Symbol	Term
F_h	Horizontal seismic force
F_P	Resultant of normal and frictional forces of passive wedge
F.S.	Factor of safety
g	Gravitational constant
H	Height of embankment
H_D	Height of drawdown
h	Vertical distance to failure surface from slope surface
h'	Modified height obtained from $h(\gamma/\gamma_{base})$
h_w	Piezometric level above the failure surface; height of maximum pool above sliding surface
K	Ratio of horizontal to vertical earth pressures
K_A	Active earth pressure coefficient
K_o	Coefficient of at-rest earth pressure
K_P	Passive earth pressure coefficient
k	Coefficient of permeability
L	Length of arc or failure surface; length beneath passive block along which cohesive shear resistance is assumed to develop
L'	Width of the slice parallel to the saturation line
ΔL	Length of base of slice
N	Total normal force
N_D	Developed normal force
N_K	Active earth pressure stability number, $\frac{bc_D}{\gamma H}$
N_s	Stability factor, $\frac{\gamma H}{c_D}$
n	Porosity
n_e	Effective porosity
P_D	Dimensionless parameter $= \frac{k}{n_e V}$
p_h	Horizontal pressure at depth z
Q	Shear test for specimen tested at constant water content (unconsolidated-undrained)
$\overline{Q}$	Q shear test with pore pressure measurements

Symbol	Term
R	(a) Radius of failure arc (b) Shear test for specimen consolidated then sheared at constant water content (consolidated-undrained)
$\overline{R}$	R shear test with pore pressure measurements
S	Shear test for specimen consolidated and sheared without restriction of change in water content (consolidated-drained)
s	Shear strength; $s = c + \sigma \tan \phi$
s_D	Developed shear strength; $s_D = c_D + \sigma \tan \phi_D$
U	Hydrostatic force
u	Pore water pressure
V	Velocity of pool drawdown
W	Total weight of slice or soil mass above failure plane
W_p	Weight of passive block or subblocks above plane along which frictional shear resistance is assumed to develop
X	Dimensionless height ratio (Appendix III)
z	Distance beneath crest
α	Angle of inclination of the saturation line with the horizontal
α_f	Angle of inclination of failure plane (based on laboratory shear test results)
β	Angle of inclination of the embankment slope with the horizontal
γ	Weight per unit volume
γ'	Buoyant unit weight of the soil
γ_{base}	Base unit weight used in graphical integration procedure of modified Swedish method
γ_m	Moist unit weight of the soil
γ_{sat}	Saturated unit weight of the soil
γ_w	Unit weight of water
Δ	Increment or small part
θ	Angle of inclination of the failure arc with the horizontal
θ_A	Angle of inclination of the base of the active wedge with the horizontal

Symbol	Term
θ_P	Angle of inclination of the base of the passive wedge with the horizontal
σ	Normal stress
σ_{ff}	Normal stress on failure plane at failure (in laboratory shear test specimen)
σ_h	Horizontal stress on vertical plane
σ_i	Conjugate stress on a plane parallel to the outer slope
σ_1	Major principal stress
σ_3	Minor principal stress
$\sigma_1 - \sigma_3$	Deviator stress
$\bar{\sigma}_{fc}$	Effective normal stress on failure plane prior to start of test
$\bar{\sigma}_{ff}$	Effective normal stress on failure plane at failure
$\bar{\sigma}_1$	Effective major principal stress
$\bar{\sigma}_3$	Effective minor principal stress
τ	Shear stress
τ_{fc}	Shear stress on failure plane at end of consolidation
τ_{ff}	Shear stress on failure plane at failure
ϕ	Angle of internal friction (or slope angle of strength envelope) based on total stresses
ϕ'	Angle of internal friction (or slope angle of strength envelope) based on effective stresses
ϕ_D	Developed angle of internal friction (required for equilibrium)
ψ	Seismic coefficient, $\frac{a_h}{g}$

APPENDIX III

Estimating the Lowering of the Seepage Line in Pervious Upstream Embankment Zones During Reservoir Drawdown

1. General. In stability analyses of pervious embankment slopes subjected to various time rates of drawdown, it is often desirable to construct flow nets for use in determining seepage forces. To construct such flow nets, it is necessary to determine the lowering of the intercept of the line of seepage at the face of the impervious core. The lowering of the seepage line can be estimated as shown in a method by Schnitter and Zeller[10] that relates fill permeability and drawdown rate. This relation is valid only in materials such as sands and gravel which do not change volume as the water content changes during drawdown.

2. Mathematical Relation. The equations for the dimensionless height ratio X (i.e., the ratio of height of saturation line at face of core at end of drawdown expressed in percent of drawdown) and the dimensionless parameter P_D are

$$X = \frac{H_D - \Delta H_D}{H_D} \times 100$$

$$P_D = \frac{k}{n_e V}$$

where

H_D = height of drawdown

ΔH_D = change in height of saturation line at face of impervious core

k = coefficient of permeability of shell material

$n_e = \frac{n}{100} \times \frac{w_1 - w_2}{w_1}$ = effective porosity; i.e., the ratio of void space drained to unit volume of soil where n is porosity, w_1 is saturated water content, and w_2 is water content after drainage

V = velocity of pool drawdown

All quantities should be expressed in consistent units.

3. Computations. Although the curves presented in plate III-1 were developed for the case of full reservoir drawdown, they may also be used when drawdown is to some intermediate pool level above the embankment base by considering the intermediate pool elevation as the base of the embankment. The following example illustrates the use of the chart in plate III-1.

a. Assume a 105-ft-high dam with a narrow central impervious core and a 1-on-3 upstream slope. The pool is 100 ft above the embankment base and is to be drawn down 60 ft in 30 days. The shell is assumed to be a sandy gravel having a permeability of 500×10^{-4} ft per min and a porosity of 20 percent. The average saturated water content is 12 percent, and after drainage the water content is 3 percent.

The effective porosity n_e is

$$n_e = \frac{12 - 3}{12} \times \frac{20}{100} = 0.15$$

The velocity of pool drawdown V is

$$= \frac{60\ (\text{ft})}{30 \times 24 \times 60\ (\text{min})}$$

$$V = 0.00139 \text{ ft per min} = 13.9 \times 10^{-4} \text{ ft per min}$$

$$P_D = \frac{k}{n_e V} = \frac{500 \times 10^{-4}}{0.15 \times 13.9 \times 10^{-4}} = 240$$

From the chart, for a 1-on-3 slope, X = 10 percent. Solving the equation

$$\frac{X}{100} = \frac{H_D - \Delta H_D}{H_D} \quad \text{for } \Delta H_D$$

$$\frac{10}{100} = \frac{60 - \Delta H_D}{60} \quad \text{or} \quad \Delta H_D = 54 \text{ ft}$$

Thus, the height of saturation at the core is 54 ft below the original pool level, or 46 ft above the base of dam, or 6 ft above the lowered pool.

b. Assume the same conditions except that the shell is constructed of less pervious soil with $k = 5 \times 10^{-4}$ ft per min and the water content after drainage is 9 percent.

$$n_e = \frac{12 - 9}{12} \times \frac{20}{100} = 0.05$$

$$P_D = \frac{5 \times 10^{-4}}{0.05 \times 13.9 \times 10^{-4}} = 7.2$$

A value of X equal to 51 percent is obtained from the curve in plate III-1 for a 1-on-3 slope. Solving for ΔH_D

$$\frac{51}{100} = \frac{60 - \Delta H_D}{60} \text{ or } \Delta H_D = 29.4 \text{ ft}$$

In this case, the height of saturation is 29.4 ft below the original pool or 70.6 ft above the base of the dam, or 30.6 ft above the lowered pool.

4. Limitations. The curves in plate III-1 give only approximate criteria for determining the rate of drainage of shell material and lowering the line of seepage at the face of central core embankments.* Judgment must be used in determining probable velocity of drawdown, and reasonable values of n_e and k. Information given by Terzaghi and Peck[11] may be used as a guide in selecting values of n_e. In order for values of X to approach 0 percent (i.e. complete, virtually instantaneous drainage of the shell material), the shell must approach a highly pervious condition.

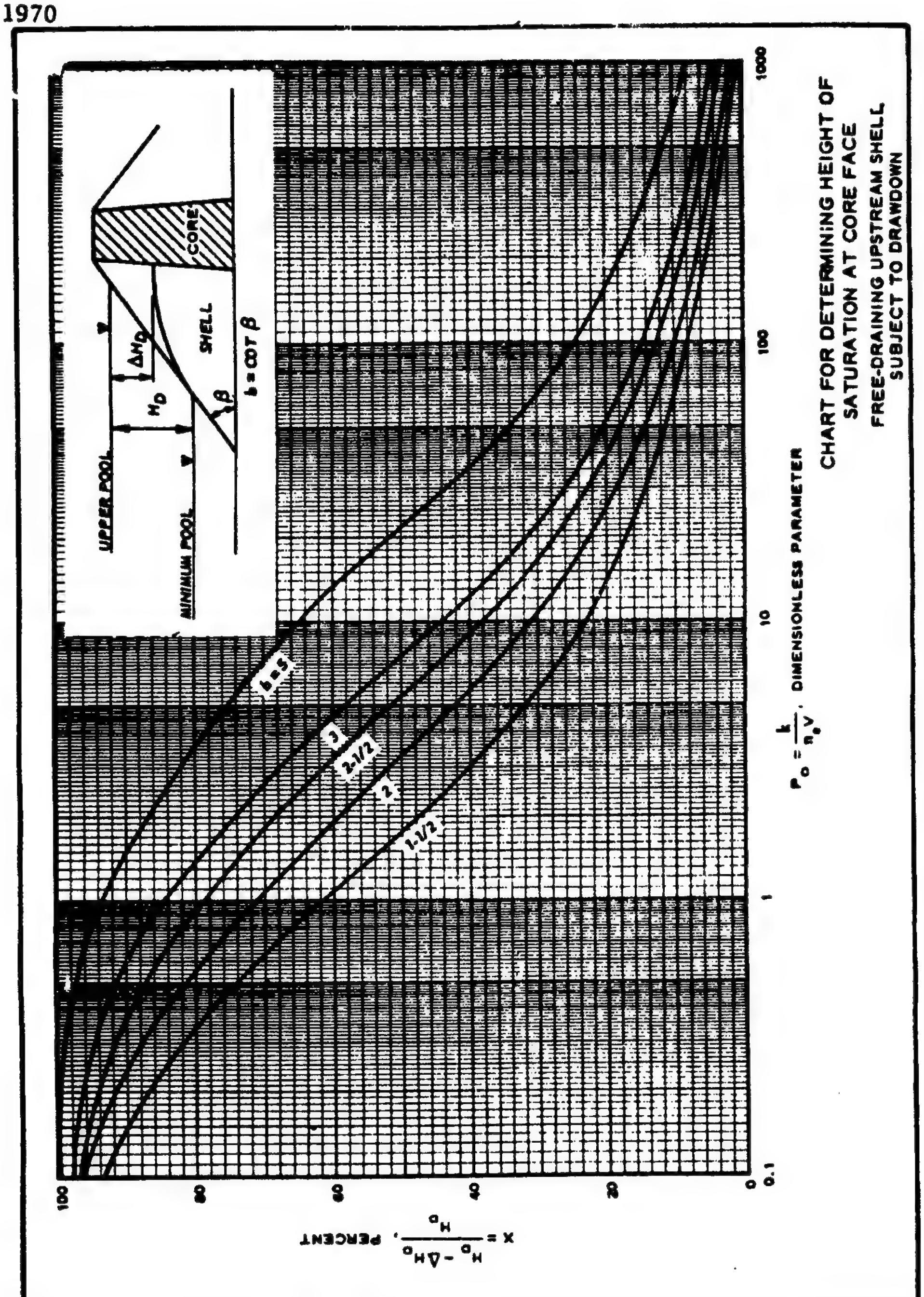
CHART FOR DETERMINING HEIGHT OF
SATURATION AT CORE FACE
FREE-DRAINING UPSTREAM SHELL
SUBJECT TO DRAWDOWN
UPPER POOL
MINIMUM POOL
H_D
ΔH_D
SHELL
CORE
β
$b = \cot \beta$
$b = 5$
3
2-1/2
2
1-1/2
$P_o = \frac{k}{n_e V}$, DIMENSIONLESS PARAMETER
0.1
1
10
100
1000
$X = \frac{H_o - \Delta H_o}{H_o}$, PERCENT
0
20
40
60
80
100

Plate III-1

APPENDIX IV

Simplified Procedures for Preliminary Determination of Embankment Slopes

1. General. Two methods for determining approximate embankment slopes using design charts are presented in this appendix. The methods are useful for determining approximate embankment slopes prior to more detailed analyses by the methods outlined in Appendixes VI, VII, and VIII. The first method is applicable to homogeneous clay embankments and foundations overlying a rigid boundary and assumes that failure occurs along a circular arc as shown in plate IV-1. The second method is applicable to homogeneous cohesionless embankments on shallow clay foundations overlying a rigid boundary and assumes that failure occurs along plane surfaces in the foundation and in the embankment as shown in plate IV-6. These methods of analyses are applicable for cases involving no seepage. Due to the differences in the basic assumptions of the two methods presented, comparisons of factors of safety should be made with caution. Other charts such as those prepared by Janbu[12] or Scott[13] may also be used; they yield more conservative results because they apply to slopes having horizontal or wide crests.

2. Homogeneous Embankment and Foundation Overlying a Rigid Boundary.

a. The design charts are developed for the general case of a homogeneous embankment and foundation overlying a rigid boundary as shown in plate IV-1. The embankment slopes are assumed to be symmetrical, and the crown width is equal to one-eighth the embankment height. In plates IV-2 through IV-5, the stability factor $N_s = \frac{\gamma H}{c_D}$ is presented for ratios of thickness of foundation layer D to embankment height H between 0 and 1. Embankment slopes are limited in these plates to those between 1 vertical on 2 horizontal and 1 vertical on 4 horizontal. The stability factor is related to shear strength of the soil by values of developed angles of internal friction ϕ_D for the embankment and foundation between 0 and 25 deg, with no restrictions as to developed values of cohesion. The critical arc

originates on the slope opposite that under investigation and emerges at or beyond the toe of the embankment, depending on the relative thickness of the impervious embankment and foundation layer. (The method given in this section is not suitable for cohesionless embankments on clay foundations.) The following example illustrates the use of the charts.

Example: A homogeneous earth embankment, 120 ft high, is to be constructed on a clay foundation, 40 ft thick, underlain by bedrock. The unit weight of the foundation and the unit weight estimated for the compacted embankment are 110 lb per cu ft. Results of Q tests indicate that a design shear strength of $c = 950$ lb per sq ft, $\tan \phi = 0.165$ may be used for the foundation and embankment. What slope having a factor of safety of 1.3 should be used as a basis for a detailed analysis of the end-of-construction condition? The values to be used in the appropriate design charts are as follows.

$$\frac{D}{H} = \frac{40}{120} = 0.33$$

$$c_D = \frac{950}{1.3} = 731 \text{ lb per sq ft}$$

$$\tan \phi_D = \frac{0.165}{1.3} = 0.127 \text{ and}$$

$$\phi_D = 7.2 \text{ deg}$$

$$\text{Stability factor } N_s = \frac{\gamma H}{c_D} = \frac{110 \times 120}{731} = 18$$

From plate IV-4, the stability chart for $D/H = 0.25$, the slope corresponding to a stability factor of 18 and a $\tan \phi_D$ of 0.127 is approximately 1 on 3.30; from plate IV-3, the stability chart for $D/H = 0.50$, the slope is found to be 1 on 3.55. By interpolation, an embankment slope of 1 on 3.38 is indicated for $D/H = 0.33$. Thus, an embankment slope of 1 on 3.5 may be chosen for more detailed analysis.

b. The design charts are limited to cases where the embankment and foundation soils have similar unit weights and shear strengths. Otherwise, weighted averages are required and a trial failure arc must be selected. Such a refinement is not considered justified since the effort involved can be more appropriately used in detailed stability analyses.

3. Embankment on Shallow Clay Foundations Overlying a Rigid Boundary. The outer slopes of a symmetrical embankment of cohesionless material resting on a shallow clay foundation overlying a rigid boundary, as shown in plate IV-6, can be approximated from figure 1 in plate IV-7. This chart utilizes an active earth pressure coefficient K_A corresponding to the ratio of the horizontal to vertical earth pressures at the center of the dam. Figure 2 in plate IV-7 gives values of K_A for a horizontal ground surface and for negative slopes (i.e. reverse slope on opposite side of embankment). A design slope can be estimated by determining a value of K_A from figure 2 of plate IV-7 for an assumed embankment slope and substituting this trial value of K_A in figure 1 to obtain a value of the stability number $N_K = \frac{b\,c_D}{\gamma H}$ and a corresponding slope. This slope can then be used to determine a second trial value of K_A from figure 2, if necessary, and a revised stability number and slope from figure 1. A few trials are adequate, as the value of K_A changes slowly for small changes in slope angles and the stability number is relatively insensitive to small changes in K_A. The stability chart in figure 1 of plate IV-7 assumes that the thickness of plastic foundation soil is small. The shear strength of the foundation soil corresponds to the Q shear strength and is expressed in terms of an equivalent cohesion c. The shear resistance along the failure plane in the embankment is taken into account by the earth pressure coefficient. The following example illustrates the use of the chart.

Example: A homogeneous embankment, 100 ft high, having a shear strength corresponding to an angle of internal friction of 28 deg and a unit weight of 120 lb per cu ft is to be constructed on a layer of clay, 10 ft thick, having a shear strength of 1200 lb per sq ft. What approximate slope should

be used in an analysis of the stability of the dam for a factor of safety of 1.3? The developed angle of internal friction ϕ_D of the embankment is 22 deg $\left(\tan \phi_D = \frac{0.532}{1.3} = 0.409\right)$. The developed cohesion c_D of the foundation is $\frac{1200}{1.3} = 923$ lb per sq ft. The ratio of D/H is 0.1. As a first trial, the value of K_A, assuming a slope of 1 on 4-1/2, is 0.40. From figure 1 of plate IV-7 for D/H = 0.1 and $K_A = 0.40$, the stability number N_K is 0.300. Solving for b in the equation

$$N_K = \frac{b\,c_D}{\gamma H} \quad \text{or} \quad b = \frac{N_K\,\gamma H}{c_D}$$

$$b = \frac{0.300 \times 120 \times 100}{923} = 3.9$$

Thus, a slope of 1 on 4 may be selected for detailed analysis; additional trial values of K_A are unnecessary.

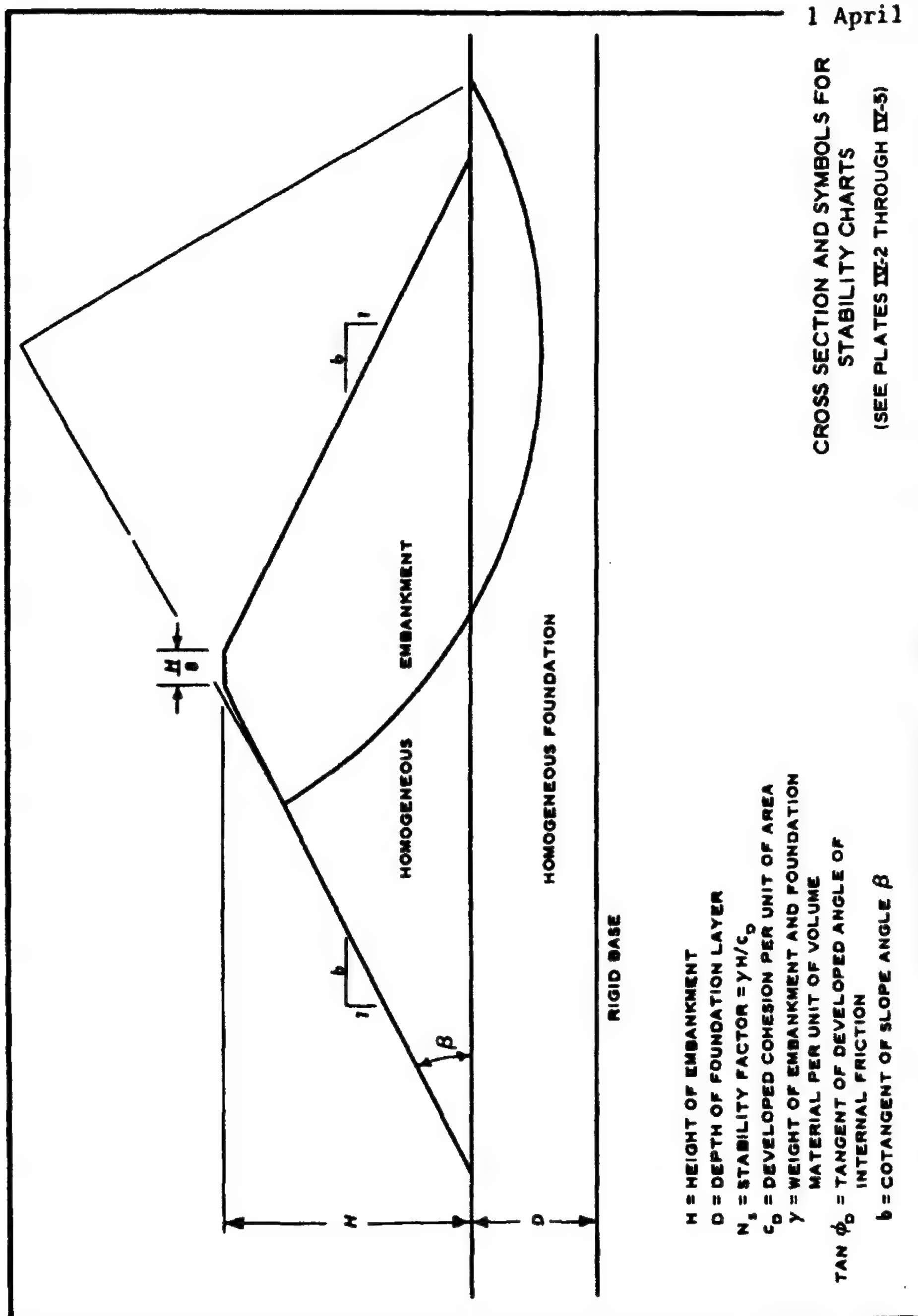

CROSS SECTION AND SYMBOLS FOR STABILITY CHARTS

(SEE PLATES IV-2 THROUGH IV-5)

Plate IV-1

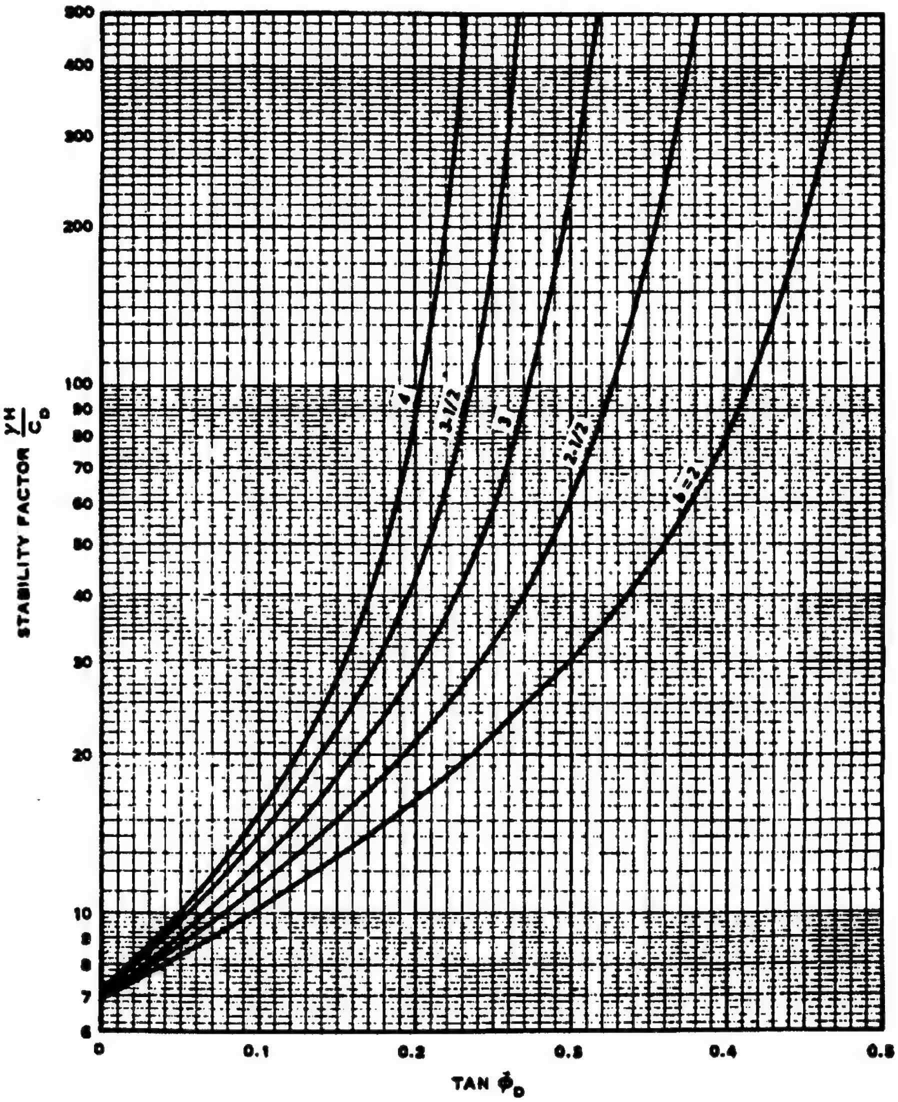

NOTE: SEE PLATE IV-1 FOR DEFINITIONS OF SYMBOLS.

STABILITY CHART FOR HOMOGENEOUS EMBANKMENT AND FOUNDATION.
FOUNDATION DEPTH-EMBANKMENT HEIGHT RATIO, D/H = 1.0

Plate IV-2

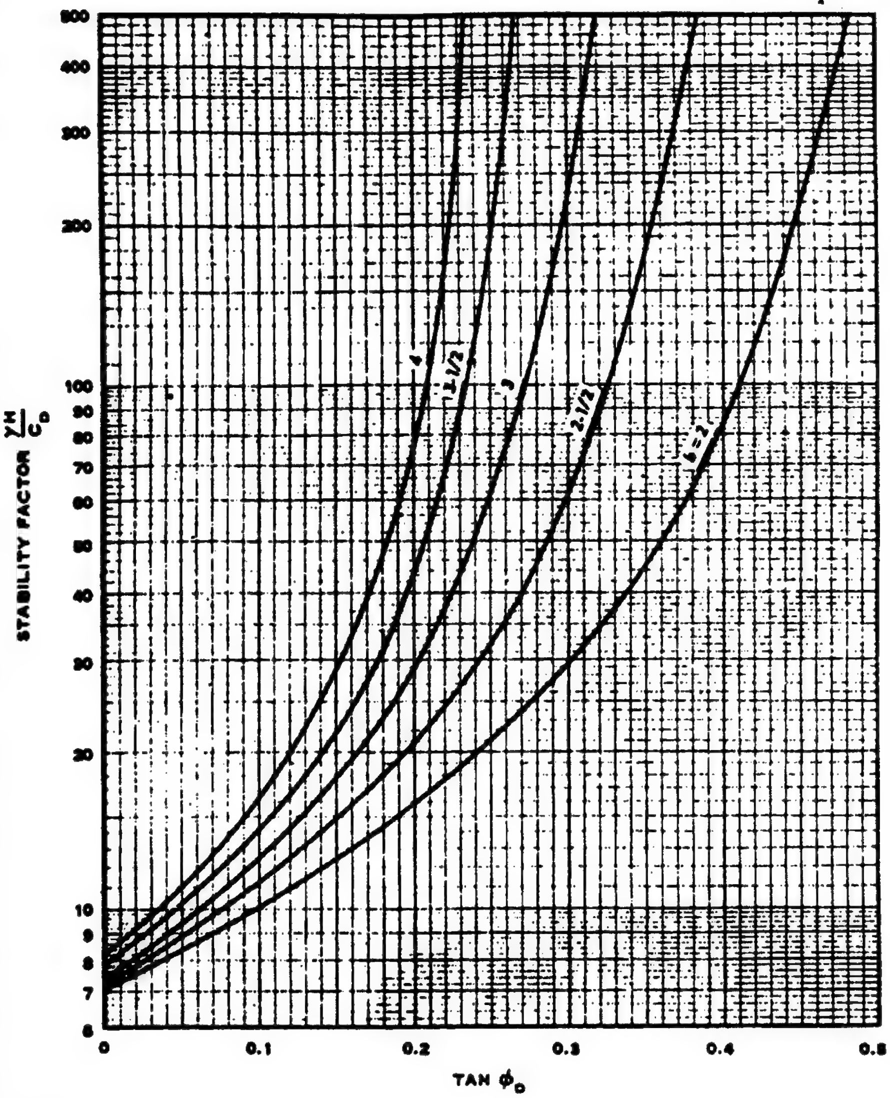

NOTE: SEE PLATE IV-1 FOR DEFINITIONS OF SYMBOLS.

STABILITY CHART FOR HOMOGENEOUS EMBANKMENT AND FOUNDATION

FOUNDATION DEPTH-EMBANKMENT HEIGHT RATIO, D/H = 0.50

Plate IV-3

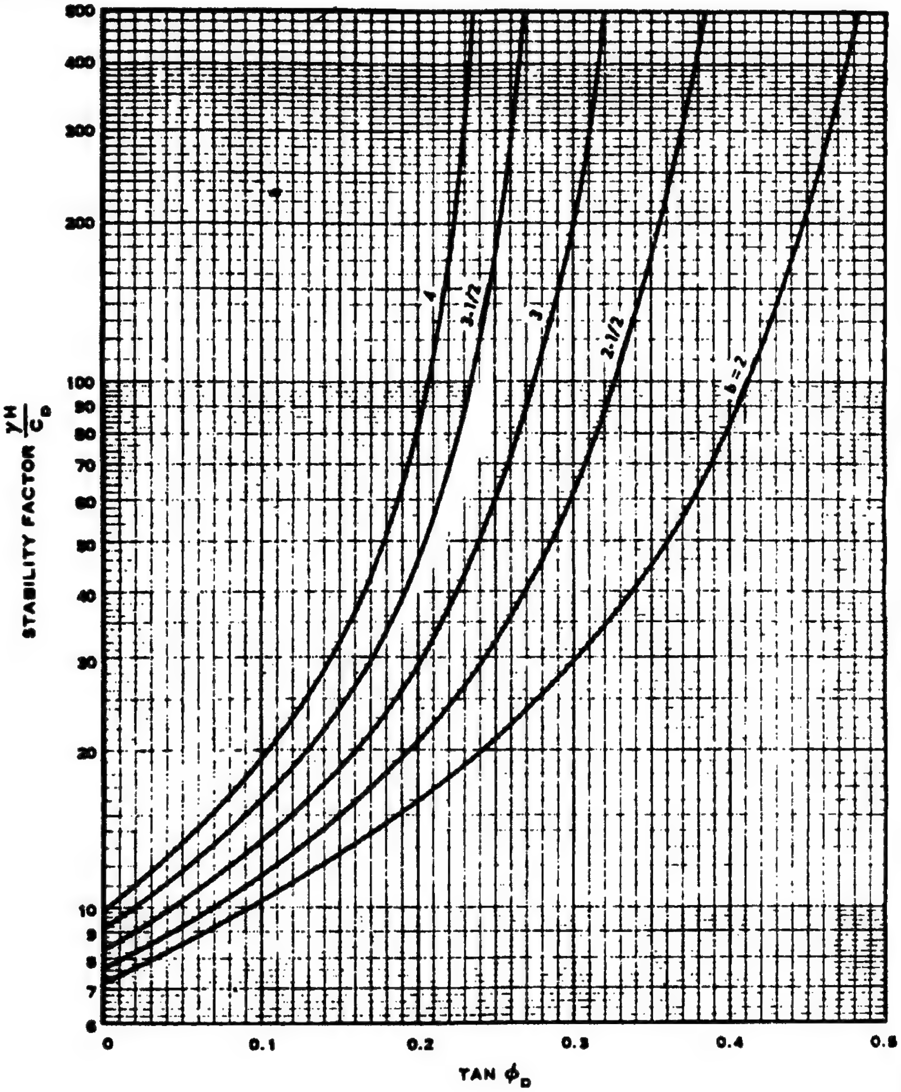

NOTE: SEE PLATE IV-1 FOR DEFINITIONS OF SYMBOLS.

STABILITY CHART FOR HOMOGENEOUS EMBANKMENT AND FOUNDATION

FOUNDATION DEPTH-EMBANKMENT HEIGHT RATIO, D/H = 0.25

Plate IV-4

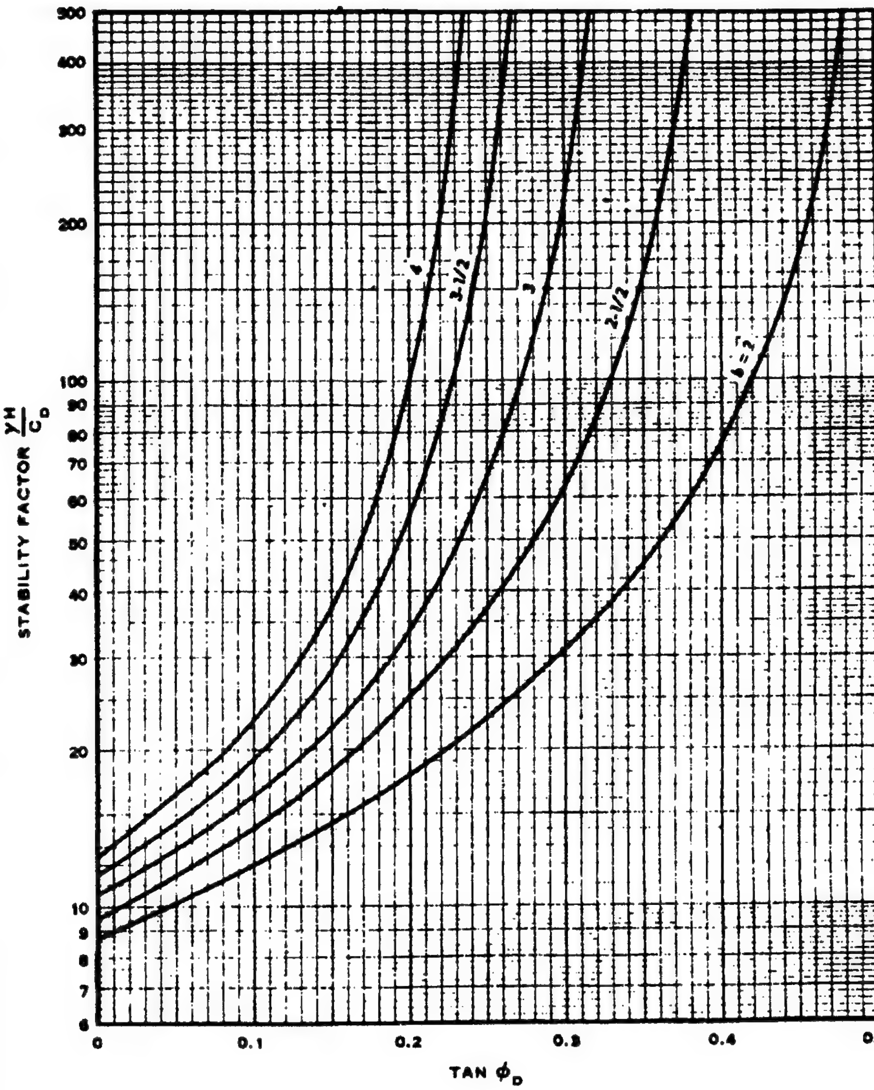

NOTE: SEE PLATE IV-1 FOR DEFINITIONS OF SYMBOLS.

STABILITY CHART FOR HOMOGENEOUS EMBANKMENT AND FOUNDATION

FOUNDATION DEPTH-EMBANKMENT HEIGHT RATIO, D/H = 0

Plate IV-5

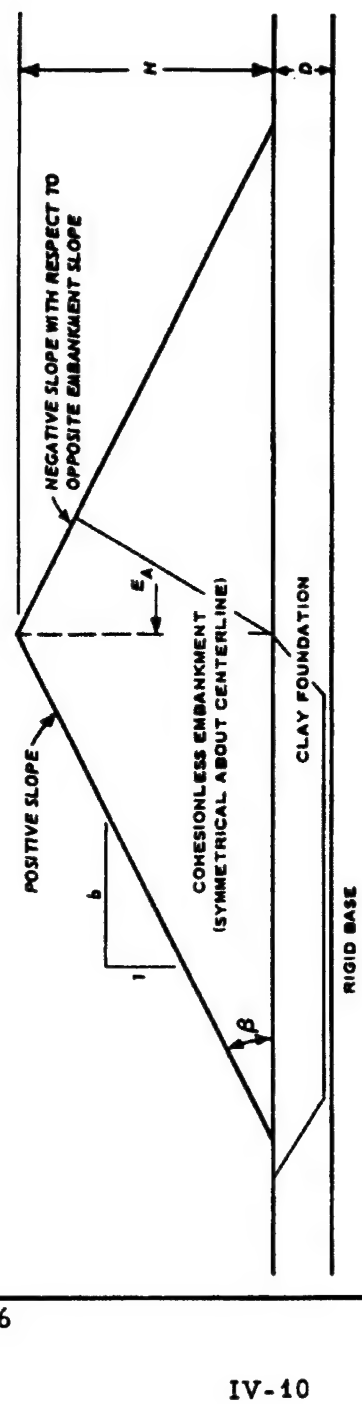

H = HEIGHT OF EMBANKMENT
D = THICKNESS OF CLAY FOUNDATION LAYER
K_A = RATIO OF HORIZONTAL TO VERTICAL EARTH PRESSURES, ACTIVE CASE
b = COTANGENT OF SLOPE ANGLE, β
γ = WEIGHT OF EMBANKMENT AND FOUNDATION MATERIAL PER UNIT OF VOLUME
c = COHESION PER UNIT AREA OF FOUNDATION SOIL

CROSS SECTION AND SYMBOLS FOR STABILITY CHART

(SEE PLATE IV-7)

Plate IV-6

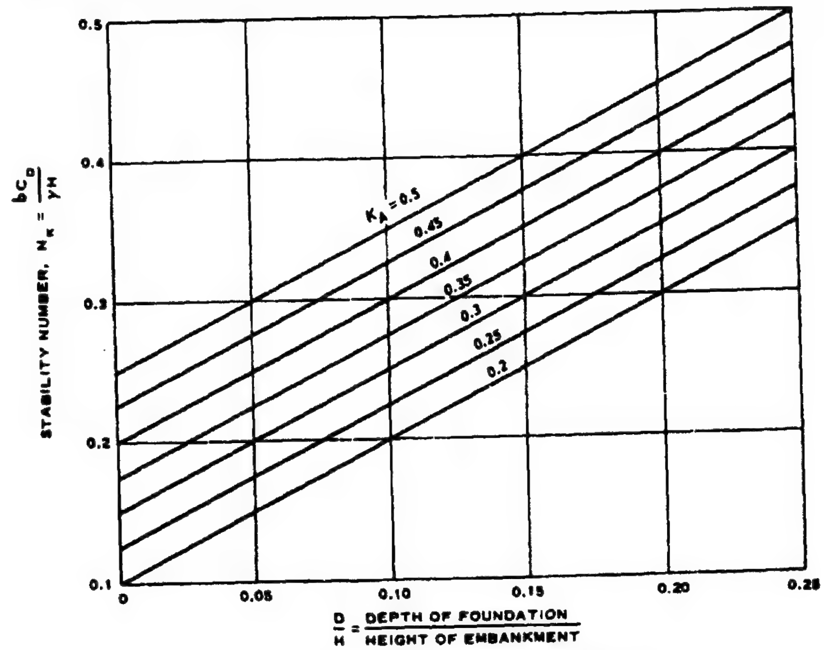

FIGURE 1. N_K VERSUS K_A AND $\frac{D}{H}$

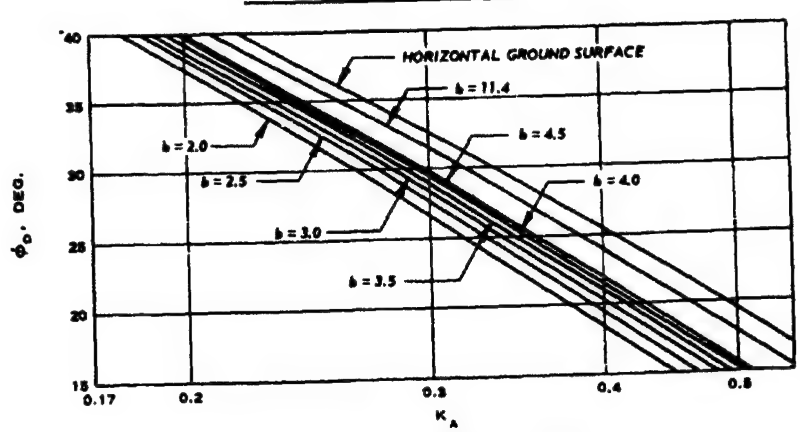

FIGURE 2. ϕ_D VERSUS b AND K_A

**STABILITY CHART FOR
COHESIONLESS EMBANKMENT
ON PLASTIC FOUNDATION**

Plate IV-7

APPENDIX V

Infinite Slope Analysis for Cohesionless Soils

1. Infinite Slope Computations. For cohesionless materials $(c = 0)$, equations applicable to an infinite slope may be used to obtain an estimate of the stability of the slope of an embankment where seepage is involved. It is assumed that the seepage flow is uniform throughout the soil mass.

2. General Case. The safety factor for the general case where seepage flow is neither parallel nor horizontal to the outer slope is

$$F.S. = \frac{\gamma' - (\gamma_w \frac{\tan \alpha}{\cot \beta})}{\gamma_{sat}} \cot \beta \tan \phi$$

where

γ' = submerged unit weight of soil
γ_w = unit weight of water
α = angle between seepage flow line and embankment slope
β = angle of inclination of embankment slope with horizontal $(\cot \beta = b)$
γ_{sat} = saturated unit weight of soil
ϕ = angle of internal friction

3. Seepage Parallel to Slope. For seepage flow parallel to and coincident with the embankment slope $(\alpha = 0)$, the safety factor becomes

$$F.S. = \frac{\gamma'}{\gamma_{sat}} \cot \beta \tan \phi = \frac{\gamma'}{\gamma_{sat}} b \tan \phi$$

where

$b = \cot \beta$

4. Horizontal Seepage. Where seepage flow is horizontal $(\alpha = \beta)$, the factor of safety is

$$F.S. = \frac{\gamma' - \frac{\gamma_w}{\cot^2 \beta}}{\gamma_{sat}} (\cot \beta \tan \phi) = \frac{b^2 \gamma' - \gamma_w}{b \gamma_{sat}} (\tan \phi)$$

5. No Seepage. Where no seepage forces exist, i.e. for a dry slope, the factor of safety is

$$F.S. = \frac{\tan \phi}{\tan \beta} = b \tan \phi$$

6. Earthquake. The effects of an earthquake loading can be applied to all of the previous equations for factor of safety by replacing b with the term b' where

$$b' = \frac{b - \psi}{1 + b_{\psi}}$$

ψ = seismic coefficient (see fig. 6, main text)

7. Example. An example of the influence of the direction of seepage flow on the factor of safety is illustrated in the following tabulation.

	Factor of safety for		
Assumed design values	Seepage parallel to outer slope	Horizontal seepage	No seepage
$b = 3.5$			
$\gamma_{sat} = 2\gamma_w$	1.23†	1.13†	2.45†
$\tan \phi = 0.7$			
$\psi = 0.1$	0.88††	0.74††	1.76††
$b' = 2.52$			

† Without earthquake loading.
†† With earthquake loading.

APPENDIX VI

Modified Swedish Method of Analysis Using Slice Procedure

1. General. The procedures presented in this appendix are for use in making detailed slope stability analyses assuming failure would occur along a circular arc or along a surface of any arbitrary shape. For uniformity and simplicity of presentation, failure is assumed to occur along a trial circular arc. In the modified Swedish method, the sliding mass is divided into slices of either finite or unit width, and a number of trial failure arcs or arbitrary sliding surfaces are investigated to determine which is most critical. An important feature of this method is that earth forces acting on the sides of the slices are considered. The direction of the side forces should be assumed parallel to the average slope of the embankment. Since the side forces are internal forces, they must be balanced to obtain a solution. This requires either the use of analytical procedures using a digital computer to solve a set of simultaneous equations by iteration or the use of graphical procedures involving composite force polygons or graphical integration to balance internal earth forces. The graphical procedures are described in this appendix because of their relative simplicity and clarity. While the modified Swedish method is particularly applicable to homogeneous dams and dikes, it is also used for analyzing zoned embankments. The decision whether to use the modified Swedish method or the wedge method should be based on the stratification or lack of stratification of the soil mass. The circular arcs shown in the examples of this appendix are not necessarily the most critical trial failure surfaces, since the examples have been developed only to illustrate the various methods and procedures.

2. Procedure of Finite Slices. a. Embankment Without Seepage Forces. The sliding mass is divided into a number of slices of convenient width as shown in figure 1 of plate VI-1. Generally, six to twelve slices are sufficient for reasonable accuracy, depending on the embankment zonation and

foundation conditions. A typical slice with forces acting on it is shown in figure 2 of plate VI-1. The force W is the total weight of the slice. The resisting cohesive force C_D is assumed to act parallel to chord AB (fig. 2) and is equal to chord AB times the developed unit cohesion C'_D. The force F_D acting at an angle ϕ_D with the normal to AB is the resultant of the effective normal force at the base and the developed frictional force. Assuming a trial factor of safety, the forces acting on each slice are combined into the composite force polygon shown in figure 3 of plate VI-1, using a convenient force scale and following steps 1 through 5 as outlined below:

(1) Draw the weight vector of the uppermost slice (slice 1).

(2) Draw the developed cohesion vector C_D parallel to the base of the slice.

(3) Draw a line normal to the base of the slice from the upper end of the weight vector.

(4) Construct a line at an angle of ϕ_D from the normal line. This establishes the direction of the vector F_D, the resultant of the normal and frictional forces on the base of the slice.

(5) From the head of the cohesion vector, draw the side earth force vector parallel to the average embankment slope to intersect the resultant vector, thereby closing the force polygon. This establishes the magnitude of the developed vector F_D. The forces on each subsequent slice are then constructed, using the side earth force vector of the previous slice as a base. The composite force polygons must be drawn to a large scale to ensure accurate results, since they are cumulative-type diagrams in which small errors can have a large effect on the error of closure. To obtain the safety factor of balanced external forces, composite force polygons for different trial factors of safety are constructed to determine what safety factor results in closure of the composite force polygon. The errors of closure for each trial composite force polygon are plotted versus the trial factors of safety, as shown in figure 4 of plate VI-1. A smooth curve drawn through the plotted points establishes the factor of safety corresponding to zero error of closure.

b. Sudden Drawdown. Two analyses for each trial failure arc are made for impervious embankments subject to sudden drawdown, one for conditions before drawdown to determine developed normal forces and one after drawdown using the developed normal forces before drawdown. The procedure is illustrated in plate VI-2. A typical slice in an embankment with forces acting before drawdown is shown in figure 1, and corresponding sections of the composite force polygons are shown in figures 2(a) and 2(b) of plate VI-2. In this procedure it is assumed that no seepage has occurred and that the pore pressures acting on the bases of the slices after drawdown reflect the increase in soil weight from submerged to saturated in the drawdown zone. The value of the developed normal force N_D is determined from the before-drawdown analysis and is used in the after-drawdown force polygon, since no increase in developed normal force over the before-drawdown state is considered for an impervious embankment. For any slice with a base located above the upper pool (i.e., the entire slice is composed of material having moist unit weight before and after drawdown), the magnitude of the side earth force determined in the before-drawdown analysis is used in the after-drawdown force polygon. Steps in constructing the composite force polygon before drawdown are the same as those shown in figure 3 of plate VI-1. The magnitude of the developed normal forces is determined from the before-drawdown balanced composite force polygons (zero error of closure) by constructing lines perpendicular to the normal force lines from the tail of the developed friction vectors as shown for one slice in figure 2(a) of plate VI-2. Steps in constructing the after-drawdown force polygon are indicated in figure 2(b). In determining the weight of the slice before drawdown, submerged weights are used for that portion of the slice below the upper pool level. The upper pool level is conservatively assumed to extend horizontally through the embankment to the trial sliding surface. The weight of the slice after drawdown is based on the saturated or moist weight above the upper pool, saturated weight between the upper pool and horizontal extension of the lowered pool, and submerged weight below the lowered pool. When the trial failure

surface is a circular arc, the factor of safety after drawdown can be computed as indicated by the equation in plate VI-2. This eliminates the necessity of constructing the after-drawdown composite force polygon in figure 2(b), plate VI-2. The use of a sudden drawdown flow net for semipervious embankment zones and the procedures for this type of analysis are given in plate VI-11.

c. Embankment with Steady Seepage. In the case of steady seepage as shown in figure 1 of plate VI-3, the water forces acting on each slice must be determined. They can be determined from flow nets or assumed to vary linearly below the saturation line. The forces on typical slices are shown in figure 2 of plate VI-3. To simplify construction of the composite force polygon, the resultant R of the weight and water forces for each slice having a sloping water surface is determined, as shown in figure 3 of plate VI-3. The composite force polygon for one trial factor of safety is shown in figure 4 of plate VI-3. The procedure for determining the factor of safety for zero error of closure is the same as that shown in figure 4 of plate VI-1.

d. Earthquake. To consider earthquake effects in a stability analysis, it is assumed that the earthquake imparts an additional horizontal force F_h acting in the direction of potential failure as discussed in paragraph 11f of the main text. This force is computed from the equation

$$F_h = \psi W$$

where

W = weight of sliding mass
ψ = assumed seismic coefficient

The weight W is based on saturated unit weight below the saturation line and moist unit weight above this line, and does not include the weight of any water above the embankment slope. Figure 6 of the main text can be used as a guide in selecting the seismic coefficient. The horizontal force F_h is computed for each slice and included in the force polygon as shown in

figure 1(a), plate VI-4. In the case of steady seepage, F_h can be combined with the weight and water forces for each slice as shown in figure 1(b), plate VI-4, and the resultant R can be used in the composite force diagram.

e. Use of Composite Strength Envelopes. Stability analyses for sudden drawdown and steady seepage (including partial pool) require the use of composite strength envelopes. The applicable shear strength depends on the developed normal force, which is influenced by the side earth forces. Consequently, the applicable shear strength must be determined by trial and error as the composite force polygon is constructed. In analysis for sudden drawdown, the S strength is assumed as a basis for ϕ_D and the developed normal force is determined for each slice as the composite force polygon is constructed. The developed normal force N_D divided by ΔL is compared with the normal stress value at the intercept of the S and R envelopes to determine if the R or the S strength governs. For the steady seepage analyses (including partial pool), the developed normal force must also be determined in a manner similar to the procedure illustrated in figure 2(a) of plate VI-2. The S strength is assumed as a basis for ϕ_D in the first portion of the composite force polygon, and the resulting developed normal force divided by ΔL is compared with normal stress at the intercept of the S and R envelopes to determine when the $\frac{R + S}{2}$ strength or the S strength governs. Where the failure arc passes through more than one type of soil, applicable values of shear strength are used for each slice.

3. Graphical Integration Procedure. Graphical integration may be used in stability analyses to balance the internal side earth forces and determine the factor of safety for balanced external forces. Vertical slices of unit width are taken at appropriate intervals along the cross section above the trial failure arc or surface of sliding. Using the trial factor of safety, the resultant of the side earth forces $\Delta E'$ determined from the force polygon for each unit width slice is plotted to form an area diagram. A sufficient number of unit width slices must be used to define accurately the area diagram. $\Delta E'$, which is the resultant of the earth forces acting on the left and right

sides of the unit width slice, is assumed to act parallel to the average embankment slope being analyzed. The trial factor of safety for which the net area of the $\Delta E'$ diagram is zero is the factor of safety for a balance of external forces for the sliding surface being analyzed.

a. Embankment Without Seepage. If the soil mass is not homogeneous with respect to density, the cross section above the arc may be transformed into an equivalent section of uniform density for use in obtaining force polygons (in units of feet) for the unit width slices. This procedure is illustrated in figure 1 of plate VI-5. The height of the equivalent section h' at any point is equal to the height of a unit slice times the ratio of the unit weight of embankment soil in the slice to the unit weight used as a base. Where a slice includes two or more soil types having different unit weights, h' is obtained by adding together the incremental height of each soil type times its unit weight divided by a selected base unit weight γ_{base}. The unit weight of water is often used as the base, but where more convenient the unit weight of one of the soil strata or zones may be used. The force polygon (in units of feet) is constructed for each unit width slice as illustrated in figure 1 of plate VI-5 using the following steps:

(1) Construct h'.

(2) Draw $C'_D = \frac{c}{F.S.} \times \frac{1}{\gamma_{base}} \times \frac{1}{\cos\theta}$ at the base of the width slice h'

(3) Construct a normal line from the head of C'_D.

(4) Construct a resultant friction and normal force vector at an angle of ϕ_D from the normal.

(5) Construct $\Delta E'$ from the top of the unit width slice h' to intersect the friction vector.

(6) The magnitude of F'_D is defined by step 5.

(7) Construct a line from the intersection of F'_D and $\Delta E'$ perpendicular to the normal. This step defines the developed normal force N'_D and $N'_D(\tan\phi_D)$.

The embankment section must be drawn to a large scale so that the force

polygons for each unit slice can be constructed accurately. A plot of $\Delta E'$ for each unit slice is then made as shown in figure 2 of plate VI-5. It should be noted that the force polygons for each unit slice are continuous vector plots in either a clockwise or counterclockwise direction so that $\Delta E'$ acts toward the crest in the upper part of the embankment section and toward the toe near the bottom of the embankment section. Consequently, in the area diagram in figure 2 of plate VI-5, minus and plus areas are obtained. When these two areas are equal, the summation of $\Delta E'$ equals zero and the corresponding factor of safety is correct for the sliding surface being analyzed, corresponding to balanced internal forces. It is useful to note that using a lower factor of safety increases the size of the $-\Delta E'$ area and decreases the size of the $+\Delta E'$ area. The areas can be measured, using any arbitrary units, by planimeter or approximated by Simpson's rule. A plot of $\Sigma \Delta E'$, which is the net area of the area diagram, versus trial factors of safety as shown in figure 3 of plate VI-5, can be used to determine the factor of safety for balanced internal forces. The graphical integration procedure requires substantially less time to complete manually than the finite slice procedure (except for the sudden drawdown analysis), and various techniques can be utilized to reduce further the time required. For example, proportional dividers (or a slide rule) can be used when constructing the equivalent section of uniform density shown in figure 1 of plate VI-5. Dividers can be used to transfer $\Delta E'$ vectors to the area diagram.

b. Sudden Drawdown. The use of the graphical integration procedure for sudden drawdown requires two analyses for an impervious embankment, as in the finite slice procedure. The cross section of the embankment above the trial failure arc is transformed into an equivalent section for conditions before drawdown and also for conditions after drawdown as shown in figure 1 of plate VI-6. For conditions before drawdown, moist or saturated unit weights are used above the upper pool level and submerged weights are used below this level. The unit slice force polygon before drawdown is shown in figure 2(a) of plate VI-6. The developed normal stress, using ϕ_D based on

the S strength, must be compared with the normal stress at the intersection of the S and R envelopes to determine if the R or S strength governs. The developed normal stress is determined by multiplying the developed normal force for N'_D by $\gamma_{base} \cos \theta'$. An area diagram and a plot of $\Sigma \Delta E'$ versus trial factors of safety similar to that shown in plate VI-5 are used to determine the factor of safety for balanced side forces. After drawdown, the magnitude of h' is increased to include the weight of water in the embankment between the upper pool and drawdown pool. The values of the developed normal force N'_D found from the condition before drawdown (where $\Sigma \Delta E' = 0$) are used in the unit force polygons for conditions after drawdown as shown in figure 2(b) of plate VI-6. The factor of safety for balanced side forces with $\Sigma \Delta E' = 0$ before drawdown will be greater than the factor of safety for balanced forces with $\Sigma \Delta E' = 0$ after drawdown. Consequently, separate sections and diagrams should be used for the two analyses to minimize possible errors. The above-described procedure must be performed for each trial failure surface investigated. The procedures for this type of analysis are given in plate VI-12.

c. Embankment with Seepage. (1) Water forces on the sides and base of each slice of unit width influence the effective normal force on the base of the slice, as shown in figures 1 and 2 of plate VI-7. The influence of these forces can be accounted for in any appropriate manner, but the following procedure simplifies the computations required. The variation of water pressure with depth is assumed to be the same on both sides of the slice (fig. 1(a)). Therefore, the total forces, U_L and $U_R - U_1$, are equal and opposite and cancel each other. Note that force $U_R - U_1$ applies to that portion of the right side of the slice from the saturation line to a line parallel to it, as shown in figure 1(a), and U_1 applies to the remaining portion of the side of the slice. Although the resultant U of all water forces acting on the slice can be determined from forces U_1 and U_2 alone as shown in figures 1(b), 1(c), and 1(d), it is not necessary to compute these forces separately to determine the resultant force U; however, this can be done if desired.

(2) It can be shown that the resultant force U' (i.e. U/γ_w) acts in a direction perpendicular to the saturation line. This makes it possible to use the simple graphical procedure illustrated in figure 2(a) of plate VI-7 for determining both the magnitude and direction of the resultant force U without determining either U_1 or U_2. The graphical determination of (a) the developed friction force F'_D, (b) the developed normal force on the base of the slice N'_D, and (c) the resultant side earth force on the slice $\Delta E'$ are illustrated in figure 2(b). This construction is valid only when the unit weight of water is used as the base unit weight in the unit slice procedure. Details required for verifying the validity of this procedure are shown in figure 1 of plate VI-7. The $\Delta E'$ forces are plotted and summed as shown in plate VI-4 to obtain the correct safety factor, which corresponds to $\Sigma \Delta E' = 0$.

(3) In analyses for steady seepage (including partial pool) using the graphical integration procedure, the developed normal force multiplied by $\gamma_w \cos \theta$ must be compared to the normal stress at the intersection of the S and R envelopes to determine when the S and $\frac{R + S}{2}$ strength governs. When the trial sliding surface passes through different materials, the appropriate composite strength envelope should be used for each material.

d. Earthquake. For the earthquake case it is assumed that the earthquake imparts an additional horizontal force F_h acting in the direction of potential failure as discussed in paragraph 11f of the main text and in paragraph 2d. The force F_h should be computed for each unit slice and added to the force polygons of the unit slices as shown in figure 2, plate VI-4. Note that in the equation $F_h = \psi h'$ (total), the term h' (total) is equal to the equivalent height for the total weight of the soil mass in the unit slice based on the saturated unit weight below the water table and moist unit weight above the water table. This equivalent height is not the same as the effective equivalent height h' (effective) based on submerged unit weight below the saturation line and moist unit weight above it.

4. End of Construction--Case I.† Unit weights and shear strengths used in analyzing this condition should correspond to those expected at the end of construction as discussed in paragraph 9 of the main text. Examples of stability analysis for the end of construction condition using the finite slice procedure and the graphical integration procedure are given in plates VI-8 and -9, respectively. Additional analyses should be made during construction using results of field instrumentation measurements and of tests on record samples where high pore water pressures are measured. This is further discussed in Appendix VIII.

5. Sudden Drawdown--Cases II and III. Appropriate unit weights, shear strengths, and design assumptions to be used in sudden drawdown analyses are described in paragraph 11b of the main text. In some extreme cases where a rapid drawdown condition is possible before pore water pressures developed during construction are dissipated, an appropriate reduction in effective stresses should be made using excess pore water pressures expected at the time of rapid drawdown.

a. Finite Slices. (1) Plate VI-10 shows an example of computations for a trial failure arc using slices of finite width for the sudden drawdown case of a homogeneous dam of impervious material. For each trial arc two analyses are required, one to determine the normal forces that develop before drawdown and the second to determine the factor of safety of the slope after drawdown using the normal forces determined in the first analysis. Submerged unit weights below the maximum pool are used for the "before-drawdown" condition; saturated unit weights in the drawdown zone and submerged unit weights below the minimum pool level are used for the "after-drawdown" condition. For the before-drawdown analysis, trial factors of safety are assumed, and errors of closure are determined until a factor of safety for approximate zero closure is found (fig. 3). The force polygon for the zero error of closure is then constructed as shown in figure 4, and the

† Case designations are those described in paragraph 11 of the main test.

normal forces from this force polygon are used for computing the factor of safety for the after-drawdown condition, as shown in tabular form in plate VI-10. The factor of safety after drawdown is determined from the equation shown in plate VI-2.

(2) The effect of seepage forces must be considered in stability analyses of upstream slopes of semipervious soils. In these cases, a drawdown flow net can be used in conjunction with saturated unit weights to determine effective normal stresses and forces as shown in plate VI-11. The water forces on the sides and base of each slice are determined from the flow net. The resultant R of the weight and water forces for each slice (fig. 4, plate VI-11) is used to construct the force polygon (fig. 5). Saturated unit weights are used below the minimum pool level, and it is necessary to consider the water on the outer slopes as part of the slice. In this way, both the weight of water above the slice and the water forces on the sides of the slice can be evaluated. Seepage forces may create a more critical condition near the lowered pool level than is shown by failure arcs through the top of the embankment, and additional analyses for failure arcs emerging part way up the upstream slope may be desirable. Such analyses should consider the riprap as a free-draining material.

b. Graphical Integration Procedure. Plate VI-12 shows computations for a trial failure arc using the graphical integration procedure for the sudden drawdown case of a homogeneous dam of impervious material. Two analyses are required for each trial arc, as in the finite slice procedure. The developed normal forces N'_D for before-drawdown condition are used to construct the after-drawdown force polygons. The factor of safety for the trial arc was determined using the following steps:

(1) Before-Drawdown Analysis. Trial factors of safety were assumed and the net area of the $\Delta E'$ diagram $(\Sigma \Delta E')$ was determined for each trial until a factor of safety for $\Sigma \Delta E' = 0$ was found (fig. 4a, plate VI-12). Shear resistance along the base of each slice of unit width corresponds to the S or R strength, depending on the effective normal stress $(N'_D \cos \theta)$ on the base

of the slice. The shear strength developed along the arc was determined by plotting the developed normal stresses, $N'_D \cos\theta$, determined using the S strength, as shown in figure 2a, plate VI-12. (In this example problem, the S strength was used when the value of $N'_D \cos\theta$ was less than $\frac{4.150 \text{ kips per sq ft}}{0.073 \text{ kips per cu ft}} = 57$ ft.)

(2) Using the factor of safety found in paragraph 5b(1) above for $\Sigma\Delta E' = 0$, corresponding force polygons for before-drawdown conditions were constructed and values of N'_D were determined.

(3) Values of N'_D from paragraph 5b(2) above were then used to construct force polygons for the after-drawdown analysis. The factor of safety for after drawdown was determined by assuming trial factors of safety and determining the net area of the $\Delta E'$ diagram for each trial until a factor of safety for $\Sigma\Delta E' = 0$ was found (fig. 4b, plate VI-12).

6. Partial Pool, Upstream Slope--Case IV. The critical pool elevation is found by determining the critical failure surfaces for various pool levels. If the assumed failure surface is a circular arc, the surface of the pool should intersect the embankment slope directly below the center of the arc for the first trial. The radii of the trial circular arcs are varied until the critical radius is determined. Subsequent trials should be made with the pool above and below this level.

a. Finite Slices. A stability analysis for Case IV using slices of finite width is shown in plate VI-13. Moist weights are used for the materials above pool level and submerged unit weights are used for materials below pool level. A composite of the S and $\frac{R+S}{2}$ design shear strength envelopes is used in computing the shear strength along the assumed failure arc. A number of different pool levels should be analyzed for each trial arc to determine the most critical pool level and factor of safety, and the process repeated for other trial arcs.

b. Graphical Integration Procedure. A stability analysis for Case IV using the graphical integration procedure is illustrated in plate VI-14, using the same section and trial arc as in plate VI-13. In figure 1, the section

above the trial arc is converted into an equivalent embankment of uniform density using the submerged weight of the foundation soil as the base unit weight. The correct shear strength used can be determined by plotting values of $N_D' \cos\theta$ as shown in figure 2. There are slight differences in factors of safety between plates VI-13 and -14. These differences are attributed mainly to small differences in measurements of the small-scale diagrams.

7. Steady Seepage, Downstream Slope--Cases V and VI. A simplifying and conservative assumption often made in this analysis is that the curve of piezometric pressures along the failure arc coincides with the saturation line. However, it may be desirable to construct a flow net to determine more closely the piezometric pressures along the failure arc.

a. Finite Slices. A stability analysis for Case V using slices of finite width is shown in plate VI-15. The method of computing the forces on a finite slice is the same as that using water forces as discussed in paragraph 2c of this appendix. In this example, the water forces are assumed to vary linearly below the saturation line. Where a surcharge pool exists above the steady seepage pool (Case VI), the weight of water due to the surcharge pool must be added to those slices upon which it acts. The procedure for determining shear resisting forces using composite strength envelopes is given in paragraph 2e.

b. Graphical Integration Procedure. A stability analysis for Case V using the graphical integration procedure is illustrated in plate VI-16 using the same section and trial arc as in plate VI-15. In figure 1, plate VI-16, the height of the soil above the failure arc is converted into equivalent height of material having a unit weight equal to water for convenience in handling water pressures. Unit width slices are selected at intervals where changes in boundary conditions occur. The slight difference in factors of safety between plates VI-15 and -16 is attributed mainly to small differences in measurements of the small-scale diagrams. In Case VI the equivalent height is increased accordingly for those unit slices that pass through the surcharge pool.

8. <u>Earthquake--Case VII.</u> This case consists of an analysis of Case I, Case IV, or Case V with seismic loadings included. The analysis can be made by using either effective or total stresses, but only total weights are used to compute the earthquake force F_h.

a. <u>Finite Slices.</u> A stability analysis for Case VII using the finite slice method is shown in plate VI-17. In this example, Case V (steady seepage) is analyzed under earthquake conditions. The procedure of analysis is basically the same as that followed in the Case V example in plate VI-15 except that the horizontal earthquake force F_h is added.

b. <u>Graphical Integration.</u> An example analysis for Case VII using the graphical integration method is presented in plate VI-18. In this example, Case I (end of construction) is analyzed with an earthquake loading. The only difference in this example and the example of Case I given in plate VI-9 is that the horizontal earthquake force F_h' is added to the force polygon. Moist and saturated unit weights are used in computing F_h' while moist and submerged unit weights are used in computing the equivalent height h'.

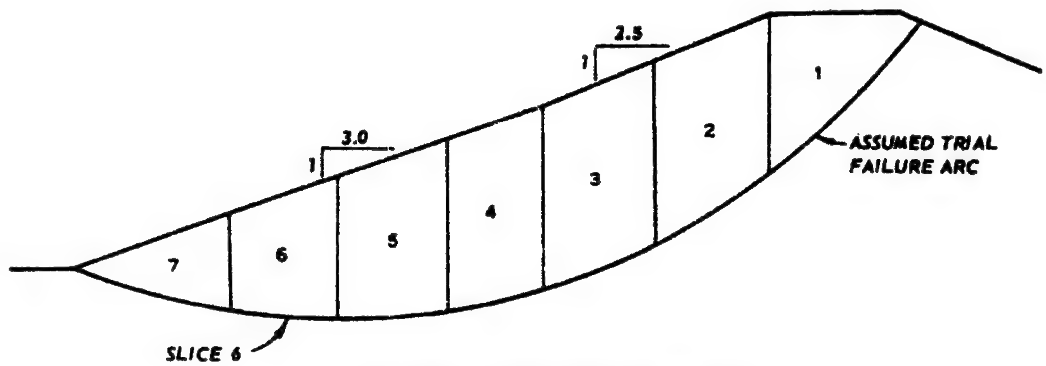

FIGURE 1. EMBANKMENT SECTION

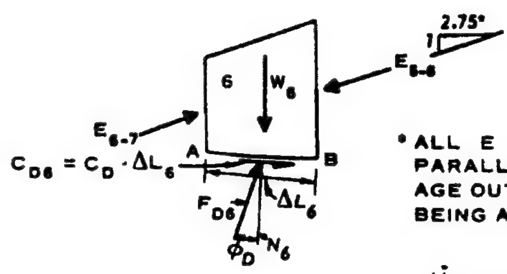

FIGURE 2. SLICE 6 WITH FORCES

* ALL E FORCES ARE PARALLEL TO AVERAGE OUTER SLOPE BEING ANALYZED.

(1) THROUGH (5) ARE STEPS IN CONSTRUCTION

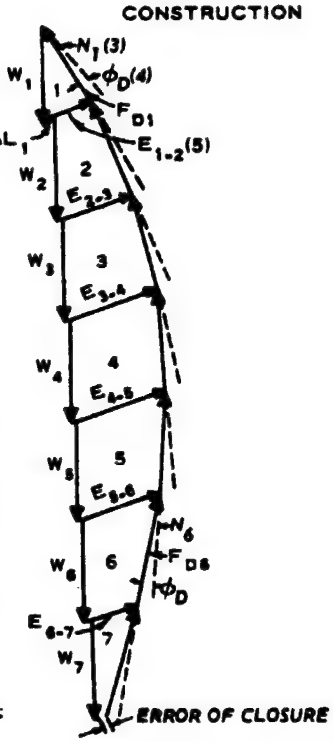

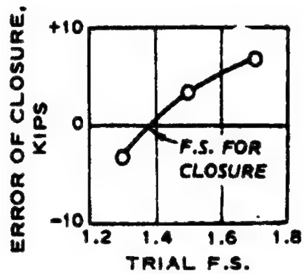

FIGURE 4. TRIAL F. S. VERSUS ERROR OF CLOSURE

FIGURE 3. COMPOSITE FORCE POLYGON FOR ONE TRIAL F. S.

LEGEND

W = WEIGHT OF SLICE
E = EARTH FORCE ON SIDE OF SLICE
N = NORMAL TO BASE OF SLICE
ΔL = LENGTH ACROSS BASE OF SLICE
C_D = DEVELOPED COHESION FORCE
F_D = RESULTANT OF NORMAL AND DEVELOPED FRICTION FORCE
ϕ_D = DEVELOPED ANGLE OF INTERNAL FRICTION OF SOIL

$C_D = \frac{C}{F.S.}, \quad \phi_D = \text{ARC TAN} \frac{\text{TAN}\,\phi}{F.S.}$

MODIFIED SWEDISH METHOD
FINITE SLICE PROCEDURE
NO WATER FORCES

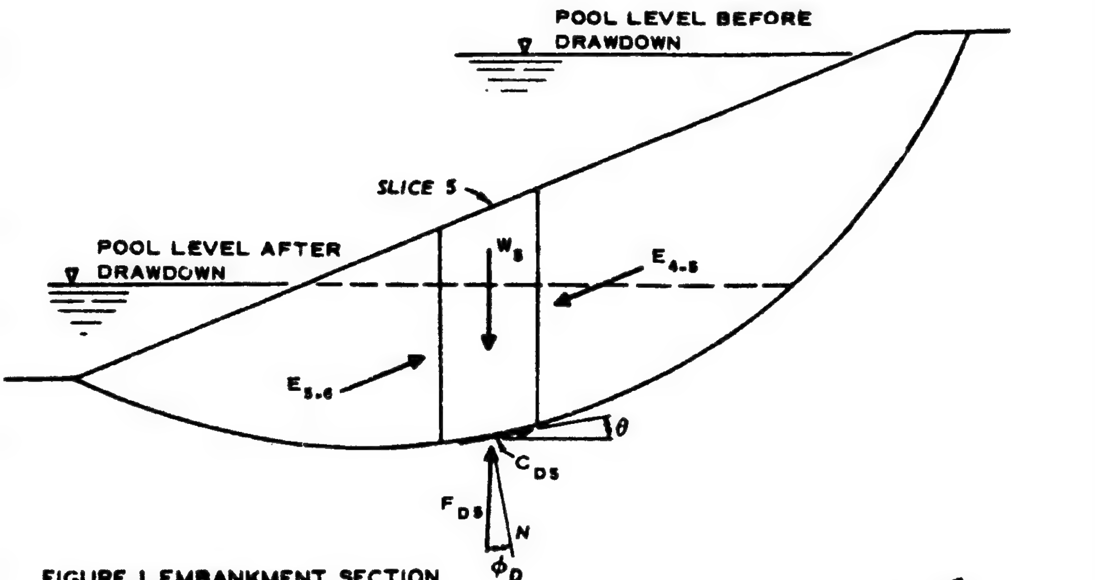

FIGURE 1. EMBANKMENT SECTION AND FORCES ON TYPICAL SLICE BEFORE SUDDEN DRAWDOWN

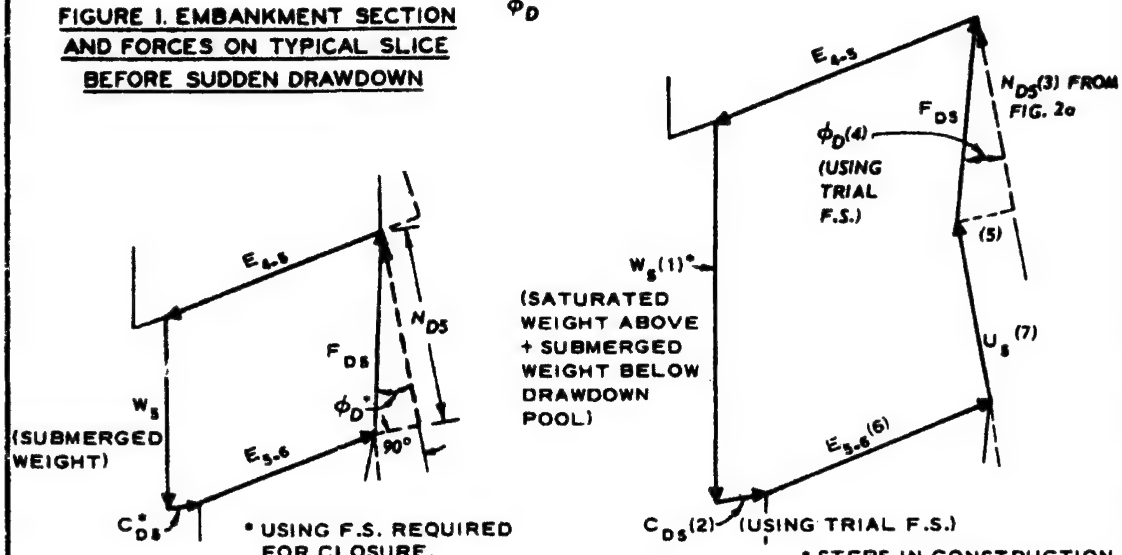

a. BEFORE DRAWDOWN

b. AFTER DRAWDOWN

FIGURE 2. PORTION OF COMPOSITE FORCE POLYGONS

EQUATION FOR F.S. AFTER DRAWDOWN
(ALTERNATIVE PROCEDURE TO 2b)

$$F.S. = \frac{\Sigma N_D \tan\phi + \Sigma C \Delta L}{\Sigma W \sin\theta}$$

N_D = DEVELOPED NORMAL FORCE BEFORE DD
W = WEIGHT OF SLICE AFTER DD
C AND ϕ ARE FOR TOTAL AVAILABLE SHEAR STRENGTH

MODIFIED SWEDISH METHOD
FINITE SLICE PROCEDURE
SUDDEN DRAWDOWN
IMPERVIOUS EMBANKMENT

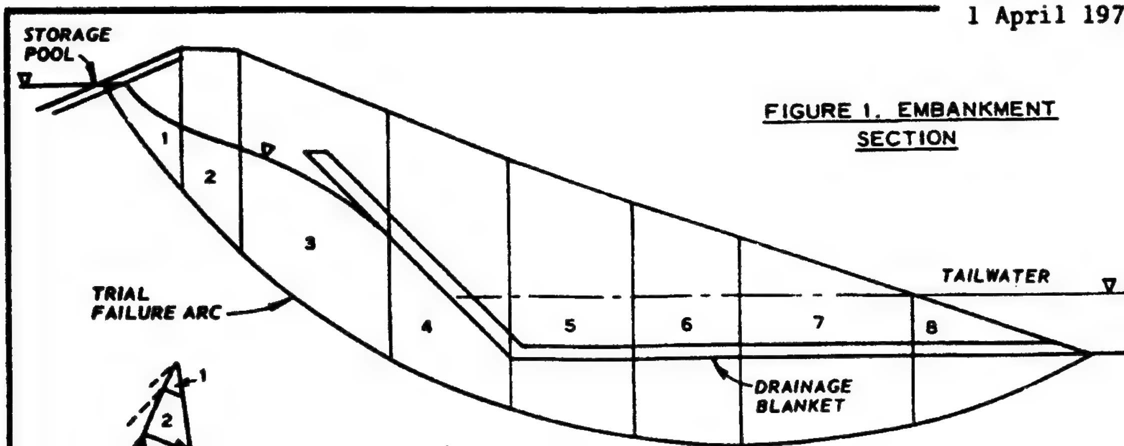

FIGURE 1. EMBANKMENT SECTION

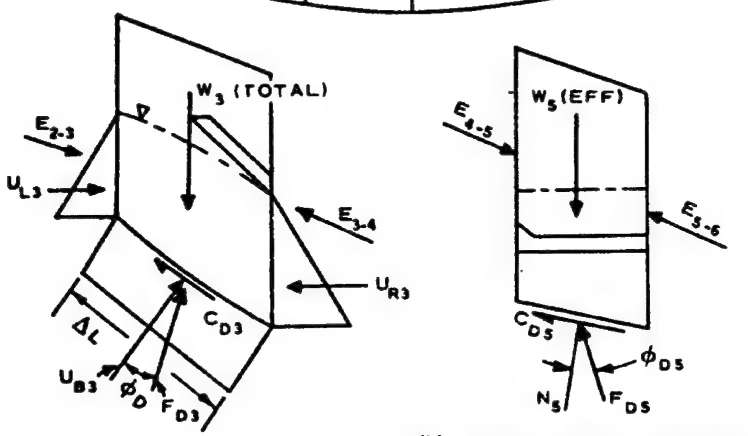

(a) SLICE WITH SLOPING WATER SURFACE

(b) SLICE WITH HORIZONTAL WATER SURFACE

FIGURE 2. FORCES ACTING ON TYPICAL SLICES

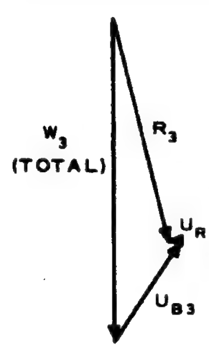

FIGURE 3. RESULTANT OF WEIGHT AND WATER FORCES

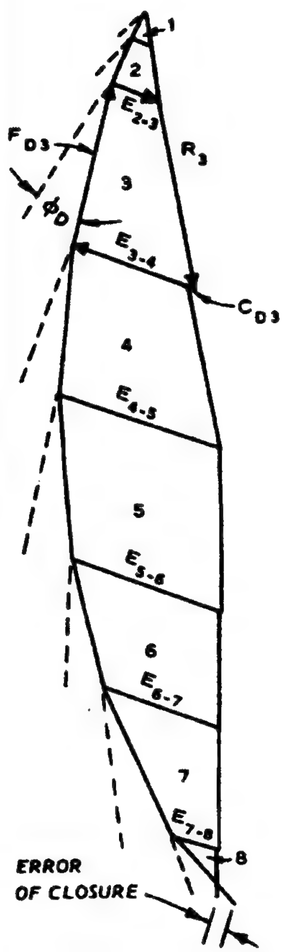

FIGURE 4. COMPOSITE FORCE POLYGON FOR ONE TRIAL F.S.

LEGEND

U_R = WATER FORCE ON RIGHT SIDE OF SLICE
U_L = WATER FORCE ON LEFT SIDE OF SLICE
U_B = WATER FORCE ON BASE OF SLICE

MODIFIED SWEDISH METHOD
FINITE SLICE PROCEDURE
WITH STEADY SEEPAGE
WATER FORCES

Plate VI-3

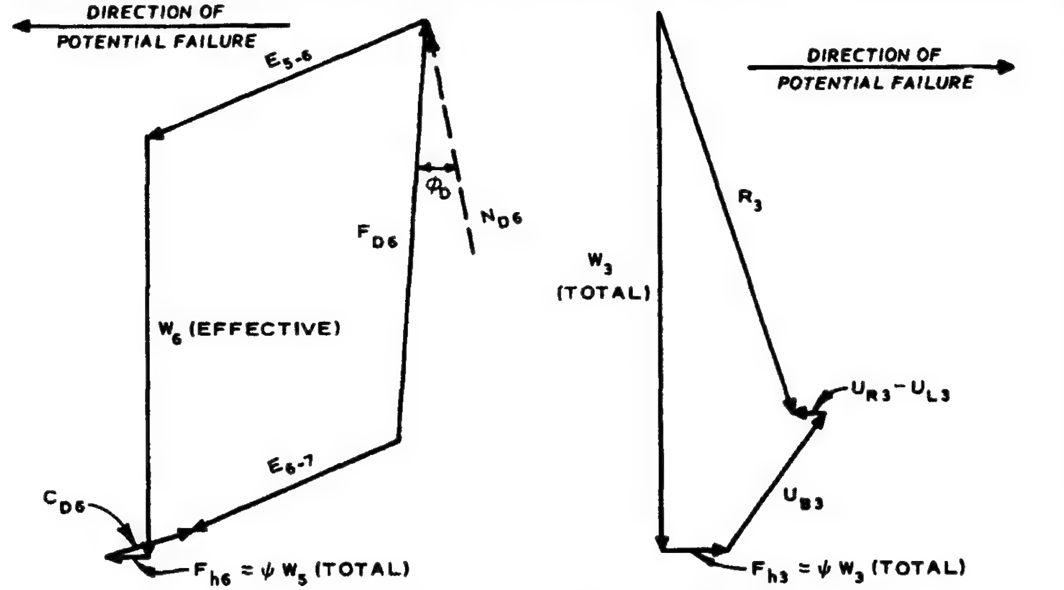

(a) NO SEEPAGE FORCES
(SEE FIG. 3, PLATE VI-1)

(b) WITH SEEPAGE FORCES
(SEE FIG. 3, PLATE VI-3)

FIGURE 1. FINITE SLICE PROCEDURE

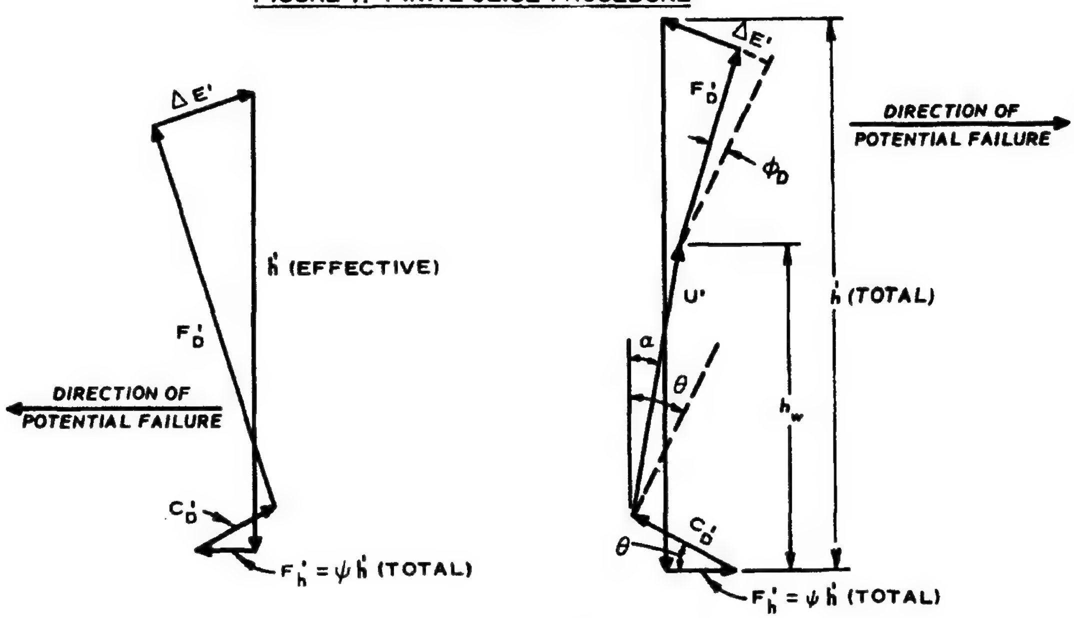

(a) NO SEEPAGE FORCES
(SEE FIG. 1, PLATE VI-5)

(b) WITH SEEPAGE FORCES
(SEE FIG. 2b, PLATE VI-7)

FIGURE 2. GRAPHICAL INTEGRATION PROCEDURE

**MODIFIED SWEDISH METHOD
FINITE SLICE AND GRAPHICAL
INTEGRATION PROCEDURE
EARTHQUAKE LOADING**

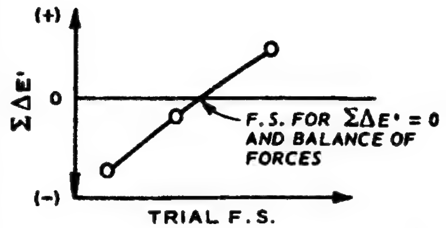

FIGURE 3. $\Sigma\Delta E'$ VERSUS TRIAL F.S.

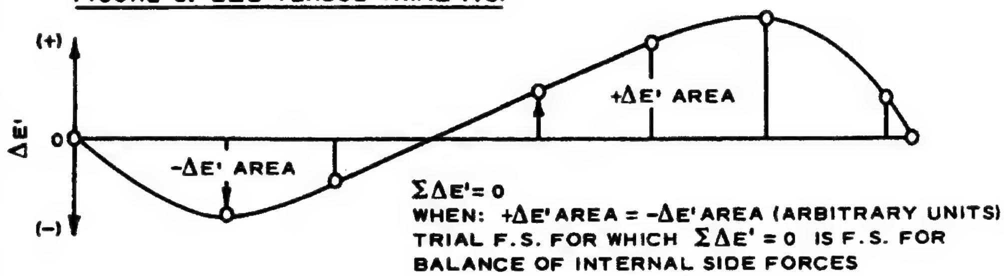

FIGURE 2. ΔE' AREA DIAGRAM

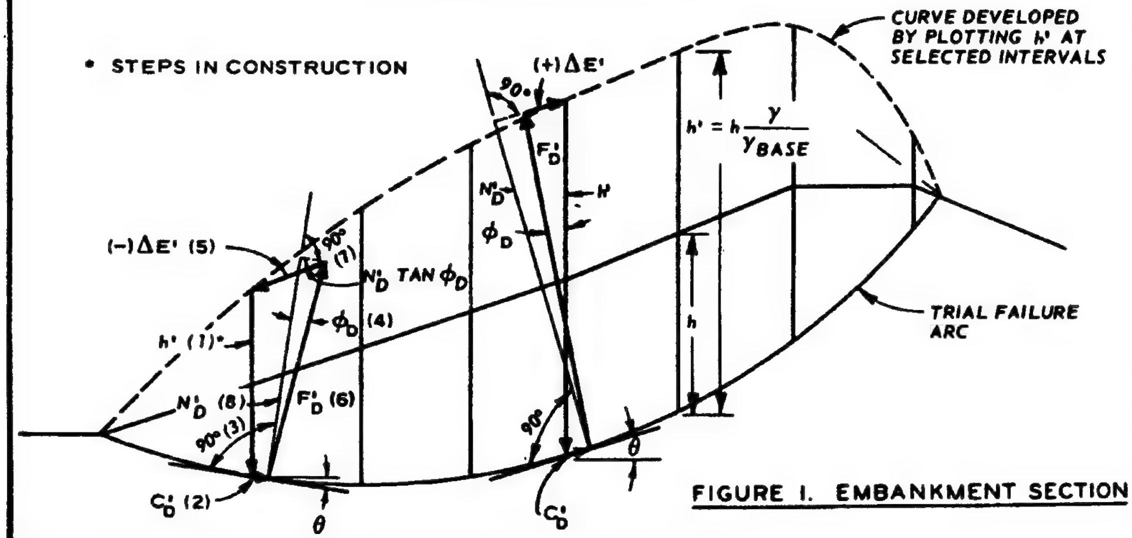

FIGURE I. EMBANKMENT SECTION

NOTE: ALL COMPONENTS OF UNIT SLICE FORCE POLYGON ARE IN UNITS OF FEET SINCE $h' = h \times \frac{\gamma}{\gamma_{BASE}}$

LEGEND

h' = HEIGHT OF UNIT WIDTH SLICE = $h \times \frac{\gamma}{\gamma_{BASE}}$

$\Delta E'$ = INCREMENT OF EARTH FORCE REQUIRED TO BALANCE FORCE POLYGON FOR UNIT WIDTH SLICE

C'_D = DEVELOPED COHESION FORCE = $\frac{C}{F.S.} \times \frac{1}{\gamma_{BASE}} \times \frac{1}{\cos\theta}$

N'_D = DEVELOPED NORMAL FORCE

F'_D = RESULTANT OF DEVELOPED NORMAL AND FRICTIONAL FORCES

ϕ_D = DEVELOPED ANGLE OF INTERNAL FRICTION

θ = ANGLE OF INCLINATION OF TRIAL FAILURE ARC WITH HORIZONTAL

MODIFIED SWEDISH METHOD
GRAPHICAL INTEGRATION
PROCEDURE
NO WATER FORCES

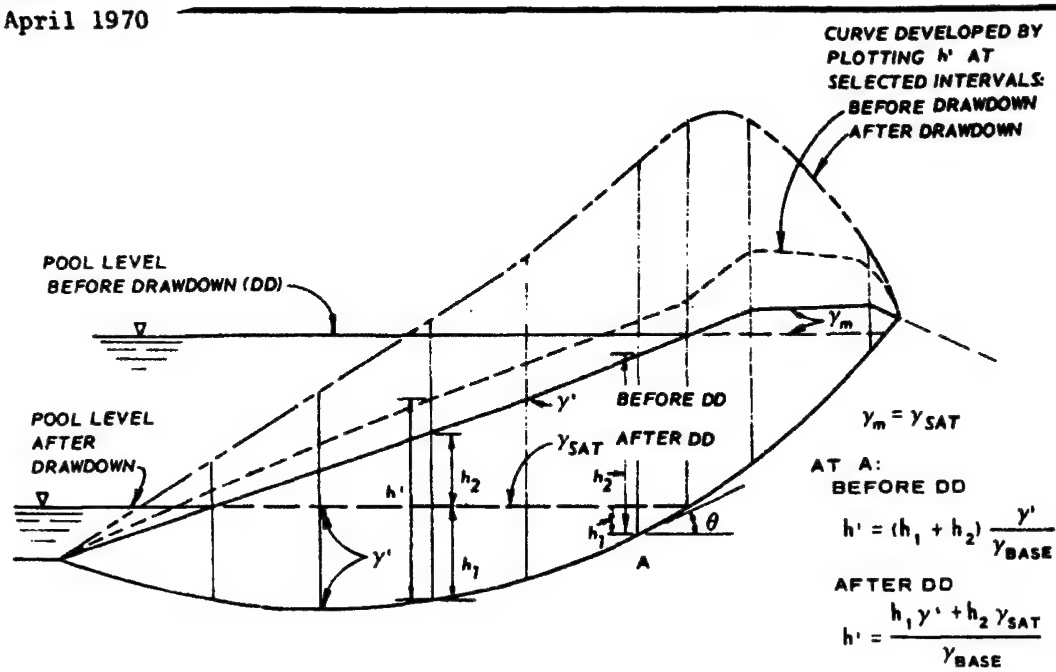

FIGURE 1. EMBANKMENT SECTION

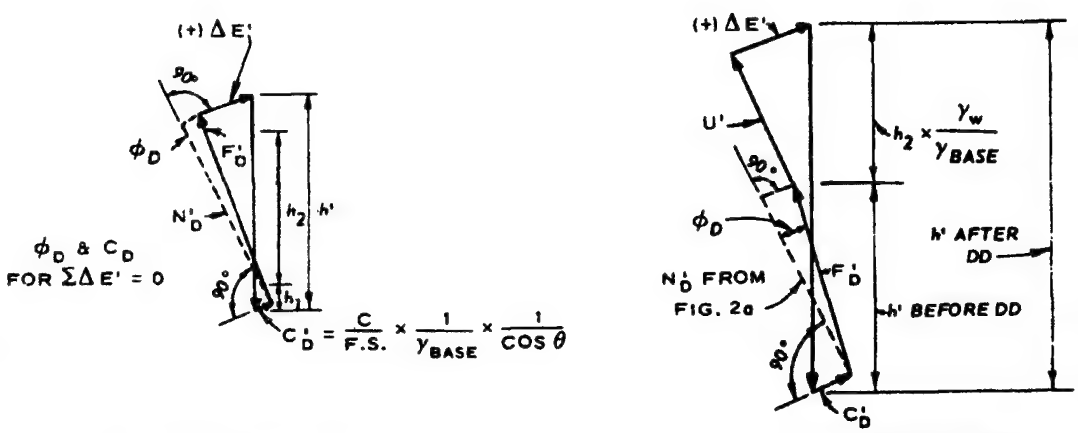

a. BEFORE DRAWDOWN

b. AFTER DRAWDOWN

FIGURE 2. UNIT SLICE FORCE POLYGON AT A

MODIFIED SWEDISH METHOD GRAPHICAL INTEGRATION PROCEDURE, SUDDEN DRAWDOWN

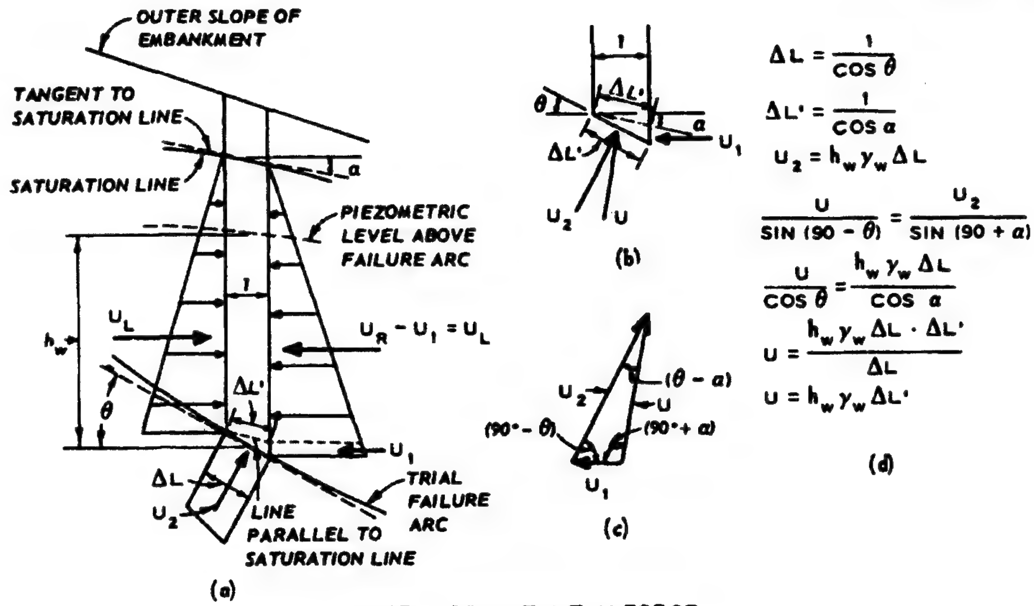

FIGURE 1. RESULTANT U FORCE

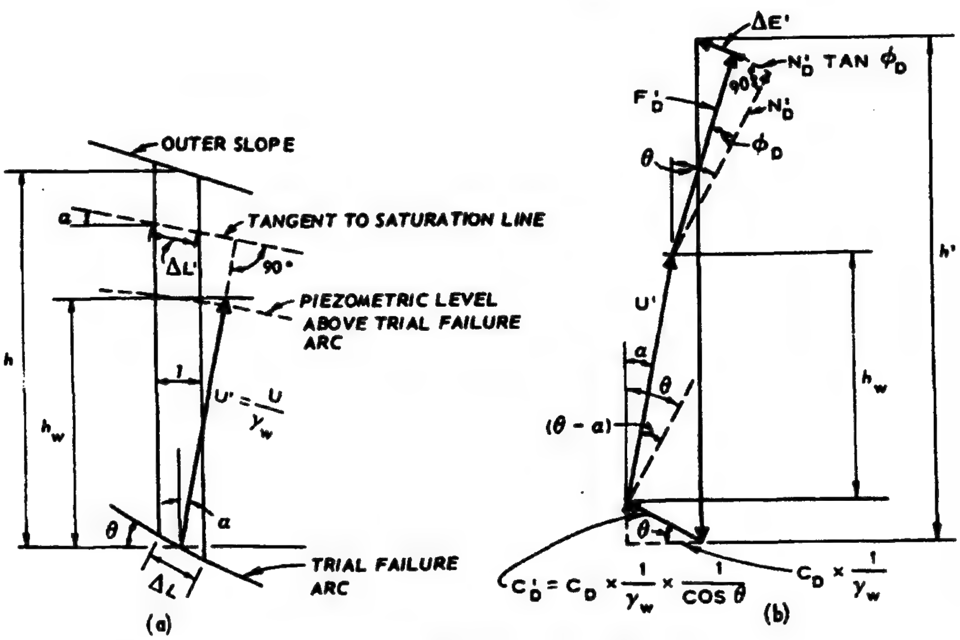

FIGURE 2. GRAPHICAL DETERMINATION OF U' AND N'$_D$

**MODIFIED SWEDISH METHOD
GRAPHICAL INTEGRATION
PROCEDURE, STEADY SEEPAGE
WATER FORCES**

Sliding surface in	Slice	Horizontal width, ft	Slice height, ft: Left side	Slice height, ft: Right side	Slice height, ft: Average	Area of slice, sq ft	Weight, kips: Moist	Weight, kips: Submerged	Weight, kips: Total	Base length of slice, ΔL, ft	$c\,\Delta L$, kips	$\frac{c\,\Delta L}{F.S.}$, kips*	ϕ_D, deg*
Embankment	1	15	23	0	11.5	172.5	23	—	23	23.0	40.9	25.6	3.2
	2	22	44	23	33.5	737.0	100	—	100	31.0	55.2	34.5	
	3	22	61	44	52.5	1155.0	156	—	156	27.5	49.0	30.6	
	4	28	67	61	64.0	1792.0	242	—	242	33.0	58.7	36.7	
	5	28	69	67	68.0	1904.0	257	—	257	31.5	56.1	35.0	
Foundation	6 6'	27	58 9	69 0	63.5 4.5	1714.0 122.0	231 —	— 8	239	29.0	46.4	29.0	1.3
	7 7'	36	47 16	58 9	52.5 12.5	1890.0 450.0	255 —	— 29	284	37.0	59.2	37.0	
	8 8'	40	33 19	47 16	40.0 17.5	1600.0 700.0	216 —	— 46	262	41.0	65.6	41.0	
	9 9'	40	19 16	33 19	26.0 17.5	1040.0 700.0	140 —	— 46	186	41.0	65.6	41.0	
	10 10'	57	0 0	19 16	9.5 8.0	542.0 456.0	73 —	— 30	103	60.0	96.0	60.0	

* FOR F.S. = 1.60

ADOPTED DESIGN DATA					
MATERIAL	Q STRENGTH: ϕ DEG	Q STRENGTH: TAN ϕ	Q STRENGTH: COHESION KIPS/SQ FT	UNIT WT LB/CU FT: γ_m	UNIT WT LB/CU FT: γ'
EMBANKMENT	5	0.088	1.78	135	—
FOUNDATION	2	0.035	1.60	—	65

FIGURE 2. DESIGN DATA

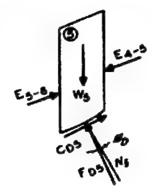

FIGURE 3. TYPICAL SLICE

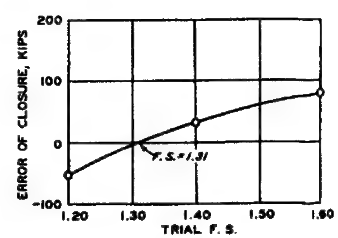

FIGURE 4. TRIAL FACTOR OF SAFETY VERSUS ERROR OF CLOSURE

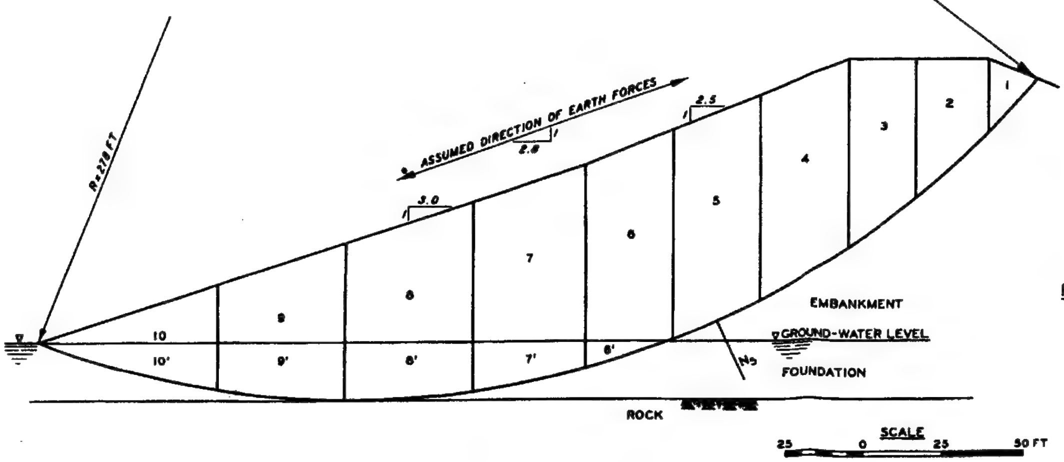

FIGURE 1. EMBANKMENT SECTION

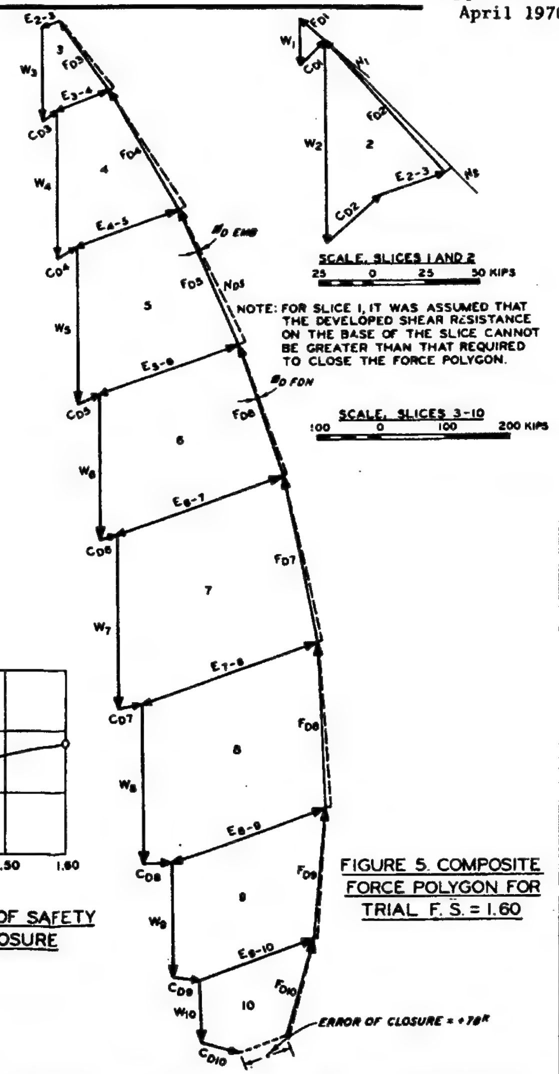

FIGURE 5. COMPOSITE FORCE POLYGON FOR TRIAL F. S. = 1.60

STABILITY ANALYSIS, CASE I - END OF CONSTRUCTION, UPSTREAM SLOPE, MODIFIED SWEDISH METHOD, FINITE SLICE PROCEDURE

ADOPTED DESIGN DATA					
MATERIAL	UNIT WT LB/CU FT		Q STRENGTH		
	γ_m	γ'	ϕ DEG	TAN ϕ	c KIPS/SQ FT
EMBANKMENT	135	–	5	0.088	1.78
FOUNDATION	–	65	2	0.035	1.60

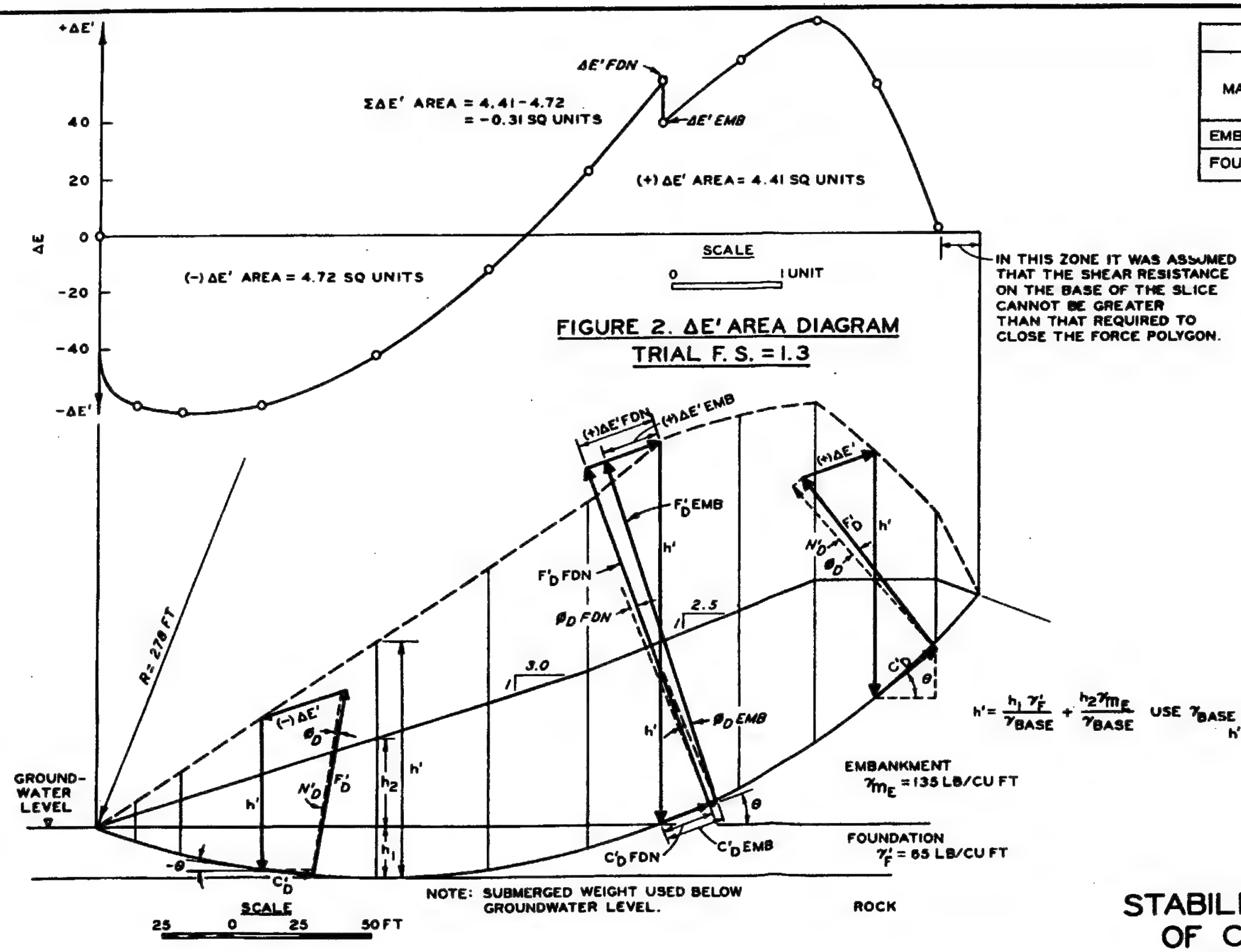

FIGURE 2. ΔE' AREA DIAGRAM
TRIAL F. S. = 1.3

FIGURE 1. EMBANKMENT SECTION AND UNIT WIDTH
SLICE FORCE POLYGONS, TRIAL F. S. = 1.3

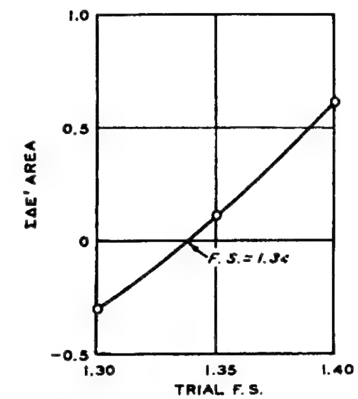

FIGURE 3. TRIAL F. S.
VERSUS ΣΔE'

STABILITY ANALYSIS, CASE I – END OF CONSTRUCTION, MODIFIED SWEDISH METHOD, GRAPHICAL INTEGRATION PROCEDURE

COMPUTATION OF FACTOR OF SAFETY-SUDDEN DRAWDOWN

$$F.S. = \Sigma \frac{N_D \tan \phi + c\Delta L}{W \sin \theta}$$

WHERE N_D = NORMAL EFFECTIVE FORCE BEFORE DRAWDOWN

W = WEIGHT OF SLICE AFTER DRAWDOWN

SLICE	N_D KIPS	TAN ϕ	N_D TAN ϕ	ΔL FT	$c\Delta L$ KIPS	W KIPS	$\theta°$	SIN θ	W SIN θ KIPS
1	35	—	—	—	—	51.5	56.2	0.831	42.8
2	67	—	—	—	—	118.6	46.7	0.728	86.3
3	64	—	—	—	—	124.6	40.0	0.643	80.1
4	122	—	—	—	—	247.8	32.0	0.530	131.3
Σ 1-4	288	0.577	166.2	—	—	—	—	—	340.5
5	123	—	—	28.0	—	230.7	24.0	0.407	93.9
6	123	—	—	27.0	—	212.9	16.3	0.281	59.8
7	119	—	—	25.4	—	183.8	8.9	0.155	28.5
8	114	—	—	25.0	—	160.7	2.2	0.038	6.1
Σ 5-8	479	0.287	137.5	105.4	126.5	—	—	—	188.3
9	123	—	—	—	—	154.2	-5.0	-0.087	-13.4
10	99	—	—	—	—	103.1	-13.8	-0.239	-24.6
11	45	—	—	—	—	41.7	-23.0	-0.391	-16.3
Σ 9-10	267	0.577	154.1	—	—	—	—	—	-54.3
Σ 1-10	—	—	457.8	—	126.5	—	—	—	474.5

$$F.S. = \frac{457.8 + 126.5}{474.5} = 1.23$$

MEASUREMENTS AND WEIGHTS

SLICE	HORIZONTAL WIDTH, FT	BASE LENGTH OF SLICE, ΔL, FT	SLICE HEIGHT, FT: LEFT SIDE	SLICE HEIGHT, FT: RIGHT SIDE	SLICE HEIGHT, FT: AVERAGE	AREA OF SLICE, SQ FT	WEIGHT, KIPS: SUBMERGED	WEIGHT, KIPS: MOIST OR SATURATED	WEIGHT, KIPS: TOTAL WT BEFORE DRAWDOWN	WEIGHT, KIPS: TOTAL WT AFTER DRAWDOWN
1' 1	20.4 18.6	40.0	6.4 26.9	6.4 0	6.4 13.5	130.6 251.1	— 18.3	17.6 33.9	35.9	51.5
2' 2	20.0	29.0	6.4 48.0	6.4 26.9	6.4 37.5	128.0 750.0	— 54.8	17.3 101.3	72.1	118.6
3' 3	16.0	20.6	0 61.0	6.4 48.0	3.2 54.5	51.2 872.0	— 63.6	6.9 117.7	70.5	124.6
4	28.5	33.5	67.7	61.0	64.4	1835.4	134.0	247.8	134.0	247.8
5 5'	26.0	28.0	57.5 11.5	67.7 0	62.6 5.8	1627.6 150.8	118.8 11.0	219.7 —	129.8	230.7
6 6'	26.0	27.0	47.3 19.0	57.5 11.5	52.4 15.3	1362.4 397.8	99.5 29.0	183.9 —	128.5	212.9
7 7'	25.0	25.4	39.0 23.0	47.3 19.0	43.1 21.0	1077.5 525.0	78.7 38.3	145.5 —	117.0	183.8
8 8'	25.0	25.0	30.7 24.0	39.0 23.0	34.9 23.5	872.5 587.5	63.7 42.9	117.8 —	106.6	160.7
9 9'	30.0	30.2	21.0 21.0	30.7 24.0	25.9 22.5	777.0 675.0	56.7 49.3	104.9 —	106.0	154.2
10 10'	30.0	31.0	11.0 14.0	21.0 21.0	16.0 17.5	480.0 525.0	35.0 38.3	64.8 —	73.3	103.1
11 11'	33.3	36.1	0	11.0 14.0	5.5 7.0	183.2 233.1	13.4 17.0	24.7 —	30.4	41.7

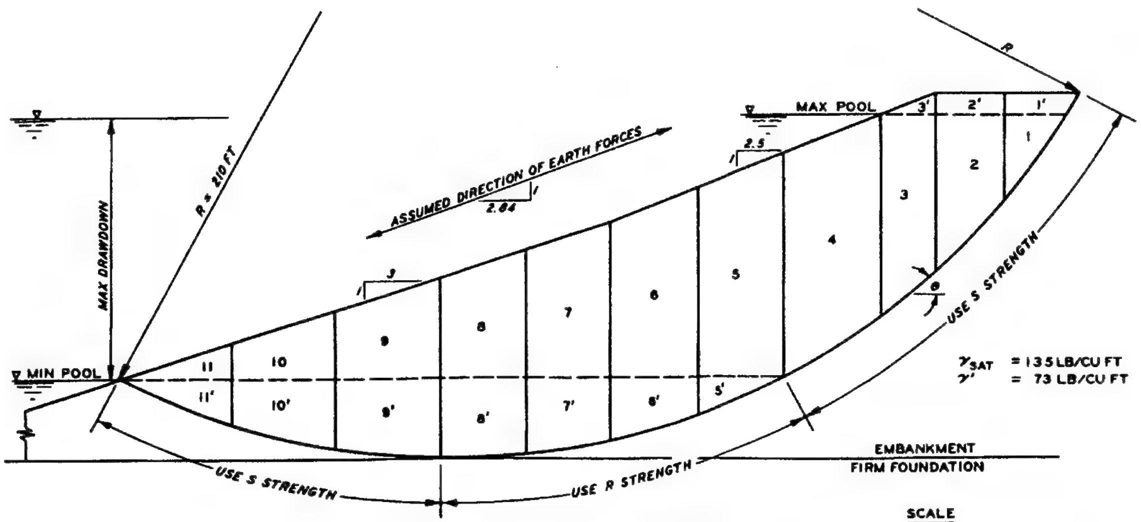

FIGURE 1. EMBANKMENT SECTION

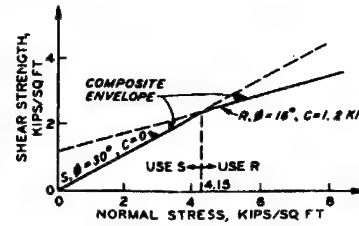

FIGURE 2. COMPOSITE STRENGTH ENVELOPE

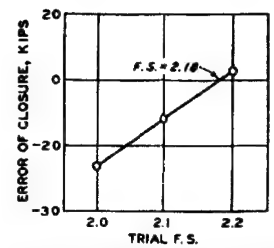

FIGURE 3. TRIAL FACTOR OF SAFETY VERSUS ERROR OF CLOSURE (BEFORE DRAWDOWN)

NOTE FOR FIG. 4:
THE SHEAR STRENGTH USED FOR EACH SLICE IN THE FORCE POLYGON IS SELECTED BY TRIAL. WHEN THE NORMAL FORCE N_D DETERMINED USING THE S STRENGTH EXCEEDS 4.15 KIPS/SQ FT TIMES THE BASE LENGTH OF THE SLICE, THE R STRENGTH IS USED FOR THAT SLICE. THIS WAS THE CASE FOR SLICES 5, 6, 7, AND 8.

FOR F.S. = 2.18:

	S	R
TAN Φ_D	0.265	0.131
Φ_D, DEG	14.8	7.5
C_D, KIPS/SQ FT	0	0.55

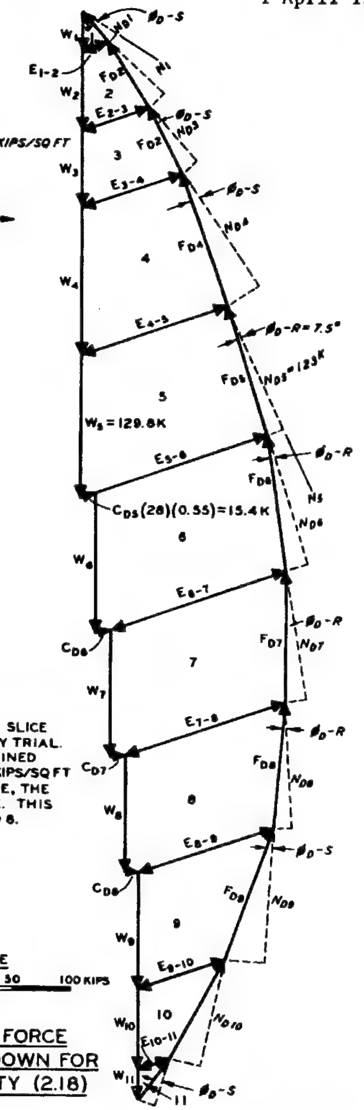

FIGURE 4. COMPOSITE FORCE POLYGON BEFORE DRAWDOWN FOR TRUE FACTOR OF SAFETY (2.18)

STABILITY ANALYSIS, CASE II – SUDDEN DRAWDOWN, UPSTREAM SLOPE, MODIFIED SWEDISH METHOD, FINITE SLICE PROCEDURE

SLICE	HORIZONTAL WIDTH, FT	BASE LENGTH OF SLICE, ΔL, FT	SLICE HEIGHT, FT: LEFT SIDE	SLICE HEIGHT, FT: RIGHT SIDE	SLICE HEIGHT, FT: AVERAGE	AREA OF SLICE, SQ FT	WEIGHT OF SLICE, KIPS(1)	WATER PRESSURE ON FAILURE ARC, KIPS/SQ FT (2): LEFT	WATER PRESSURE ON FAILURE ARC, KIPS/SQ FT (2): RIGHT	U_L, KIPS(3)	U_R, KIPS(3)	$(U_L - U_R)$, KIPS	UPLIFT (U_B), KIPS(4)
1	25	42.0	23.5	0	11.75	293.8	41.1	0.88	0	10.3	0	10.3	18.5
2	35	49.0	44.0	23.5	33.75	1181.0	165.3	2.06	0.88	45.3	10.3	35.0	72.0
3	40	50.0	58.0	44.0	51.00	2040.0	285.6	3.15	2.06	91.4	45.3	46.1	120.2
4	40	45.5	66.0	58.0	62.00	2480.0	347.2	3.88	3.15	128.0	91.4	36.6	160.0
5	40	43.0	68.0	66.0	67.00	2680.0	375.2	4.12	3.88	140.0	128.0	12.0	172.0
6	40	41.5	65.0	68.0	66.50	2660.0	372.4	4.09	4.12	132.9	140.0	-7.1	170.4
7	50	50.0	55.5	65.0	60.25	3012.0	421.7	3.50	4.09	97.1	132.9	-35.8	189.7
8	55	55.0	36.5	55.5	46.00	2530.0	354.2	2.44	3.50	44.5	97.1	-52.6	163.4
9 9'	70	72.0	0 20.0	36.5 0	18.25 10.00	1278.0 700.0	178.8 43.8	1.25	2.44	12.5	44.5	-32.0	132.8

(1) SLICE 9': MULTIPLY AREA BY γ_m TO DETERMINE WEIGHT. ALL OTHER SLICES, MULTIPLY AREA BY γ_{SAT} TO DETERMINE WEIGHT.
(2) PIEZOMETRIC HEAD AT BASE × γ_w.
(3) PIEZOMETRIC PRESSURE AT BASE × SLICE HEIGHT ÷ 2.
(4) BASE LENGTH OF SLICE × AVERAGE PIEZOMETRIC PRESSURE ON BASE.

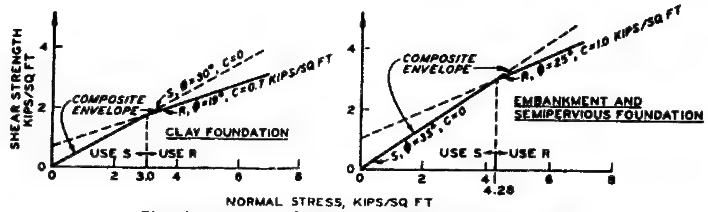

FIGURE 2. COMPOSITE STRENGTH ENVELOPES

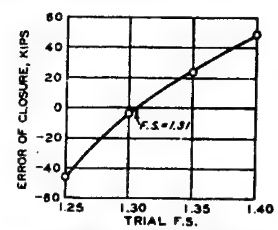

FIGURE 3. TRIAL FACTOR OF SAFETY VS ERROR OF CLOSURE

ADOPTED DESIGN DATA						
MATERIAL	TAN φ: R	TAN φ: S	COHESION KIPS/SQ FT: R	COHESION KIPS/SQ FT: S	UNIT WT LB/SQ FT: γ_{SAT}	UNIT WT LB/SQ FT: γ'
FOUNDATION CLAY	0.344	0.577	0.7	0	*	*
SEMIPERVIOUS FOUNDATION AND EMBANKMENT	0.466	0.700	1.0	0	140	78

* ASSUMED SAME AS SEMIPERVIOUS MATERIAL.

NOTES FOR FIGURE 5:
THE SHEAR STRENGTH USED FOR EACH SLICE IN THE FORCE POLYGON IS SELECTED BY TRIAL. WHEN THE NORMAL FORCE N_D (DETERMINED USING THE S STRENGTH) DIVIDED BY THE BASE LENGTH OF THE SLICE EXCEEDS 4.28 KIPS/SQ FT IN SEMIPERVIOUS MATERIAL OR 3.0 KIPS/SQ FT IN THE FOUNDATION CLAY, THE R STRENGTH IS USED FOR THAT SLICE.

FOR TRIAL F.S.=1.30:

	CLAY FOUNDATION: S_F	CLAY FOUNDATION: R_F	SEMIPERVIOUS: S_P	SEMIPERVIOUS: R_P
TAN Φ_D	0.444	0.265	0.538	0.358
Φ_D, DEG	24.0	14.8	28.3	19.7
C_D, KIPS/SQ FT	0	0.538	0	0.769

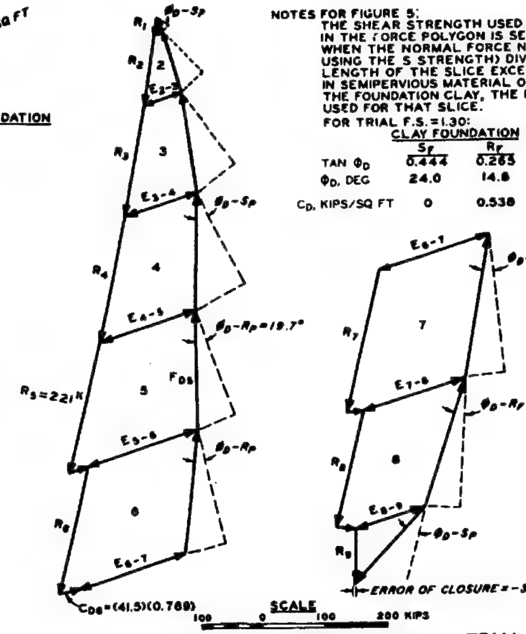

FIGURE 5. COMPOSITE FORCE POLYGON, TRIAL F.S.=1.30

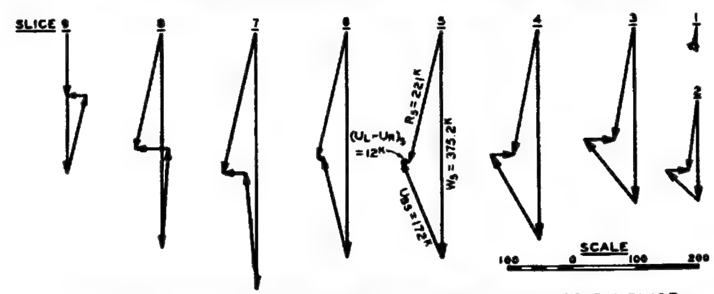

FIGURE 4. RESULTANT OF WEIGHT AND WATER FORCES ON SLICE

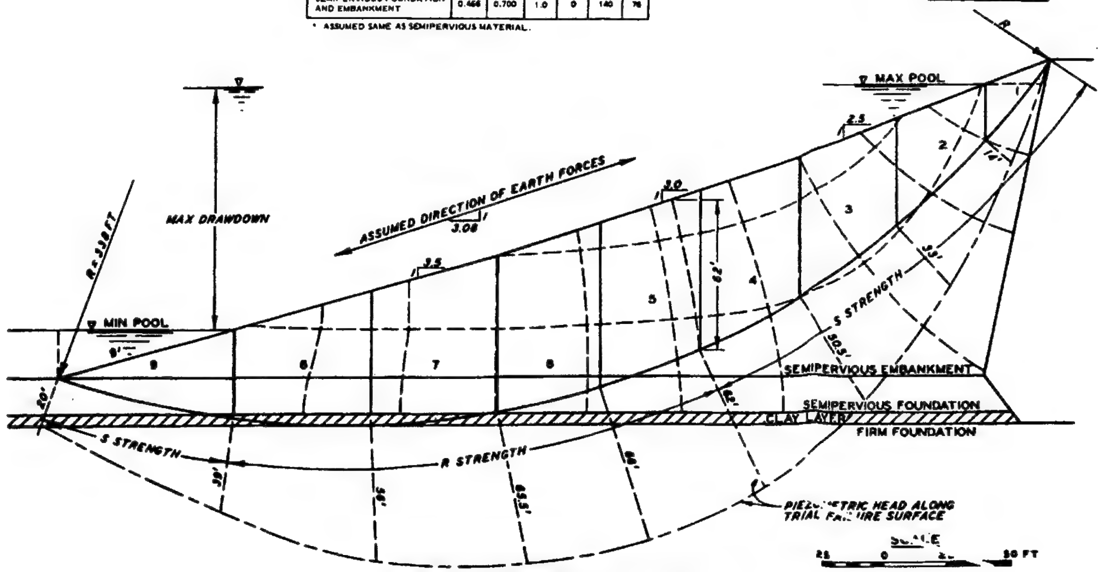

FIGURE 1. EMBANKMENT SECTION

STABILITY ANALYSIS, EMBANKMENT WITH CENTRAL CORE AND SEMIPERVIOUS SHELL, CASE II – SUDDEN DRAWDOWN, MODIFIED SWEDISH METHOD, FINITE SLICE PROCEDURE

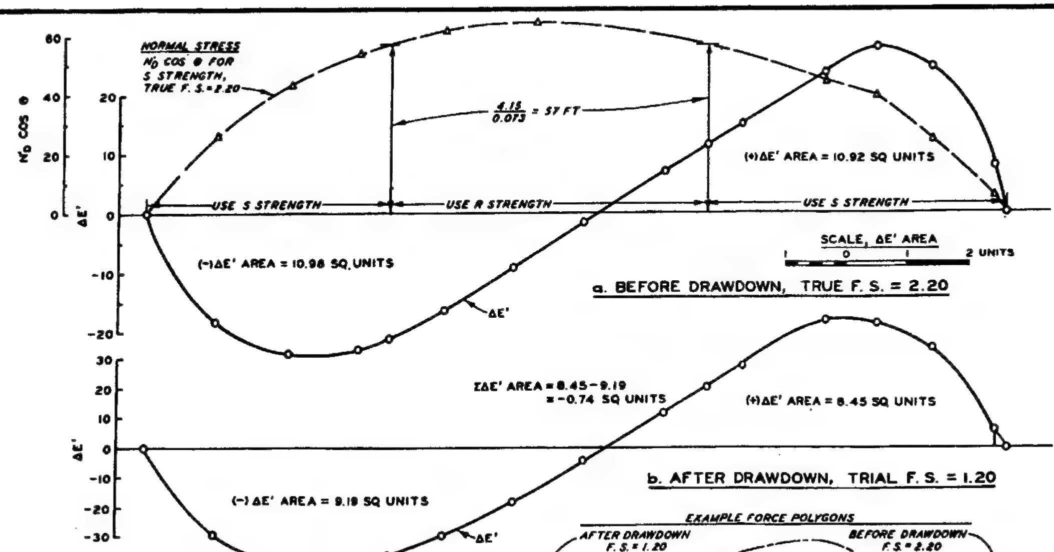

a. BEFORE DRAWDOWN, TRUE F. S. = 2.20

b. AFTER DRAWDOWN, TRIAL F. S. = 1.20

FIGURE 2. ΔE' AREA DIAGRAM

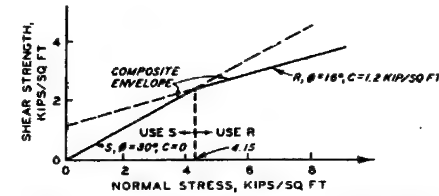

FIGURE 3. COMPOSITE STRENGTH ENVELOPE

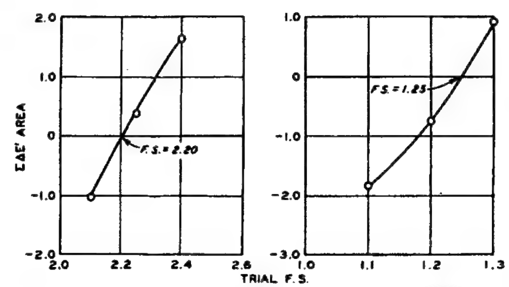

a. BEFORE DRAWDOWN

b. AFTER DRAWDOWN

FIGURE 4. TRIAL FACTOR SAFETY VERSUS ΣΔE'

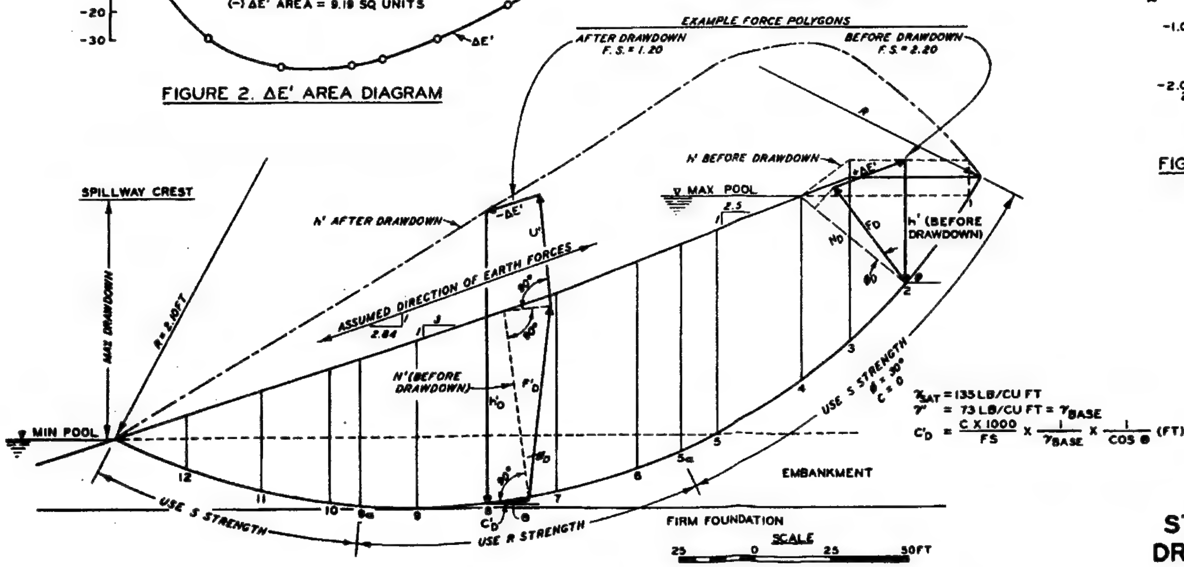

FIGURE 1. EMBANKMENT SECTION AND UNIT WIDTH SLICE FORCE POLYGON,
TRIAL F. S.: BEFORE DRAWDOWN = 2.20, AFTER DRAWDOWN = 1.20

STABILITY ANALYSIS, CASE II - SUDDEN DRAWDOWN, UPSTREAM SLOPE, MODIFIED SWEDISH METHOD, GRAPHICAL INTEGRATION PROCEDURE

SLICE	HORIZONTAL WIDTH FT	BASE LENGTH OF SLICE, ΔL, FT	SLICE HEIGHT, FT: LEFT SIDE	SLICE HEIGHT, FT: RIGHT SIDE	SLICE HEIGHT, FT: AVERAGE	AREA OF SLICE, SQ FT	WEIGHT, KIPS: MOIST	WEIGHT, KIPS: SUBMERGED	WEIGHT, KIPS: TOTAL
1	13.3	24.9	21.0	0	10.5	140.0	18.0	—	18.0
2	18.0	28.0	34.5	21.0	27.8	500.0	65.0	—	65.0
3	15.0	20.0	28.0	34.5	31.3	470.0	61.0	—	68.0
3'			13.5	0	6.7	100.5	—	7.0	
4	24.0	28.7	18.5	28.0	23.3	564.0	73.0	—	108.0
4'			29.5	13.5	21.5	515.0	—	35.0	
5	28.0	31.5	9.0	18.5	13.8	388.0	50.0	—	117.0
5'			29.5	29.5	29.5	825.0	—	56.0	
5''			12.5	0	6.3	176.0	—	11.0	
6	30.0	31.0	0	9.0	4.5	135.0	18.0	—	109.0
6'			29.5	29.5	29.5	885.0	—	60.0	
6''			20.0	12.5	16.3	489.0	—	31.0	
7'	30.0	30.5	22.0	29.5	25.8	774.0	—	53.0	93.0
7''			22.6	20.0	21.3	639.0	—	40.0	
8'	25.0	23.2	15.5	22.0	18.8	470.0	—	32.0	66.0
8''			21.0	22.6	21.8	545.0	—	34.0	
9'	31.0	32.0	8.0	15.5	11.8	366.0	—	25.0	58.0
9''			14.0	21.0	17.5	542.0	—	34.0	
10'	32.0	34.3	0	8.0	4.0	128.0	—	9.0	23.0
10''				14.0	7.0	224.0	—	14.0	

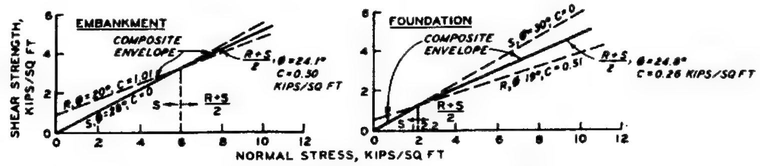

FIGURE 2. COMPOSITE STRENGTH ENVELOPES

ADOPTED DESIGN DATA								
MATERIAL	TAN φ: R	TAN φ: S	TAN φ: $\frac{R+S}{2}$	COHESION KIPS/SQ FT: R	COHESION KIPS/SQ FT: S	COHESION KIPS/SQ FT: $\frac{R+S}{2}$	UNIT WT LB/CU FT: γ_m	UNIT WT LB/CU FT: γ'
EMBANKMENT	0.364	0.532	0.448	1.01	0	0.50	130	68
FOUNDATION	0.344	0.577	0.461	0.51	0	0.26	—	63

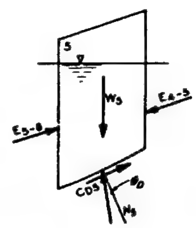

FIGURE 4. TYPICAL SLICE

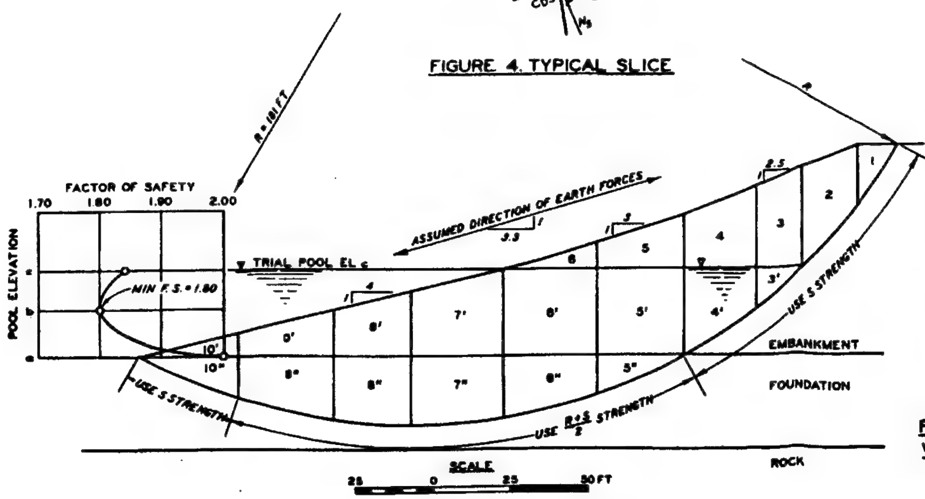

FIGURE 1. EMBANKMENT SECTION

NOTES FOR FIGURE 3:

THE SHEAR STRENGTH USED FOR EACH SLICE IN THE FORCE POLYGON IS SELECTED BY TRIAL. WHEN THE NORMAL FORCE N_D (DETERMINED USING THE S STRENGTH) DIVIDED BY THE BASE LENGTH OF THE SLICE EXCEEDS 6.0 KIPS/SQ FT IN THE EMBANKMENT OR 2.2 KIPS/SQ FT IN THE FOUNDATION, THE $\frac{R+S}{2}$ STRENGTH IS USED FOR THAT SLICE.

FOR TRIAL F.S. = 1.68:

	FOUNDATION S_F	FOUNDATION $\frac{R+S}{2}$	EMBANKMENT S_E	EMBANKMENT $\frac{R+S}{2}$
TAN Φ_D	0.344	0.274	0.317	0.268
Φ_D, DEG	18.9	15.3	17.6	14.9
C_D, KIPS/SQ FT	0	0.155	0	0.287

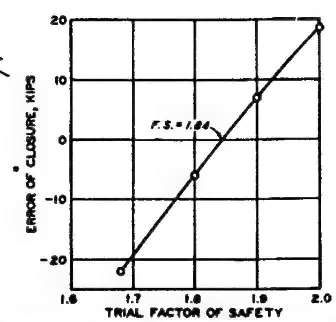

FIGURE 5. TRIAL FACTOR OF SAFETY VERSUS ERROR OF CLOSURE, POOL c

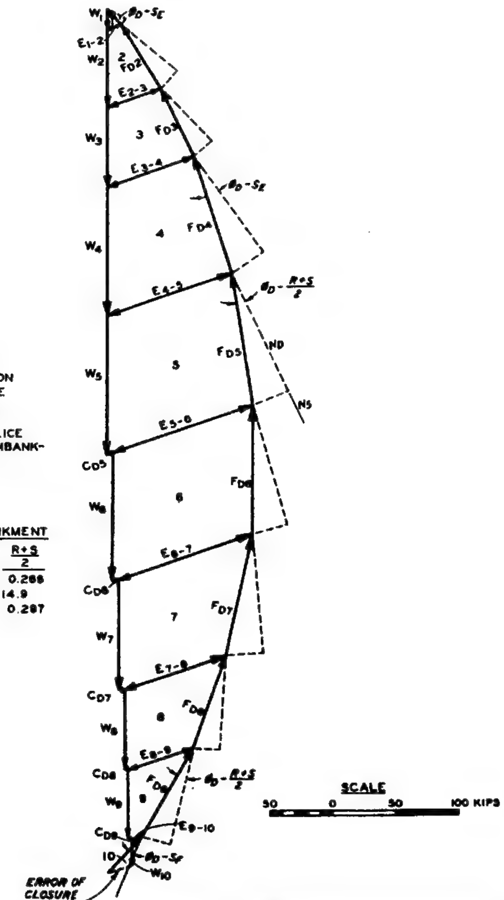

FIGURE 3. COMPOSITE FORCE POLYGON POOL EL c, TRIAL F.S. = 1.68

STABILITY ANALYSIS, CASE IV - PARTIAL POOL, UPSTREAM SLOPE, MODIFIED SWEDISH METHOD, FINITE SLICE PROCEDURE

Plate VI-13

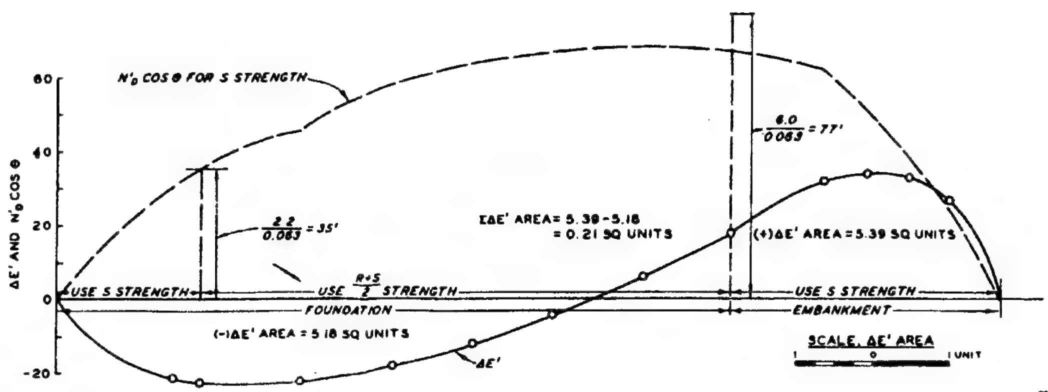

FIGURE 2. ΔE' AREA DIAGRAM AND N'D COS θ DIAGRAM
TRIAL F. S. = 1.80, POOL EL b

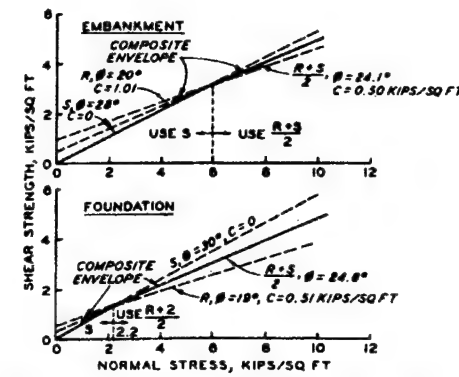

FIGURE 3. COMPOSITE STRENGTH ENVELOPES

ADOPTED DESIGN DATA								
MATERIAL	TAN φ			COHESION KIPS/SQ FT			UNIT WEIGHT LB/CU FT	
	R	S	(R+S)/2	R	S	(R+S)/2	γ_m	γ'
EMBANKMENT	0.364	0.532	0.448	1.01	0	0.50	130	68
FOUNDATION	0.344	0.577	0.461	0.51	0	0.26	—	63

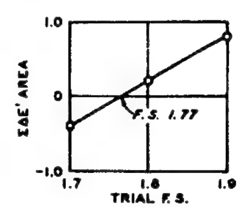

FIGURE 4. TRIAL FACTOR OF SAFETY VERSUS ΣΔE'
POOL EL b

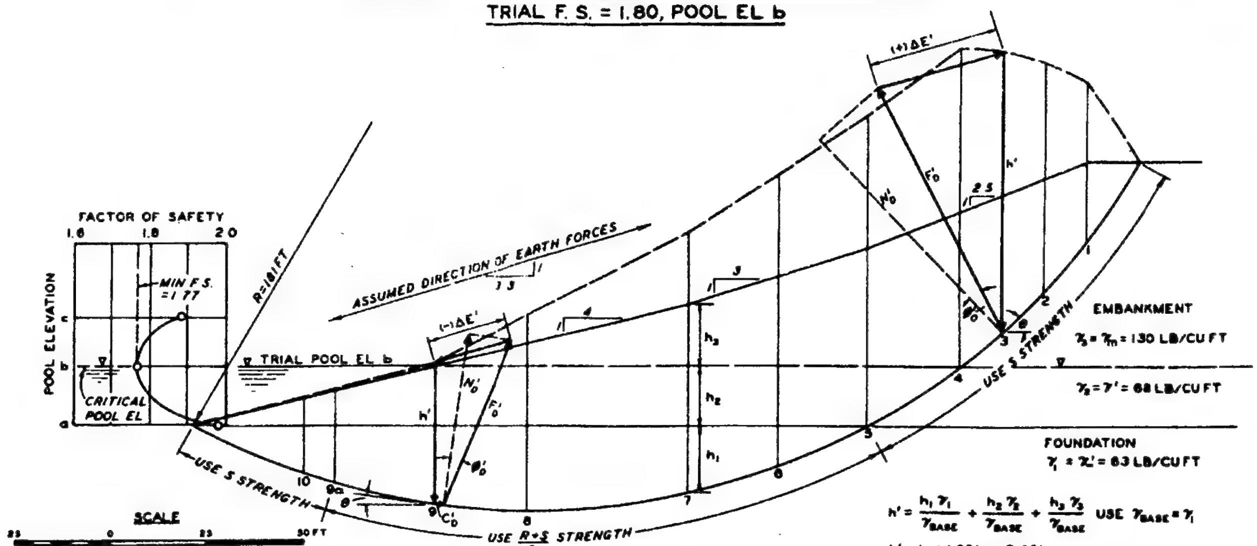

FIGURE 1. EMBANKMENT SECTION AND UNIT WIDTH SLICE
FORCE POLYGON, TRIAL F. S. = 1.80, POOL EL b

STABILITY ANALYSIS, CASE IV - PARTIAL POOL, UPSTREAM SLOPE, MODIFIED SWEDISH METHOD, GRAPHICAL INTEGRATION PROCEDURE

SLICE	HORIZONTAL WIDTH, FT	BASE LENGTH, SL FT	SLICE HEIGHT, FT: LEFT SIDE	SLICE HEIGHT, FT: RIGHT SIDE	SLICE HEIGHT, FT: AVERAGE	AREA OF SLICE, SQ FT	WEIGHT, KIPS: MOIST OR SATURATED WT	WEIGHT, KIPS: SUBMERGED WT	WEIGHT, KIPS: TOTAL WT	PIEZOMETRIC HEIGHT AT BASE OF SLICE, FT: LEFT	PIEZOMETRIC HEIGHT AT BASE OF SLICE, FT: RIGHT	WATER PRESSURE ON BASE KIPS/SQ FT: LEFT	WATER PRESSURE ON BASE KIPS/SQ FT: RIGHT	U_L, KIPS	U_R, KIPS	$(U_L - U_R)$, KIPS	UPLIFT U_B, KIPS
1	30.5	51.0	0	53.0	26.5	808	105	—	105	0	25	0	1.6	0	20.0	-20.0	40.8
2	20.5	29.0	53.0	73.5	63.2	1296	169	—	169	25	39	1.6	2.4	20.0	46.8	-26.8	58.0
3	56.3	69.0	73.5	89.5	81.5	4580	595	—	595	39	44	2.4	2.8	46.8	61.6	-14.8	179.4
4 4"	71.5	23.5	89.5 0	81.5 9.8	85.5 4.9	1030 105	238 13	— —	252	44	32	2.8	2.0	61.6	32.0	+29.6	56.4
5 5' 5"	35.0	37.5	39.0 22.5 9.8	45.5 22.5 22.0	52.3 22.5 15.9	1831 788 556	238 — —	— 53 35	326	—	—	—	—	—	—	—	—
6 6' 6"	35.0	35.5	45.5 22.5 22.0	34.0 22.5 29.8	39.8 22.5 25.9	1393 788 907	181 — —	— 53 57	291	—	—	—	—	—	—	—	—
7 7' 7"	39.0	39.4	34.0 22.5 29.8	21.0 22.5 32.5	27.5 22.5 31.2	1073 878 1217	139 — —	— 59 76	274	—	—	—	—	—	—	—	—
8 8' 8"	63.0	63.5	21.0 22.5 32.5	0 22.5 24.5	10.5 22.5 28.5	661 1417 1796	86 — —	— 96 112	294	—	—	—	—	—	—	—	—
9' 9"	67.0	—	22.5 24.5	0 0	11.3 12.3	757 824	— —	51 52	103								

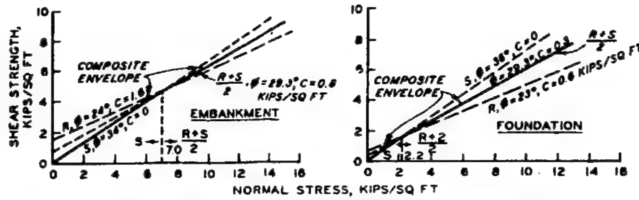

FIGURE 2. COMPOSITE STRENGTH ENVELOPES

ADOPTED DESIGN DATA								
MATERIAL	TAN φ			COHESION KIPS/SQ FT			UNIT WT LB/CU FT	
	R	S	$\frac{R+S}{2}$	R	S	$\frac{R+S}{2}$	γ_m	γ'
EMBANKMENT	0.455	0.675	0.560	1.6	0	0.8	130	67.5
FOUNDATION	0.424	0.700	0.562	0.6	0	0.3	125	62.5

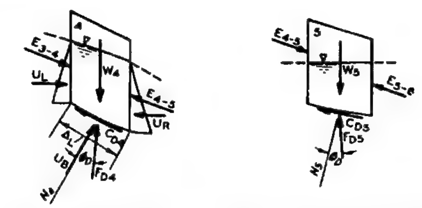

a. SLOPING WATER SURFACE (SLICES 1-4), TOTAL WEIGHTS USED

b. HORIZONTAL WATER SURFACE (SLICES 5-9), SUBMERGED WEIGHTS USED BELOW WATER SURFACE

FIGURE. 3 TYPICAL SLICES

NOTES FOR FIGURE 5:
THE SHEAR STRENGTH USED FOR EACH SLICE IN THE FORCE POLYGON IS SELECTED BY TRIAL. WHEN THE NORMAL FORCE N_D (DETERMINED USING THE S STRENGTH) DIVIDED BY THE BASE LENGTH OF THE SLICE EXCEEDS 7.0 KIPS/SQ FT IN THE EMBANKMENT OR 2.2 KIPS/SQ FT IN THE FOUNDATION, THE $\frac{R+S}{2}$ STRENGTH IS USED FOR THAT SLICE.
FOR TRIAL F. S. = 1.80:

	FOUNDATION: S	FOUNDATION: $\frac{R+S}{2}$	EMBANKMENT: S	EMBANKMENT: $\frac{R+S}{2}$
TAN Φ_D	0.375	0.311	0.389	0.312
Φ_D, DEG	20.8	17.3	21.3	17.4
C_D, KIPS/SQ FT	0	0.167	0	0.444

SCALE
200 0 200 400 KIPS

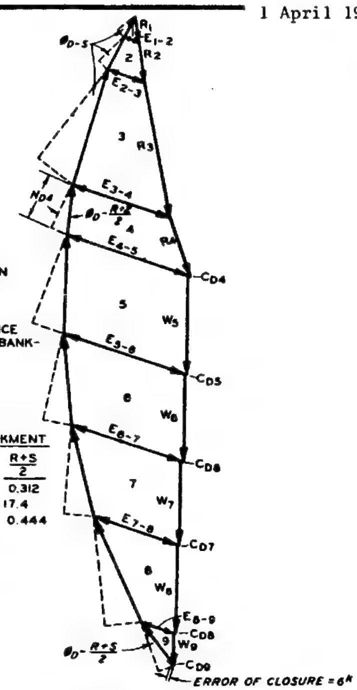

FIGURE 5. COMPOSITE FORCE POLYGON FOR TRIAL F. S. = 1.80

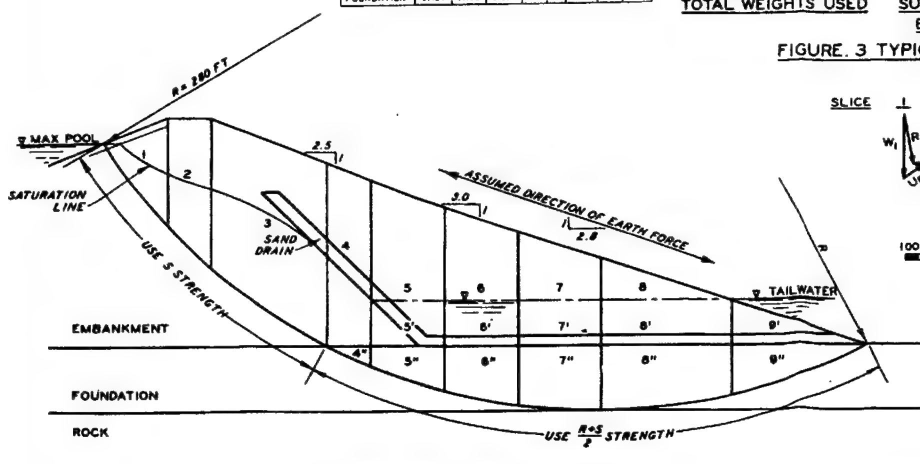

FIGURE 1. EMBANKMENT SECTION

SCALE
25 0 25 50 FT

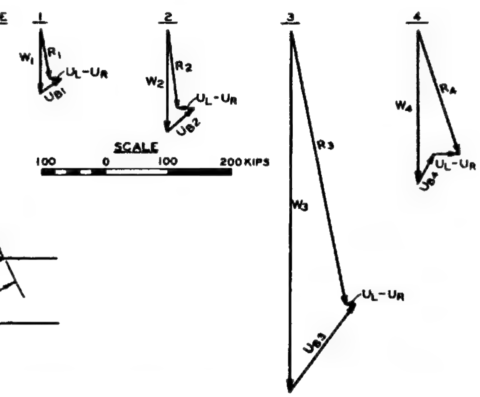

FIGURE 4. RESULTANTS OF WEIGHT AND WATER FORCES ON SLICE

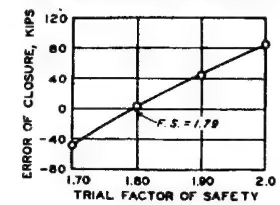

FIGURE 6. TRIAL FACTOR OF SAFETY VERSUS ERROR OF CLOSURE

STABILITY ANALYSIS, CASE V - STEADY SEEPAGE, DOWNSTREAM SLOPE, MAX STORAGE POOL, MODIFIED SWEDISH METHOD, FINITE SLICE PROCEDURE

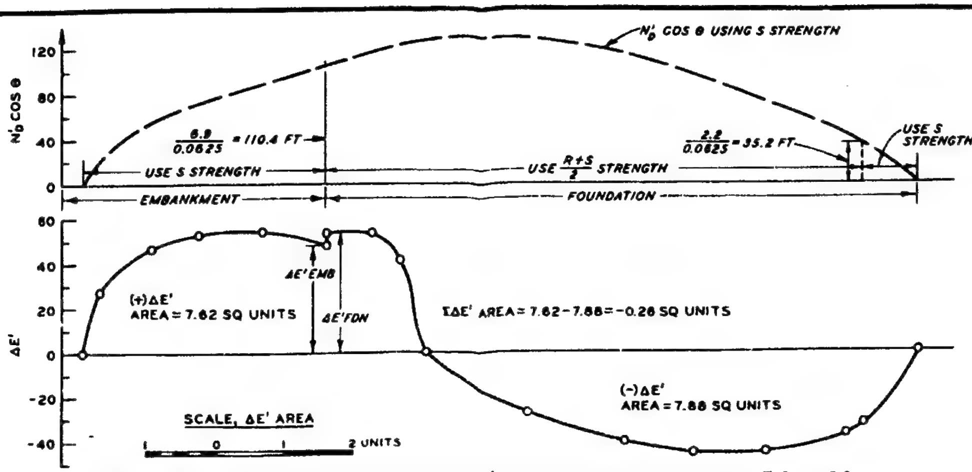

FIGURE 2. ΔE' AREA DIAGRAM AND N'_D COS Θ DIAGRAM, TRIAL F.S. = 1.80

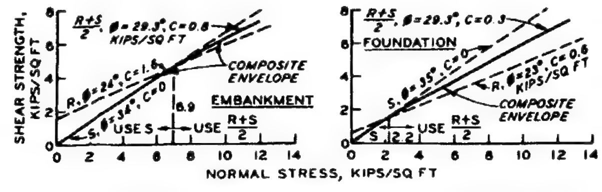

FIGURE 3. COMPOSITE STRENGTH ENVELOPES

ADOPTED DESIGN DATA							
MATERIAL	TAN Φ			COHESION KIPS/SQ FT			UNIT WT LB/CU FT
	R	S	$\frac{R+S}{2}$	R	S	$\frac{R+S}{2}$	γ_m
EMBANKMENT	0.445	0.675	0.560	1.6	0	0.8	130
FOUNDATION	0.424	0.700	0.562	0.6	0	0.3	125

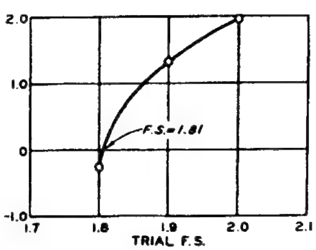

FIGURE 4. TRIAL F.S. VERSUS ΣΔE

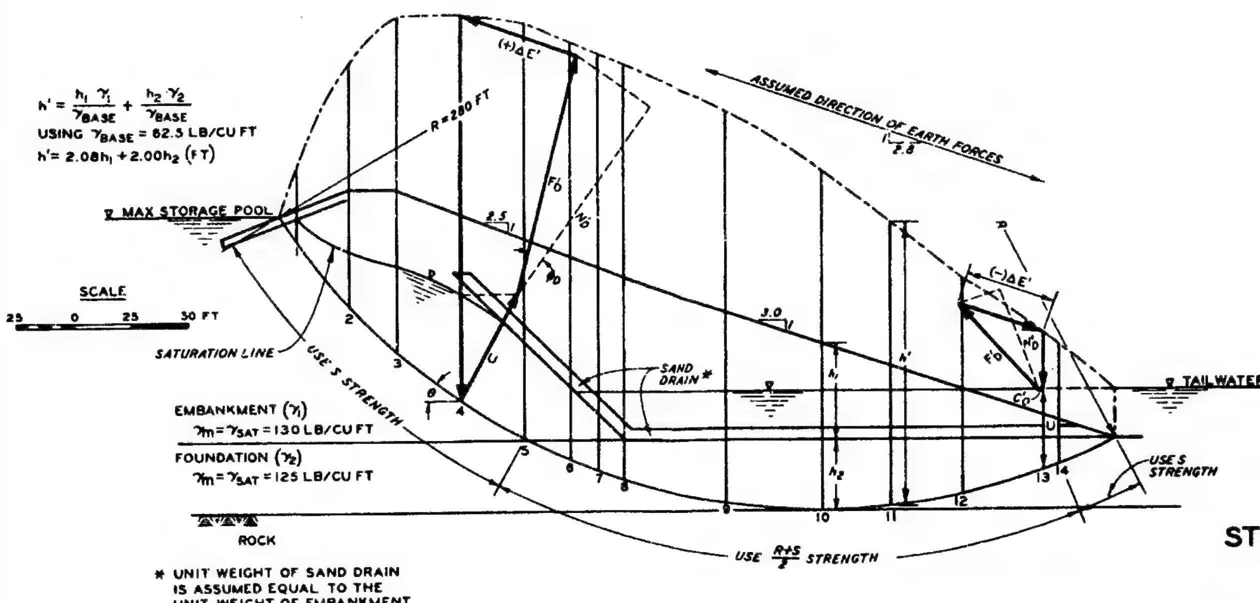

FIGURE 1. EMBANKMENT SECTION AND UNIT WIDTH SLICE FORCE POLYGONS, TRIAL F.S. = 1.8

STABILITY ANALYSIS, CASE V – STEADY SEEPAGE, DOWNSTREAM SLOPE, MAX STORAGE POOL, MODIFIED SWEDISH METHOD, GRAPHICAL INTEGRATION PROCEDURE

SLICE	HORIZONTAL WIDTH, FT	BASE LENGTH, FT	SLICE HEIGHT, FT: LEFT SIDE	SLICE HEIGHT, FT: RIGHT SIDE	SLICE HEIGHT, FT: AVERAGE	AREA OF SLICE, SQ FT	WEIGHT, KIPS: MOIST OR SATURATED WT	WEIGHT, KIPS: SUBMERGED WT	WEIGHT, KIPS: EFFECTIVE TOTAL WT	WEIGHT, KIPS: TOTAL WT FOR EARTHQUAKE	EARTHQUAKE FORCE, F_E, KIPS	PIEZOMETRIC HEIGHT AT BASE OF SLICE, FT: LEFT	PIEZOMETRIC HEIGHT AT BASE OF SLICE, FT: RIGHT	WATER PRESSURE ON BASE KIPS/SQ FT: LEFT	WATER PRESSURE ON BASE KIPS/SQ FT: RIGHT	U_L, KIPS	U_R, KIPS	$(U_L - U_R)$, KIPS	UPLIFT U_B, KIPS
1	30.5	51.0	0	53.0	26.5	808	105	—	105	105	15.8	0	25	0	1.6	0	20.0	-20.0	40.8
2	20.5	29.0	53.0	73.5	63.2	1296	169	—	169	169	25.4	25	39	1.6	2.4	20.0	46.2	-26.2	58.0
3	56.3	69.0	73.5	89.5	81.5	4588	595	—	595	595	89.4	39	44	2.4	2.8	46.2	61.6	-14.8	179.4
4 4'	21.5	23.5	89.5 0	81.5 9.8	85.5 4.9	1838 105	239 13	—	252	252	37.8	44	32	2.8	2.0	61.6	32.0	+29.6	56.4
5 5' 5"	35.0	37.5	59.0 22.5 9.8	45.5 22.5 22.0	52.3 22.5 15.9	1831 788 556	238	53 35	326	410	61.5	—	—	—	—	—	—	—	—
6 6' 6"	35.0	35.5	45.5 22.5 22.0	34.0 27.5 29.8	39.8 22.5 25.9	1393 788 907	181	53 57	291	397	59.6	—	—	—	—	—	—	—	—
7 7' 7"	39.0	39.4	34.0 22.5 29.8	21.0 22.5 32.5	27.5 22.5 31.2	1073 878 1217	139	59 76	274	405	60.8	—	—	—	—	—	—	—	—
8 8' 8"	63.0	63.5	21.0 22.5 32.5	0 22.5 24.5	10.5 22.5 28.5	661 1417 1796	86	86 112	284	495	74.3	—	—	—	—	—	—	—	—
9' 9"	67.0	—	22.5 24.5	0 0	11.3 12.3	757 828	—	51 52	103	201	30.2	—	—	—	—	—	—	—	—

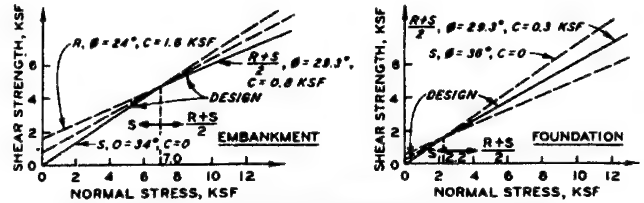

FIGURE 2. COMPOSITE STRENGTH ENVELOPES
(SAME AS IN PLATE VI-15)

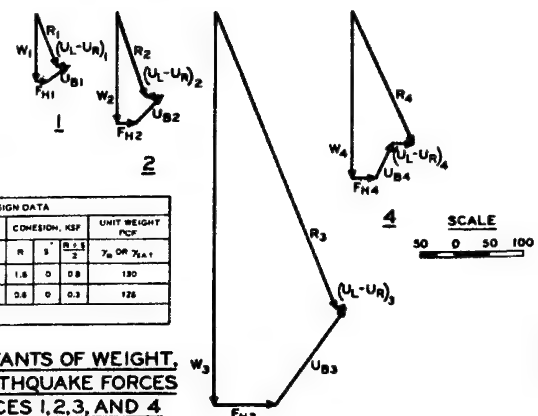

ADOPTED DESIGN DATA							
MATERIAL	TAN Ø			COHESION, KSF			UNIT WEIGHT PCF
	R	S	$\frac{R+S}{2}$	R	S	$\frac{R+S}{2}$	γ_m OR γ_{SAT}
EMBANKMENT	0.445	0.675	0.560	1.8	0	0.8	130
FOUNDATION	0.424	0.700	0.562	0.6	0	0.3	125
SEISMIC COEFFICIENT, ψ = 0.15							

FIGURE 3. RESULTANTS OF WEIGHT, WATER, AND EARTHQUAKE FORCES ACTING ON SLICES 1,2,3, AND 4

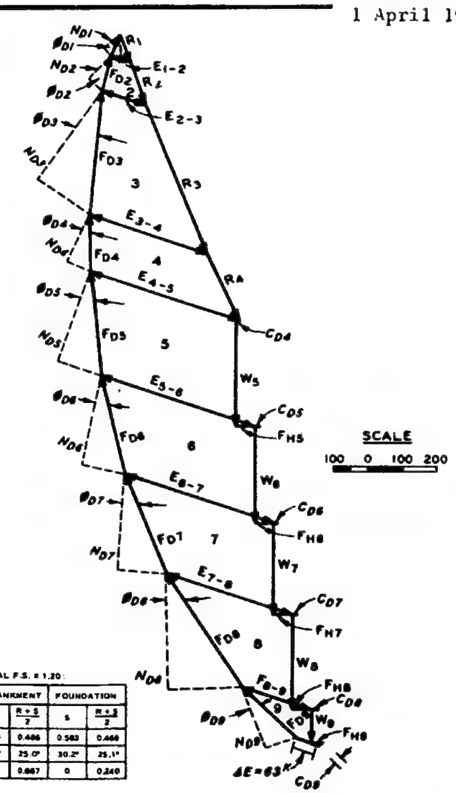

TRIAL F.S. = 1.20:

	EMBANKMENT		FOUNDATION	
	S	$\frac{R+S}{2}$	S	$\frac{R+S}{2}$
TAN $Ø_D$	0.563	0.466	0.583	0.468
$Ø_D$	29.4°	25.0°	30.2°	25.1°
C_D, KSF	0	0.667	0	0.240

FIGURE 4. COMPOSITE FORCE POLYGON FOR TRIAL F.S. = 1.20

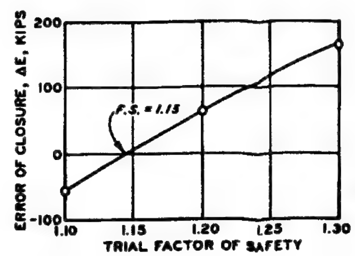

FIGURE 5. ERROR OF CLOSURE VS TRIAL FACTOR OF SAFETY

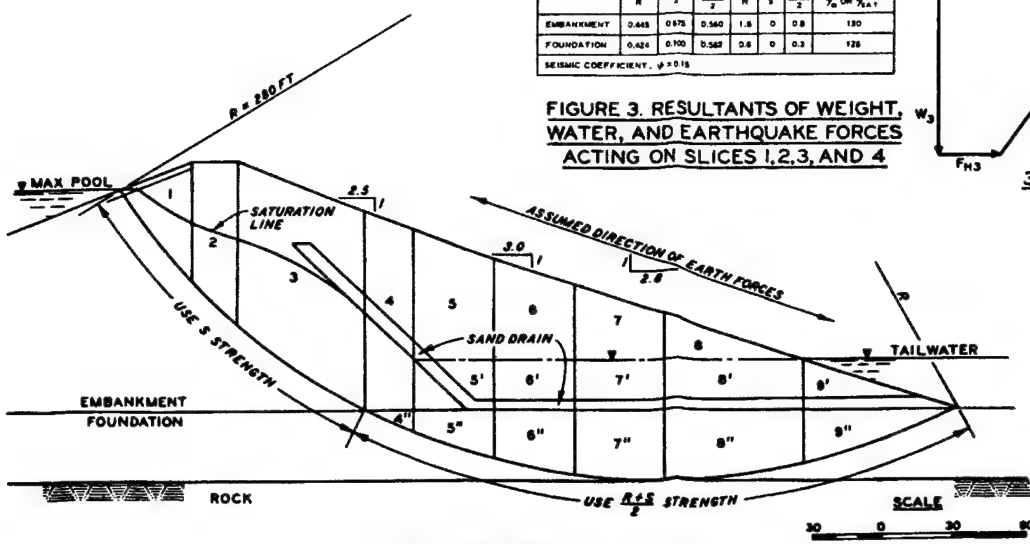

FIGURE 1. EMBANKMENT SECTION
(SAME AS IN PLATE VI-15)

STABILITY ANALYSIS, CASE VII — EARTHQUAKE, STEADY SEEPAGE, DOWNSTREAM SLOPE, MODIFIED SWEDISH METHOD, FINITE SLICE PROCEDURE

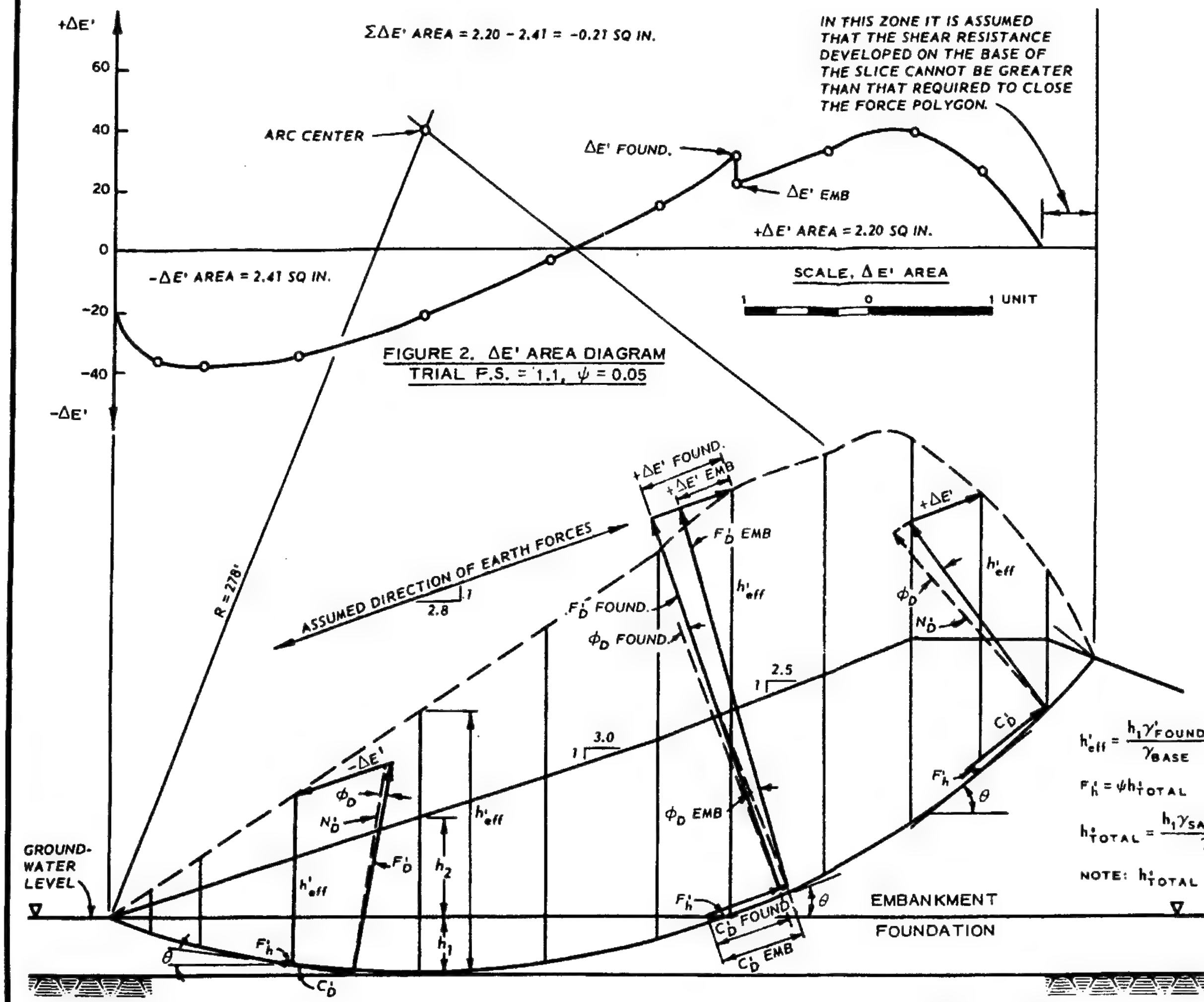

FIGURE 2. $\Delta E'$ AREA DIAGRAM
TRIAL F.S. = 1.1, ψ = 0.05

FIGURE 1. EMBANKMENT SECTION AND UNIT SLICE
FORCE POLYGONS, TRIAL F.S. = 1.1, ψ = 0.05

ADOPTED DESIGN DATA							
MATERIAL	UNIT WEIGHT PCF			Q STRENGTH			ψ
	γ	γ_{SAT}	γ'	ϕ DEG	TAN ϕ	c KSF	
EMB	135	—	—	5	0.088	1.78	0.05
FOUND.	—	127.5	65.0	2	0.035	1.60	

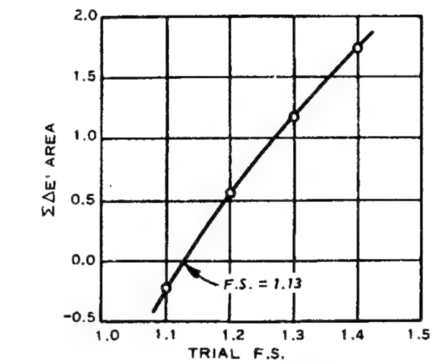

FIGURE 3. TRIAL F.S. VERSUS $\Sigma\Delta E'$

$h'_{eff} = \dfrac{h_1\gamma'_{FOUND.}}{\gamma_{BASE}} + \dfrac{h_2\gamma_{EMB}}{\gamma_{BASE}}$, USING $\gamma_{BASE} = \gamma'_{FOUND.} = 65$ PCF : $h'_{eff} = h_1 + 2.076\, h_2$

$F'_h = \psi h^t_{TOTAL}$

$h^t_{TOTAL} = \dfrac{h_1\gamma_{SAT\ (FOUND.)}}{\gamma_{BASE}} + \dfrac{h_2\gamma_{EMB}}{\gamma_{BASE}}$, USING $\gamma_{BASE} = \gamma'_{FOUND.} = 65$ PCF : $h^t_{TOTAL} = 1.96\, h_1 + 2.076\, h_2$

NOTE: h^t_{TOTAL} IS USED ONLY TO COMPUTE F'_h; h'_{eff} IS USED IN THE FORCE POLYGONS.

NOTE: EMBANKMENT SECTION AND ADOPTED DESIGN DATA ARE SAME AS IN PLATE VI-9.

STABILITY ANALYSIS, CASE VII - EARTHQUAKE, END OF CONSTRUCTION MODIFIED SWEDISH METHOD GRAPHICAL INTEGRATION PROCEDURE

APPENDIX VII

Wedge Analysis

1. General. The procedures presented in this appendix assume that shear failure may occur in an embankment and its foundation along a surface approximated by a series of planes. These procedures are variations of what is generally termed the wedge method of analysis. This method is particularly applicable to a zoned embankment containing cohesionless outer shells and a relatively thin core resting on either homogeneous or stratified foundation materials. The analyses presented in this appendix emphasize the application of the wedge method to embankments having impervious cores with gravel or rock shells and demonstrate the influence of the location of the core on embankment stability. Examples are given for embankments with central impervious cores, and for embankments with inclined impervious cores located within the upstream portions of the embankments. The planes defining the boundaries of the sliding mass that are shown in the examples are not necessarily the most critical failure planes, since the examples are presented only to illustrate the procedures involved.

2. Basic Principles. In the wedge method, the soil mass is usually divided into three segments: an active wedge, a central block, and a passive wedge, as shown in figure 1 of plate VII-1. Vertical boundaries are assumed between the central block and the active and passive wedges. The forces on each segment are considered separately as shown in figures 2 through 4 of plate VII-1. The developed values of cohesion and angle of internal friction along the failure surfaces are controlled by the assumed trial factor of safety, F.S., so that

$$c_D = c/F.S.$$

$$\tan \phi_D = (\tan \phi)/F.S.$$

Consequently, the magnitudes of the resultant earth forces E_A and E_P also

depend on the trial safety factor. The resultant earth forces acting at the vertical boundaries of the passive and active wedges are determined by constructing force polygons, as illustrated in figures 2 and 3, respectively, of plate VII-1, and are then incorporated in the force polygon for the central block (fig. 4). A condition of equilibrium will generally not be obtained on the first trial and several trial analyses with different safety factors are required. In each analysis, the force necessary to close the polygon (fig. 4, plate VII-1) is denoted as ΔE_H. The force ΔE_H is assumed to act horizontally and its magnitude and sign vary with the trial factor of safety. A plot is made of ΔE_H versus the trial factors of safety, as shown in figure 5, plate VII-1, to determine the factor of safety at which ΔE_H is zero. This factor of safety is that required to balance the forces for the sliding surface being analyzed. Various trial locations of the active and passive wedges are required to determine the minimum safety factor.

3. Basic Criteria. Criteria for selecting the direction of the active and passive earth forces are illustrated in plate VII-2. However, these criteria are illustrative only and should be modified where differential foundation settlement resulting from consolidation of soft layers or from a variable subsoil profile makes this desirable. The criteria shown in plate VII-2 apply only where the maximum settlement will occur beneath the center of the embankment. The location of the critical sliding planes is often controlled by weak zones, such as a foundation layer and/or an inclined impervious core, and must be determined by trial. In general, sliding will occur near the bottom of a weak layer. In the discussions that follow, a thin weak layer has been assumed.

a. Active Earth Forces. (1) A general rule for selecting the direction of E_A is shown in the tabulation in figure 1 of plate VII-2. When the sliding surface lies in cohesive materials or includes a portion of the crest or reverse slope (plate VII-2), the maximum value of E_A must be determined by trial force polygons using various values of θ_A. As a first trial, θ_A can be assumed equal to $45^\circ + (\phi/2)$. When the sliding plane is located within a

thin inclined core, the slope of the core will generally govern the angle of the sliding plane.

(2) The maximum value of E_A and corresponding value of θ_A can be determined using the conjugate stress procedure illustrated in plate VII-3 when (a) the active sliding surface is in cohesionless materials, (b) the entire active wedge is under the slope, (c) E_A acts parallel to the outer slope (fig. 1(b), plate VII-2), and (d) seepage forces are not present. The active earth force may also be computed by obtaining the earth pressure coefficient K_A from earth pressure tables[14] using the value of ϕ_D and the assumed angle of the active earth force as the angle of wall friction.

(3) When the active wedge is composed of different materials (fig. 1(c), plate VII-2), the angles of the active sliding surfaces depend on the shear strengths of the soils involved. However, in preliminary design analyses for dams and for design of levees, channels, miscellaneous embankments, and other structures, the active sliding surface can be assumed to be inclined at $45^\circ + \phi/2$ for each material. For final design analyses of dams and for design of more critical earth structures, θ_A should be varied within each soil zone through which the active sliding surface passes until the maximum value of E_A is found. To determine the magnitude of the resultant active force, the wedge must be subdivided as shown in figure 1(c) and the total earth force at each boundary determined as shown by the force polygon. The direction of the resultant forces E_{A1}, E_{A2}, and E_A are assumed to be in accordance with the general rule given in plate VII-2. Other trial locations of the plane ac are necessary in all analyses to determine the lowest factor of safety.

b. Central Block. (1) Where the failure plane beneath the central block passes through more than one material or where the failure plane passes through a single material but a different shear strength is used because of changing normal stress (e.g. using a composite S and R envelope), the central block should be broken up into its component parts based on material type (or shear strength) as described previously for the active wedge.

Resultant forces acting on boundaries between these "subblocks" can be assumed to be inclined at any value intermediate between the inclination of E_A and E_P, but are more conveniently assumed to be horizontal. With this latter assumption, the normal stress on the failure plane is equal to the overburden stress.

(2) The case should also be considered where a horizontal failure surface parallels a boundary between different materials (for example, a clay stratum overlying or underlying cohesionless material). In such a case, the lowest shear resistance along this failure surface may be when sliding is partially in one material and partially in the other; this occurs because sliding in the cohesionless layer may offer less shear resistance than in the clay under low effective normal stresses, whereas under high effective normal stresses the reverse may be true. The point at which this "switch" occurs can easily be determined by computing the normal stress at which the strength envelopes for the two materials intersect.

c. <u>Passive Earth Forces.</u> (1) When the passive wedge is near the toe of the embankment, as in the case shown in figure 2(a), plate VII-2, in which sliding is assumed to occur along a weak plane within the foundation, the direction of E_P is assumed to be horizontal. The passive wedge will usually be separated from the active wedge by a central block, and trial locations of the vertical boundary between the passive wedge and central block are required to determine the lowest factor of safety, as illustrated in figure 2(a). Where the passive wedge is located in cohesionless material and the vertical boundary is at the toe of the embankment (wedge A in fig. 2(a), plate VII-2), the resultant passive soil resistance E_P can be determined graphically or from the equation

$$E_P = 1/2\ \gamma\ h^2 K_P$$

in which

$$K_P = \frac{1 + \sin \phi_D}{1 - \sin \phi_D}$$

When the vertical boundary is not at the toe of the embankment, trial values of θ_P must be assumed for each trial factor of safety until a minimum value of E_P is obtained. When the passive wedge includes several soil zones, θ_P should be varied and the criteria in paragraph 3a(3) applies.

(2) Where sliding is assumed to occur along the ground surface as shown in figure 2(b), plate VII-2, the inclination of E_P is assumed to be the same as that of E_A. If a central block is present, E_P acts parallel to the outer slope. The magnitude of E_P is determined from force polygons for various trial factors of safety. When the embankment material is cohesionless and the foundation is stronger than the embankment, a passive sliding plane is assumed to intersect the toe of the embankment and make an angle of θ_P with the horizontal (fig. 2(c), plate VII-2). In this case, E_P acts parallel to the outer slope and the conjugate stress procedure (plate VII-3) may be used to determine θ_P and E_P for each trial factor of safety.

(3) Examples of the criteria above and procedures for handling water forces for various design cases are described in the following paragraphs.

4. <u>End of Construction--Case I.</u>† The end-of-construction stability of an embankment composed of a granular shell and impervious cohesive core is influenced by the core location. Accordingly, examples for embankments with both central and inclined cores are presented. Unit weights and shear strengths should correspond to those expected at the end of construction, as discussed in paragraphs 9 and 11a of the main text. In the analysis, S shear strengths are used for free-draining embankment and foundation materials and Q strengths are used for impervious core or foundation soils. The R strengths may be used for relatively thin clay strata in the foundation when consolidation will be essentially complete at the end of construction. In some cases, it may be necessary to use a design strength intermediate between Q and R. Additional analyses should be made during construction of the embankment, as discussed in Appendix VIII.

---

† Case designations are described in paragraph 11 of the main text.

a. Embankment with Central Core. (1) Where the foundation strength is equal to or greater than the strength of a cohesionless embankment shell flanking a narrow central core, the safety factor can be estimated using the infinite slope equation $F.S. = \frac{\tan \phi}{\tan \beta}$, as discussed in Appendix V.

(2) For conditions where the foundation contains a layer that is weaker than the shell, the factor of safety must be found by trial. This condition is illustrated in plate VII-4. The assumed failure mass is divided into an active wedge, a central block, and a passive wedge. A trial point 1 is selected for the upper end of a series of active wedges corresponding to various trial factors of safety. The earth force E_A and the inclination θ_A of the active sliding plane can be determined for each trial safety factor according to the conjugate stress procedure, since the earth force E_A is assumed to be parallel to the outer slope. A simplified conjugate stress procedure for determining K_A and θ_A is shown in figure 2 of plate VII-4. The direction of the earth force E_P is assumed to be horizontal. Because the upper surface of the passive wedge in the example is horizontal, the passive pressure coefficient K_P is that given in figure 2. The computation of the passive force E_P is also given in this figure. When several types of material are contained within the active or passive wedges, E_P and E_A can be determined from force diagrams.

(3) Using the values above for E_A and E_P, a force polygon for the central block can be constructed as shown in figure 3 of plate VII-4. The polygon does not close by the force ΔE_H. A plot of ΔE_H versus trial factors of safety is used as shown in figure 4, plate VII-4, to obtain the factor of safety when ΔE_H is zero and the force polygon closes. Other trial locations of the active and passive wedges should be used to find the minimum safety factor. When a portion of the active plane passes through the core, E_A is determined by trial by constructing a force polygon as shown in figure 1(c), plate VII-2.

b. Embankment with Inclined Core. (1) The failure surface for this condition will normally be located in the lower strength core material. While

the zone of minimum strength is probably near the middle of the core, because consolidation takes place at a slower rate here than at the outer faces, the failure surface is normally assumed to lie along the downstream boundary where the largest driving force is obtained. If the foundation is as strong as or stronger than the shell, the lower portion of the trial failure surface will be entirely in the shell. This case is illustrated in plate VII-5.

(2) In the embankment section shown in figure 1, plate VII-5, the toe of the passive wedge is assumed to coincide with the outer toe of the dam. The inclination of the base of the passive wedge and the magnitude of the earth force E_P are determined from the conjugate stress assumption, as discussed in paragraph 3c of this appendix and as shown in figure 2, plate VII-5, for a trial safety factor of 1.5. When the trial sliding plane of the active wedge is along the boundary of two embankment zones, the trial sliding surface plane should be located in the material having the lower developed shear strength so that the maximum resultant active earth force is obtained. In the case shown in plate VII-5, the S shear strength of the material in downstream gravel filter is less than the Q shear strength of the core under low normal stresses, but the reverse is true under higher loads; therefore minimum resistance is obtained when the upper portion of the sliding surface is in the filter and the lower portion is in the core. A method of locating the break point is illustrated in figure 1 of plate VII-5. Several trial locations (A, B, and C in fig. 1) are selected, and the weight of the active wedge to the right of each location is determined. A force polygon is constructed at each trial location using the developed shear strength of each material; the developed Q strength of the core and the developed S strength of the gravel filter are used in the case of the example in plate VII-5. The intersection of the friction vector for the developed S strength $F_{A(S)}$ with the E_A vector is located for each polygon, and a smooth curve is drawn through these points. A similar curve is drawn through the intersections of E_A and $F_{A(Q)}$ vectors. The intersection of the two curves locates the point where the two shear strengths result in the same value of E_A (point D in fig. 1).

From this point, a line parallel to the S strength friction vector $F_{A(S)}$ is drawn to the sliding surface (dashed line from point D to point E in fig. 1 of plate VII-5). This locates point E on the sliding surface, to the right of which the plane of sliding would lie in the gravel filter and to the left of which sliding would occur in the core. The force polygons for the active wedge and central block are shown in figures 3 and 4, respectively. The forces ΔE_H required to close the force polygons for the central block are plotted versus trial safety factors in figure 5, where the factor of safety to balance forces for the sliding surfaces analyzed is shown to be 1.62.

(3) If the foundation has a lower shear strength than the embankment shell, the trial failure surface will pass through the foundation.

5. Sudden Drawdown--Cases II and III. Appropriate unit weights, shear strengths, and design assumptions to be used in sudden drawdown analyses are described in paragraph 11b of the main text. In the wedge method, the active and passive forces are influenced by seepage forces when materials in the shell are semipervious.

a. Embankment with Central Core. (1) Sudden drawdown is not generally critical for embankments having free-draining shell materials and a narrow central core, and this case need not be analyzed unless a relatively weak layer is present in the foundation. The safety factor of free-draining cohesionless shell materials can be approximated using the infinite slope method described in Appendix V. However, detailed stability analyses are required when the upstream shell is composed of sands or gravels of low permeability. If the foundation contains a thin layer that is not as strong as the shell, the horizontal portion of the trial sliding surface will pass through the weaker foundation layer, as illustrated in figure 1, plate VII-6, for an embankment having semipervious shells. The potential failure mass is divided into a passive wedge, a central block, and an active wedge. Because the shell material is semipervious, it may be necessary to construct a drawdown flow net to evaluate the seepage forces. Various trial locations of the boundaries between the wedges and the central block and various

inclinations of the active and passive sliding planes must be assumed.

(2) In the example shown in plate VII-6, the boundary between the passive wedge and central block is assumed to be at the toe of the embankment; the computations for E_P are shown directly below figure 1. A trial location with θ_A = 33.5 deg is assumed for the active sliding plane.

(3) The use of the R or S shear strengths along the trial sliding planes is established by comparing the normal stress at the inflection point of the composite shear strength envelopes shown in figure 2 with the approximate effective normal stresses along the trial failure planes. The procedure for doing this is demonstrated in plate VII-6.

(4) The force polygons for the active wedge and for the central block are shown in figure 3 of plate VII-6 for a trial factor of safety of 1.3. Various safety factors are tried until a balance of forces is obtained. A plot of ΔE_H versus trial factor of safety is shown in figure 4 of plate VII-6 for the trial locations of the active and passive wedges. Other trial locations are required to determine the minimum factor of safety. A check of the lower (1 on 3.5) portion of the outer embankment slope, using the equation for horizontal flow given in Appendix V, results in a factor of safety of 1.28; the factor of safety for the upper 1-on-3 slope ranges from 1.07 for horizontal flow to 1.17 for flow parallel to the outer slope, with an average factor of safety of 1.12. Therefore, the surface of the outer slope has a low factor of safety for sudden drawdown as compared to a failure surface through the embankment and the weak foundation. If there is an appreciable thickness of riprap on the outer slope, the weight of riprap should be taken into consideration in the analysis.

b. Embankment with Inclined Core. (1) The sliding surface in the inclined core is assumed to be located along the boundary between the core and the upstream shell because the shear strength of this portion of the core is not increased by seepage forces prior to drawdown. However, stability should also be checked with the sliding surface at the downstream boundary of the core, assuming that the core along the sliding surface is fully

consolidated under the weight of overlying material and by seepage forces. When the foundation is stronger than the embankment, the failure mass consists of an active and a passive wedge, with the toe of the passive wedge coinciding with the toe of the embankment as shown in figure 1, plate VII-7. The inclination of the base of the passive wedge θ_P and the passive force E_P are determined using the conjugate stress assumption as shown in figure 3. The most critical condition for each trial factor of safety is obtained with the passive wedge completely submerged, and thus the critical lowered pool level for each trial factor of safety should be located to intersect the upstream slope at the top of the vertical boundary between the active and passive wedges. If the location of the estimated actual drawdown pool level is above or below the critical lowered pool level, the factor of safety will be slightly higher than that for the critical lowered pool level.

(2) In evaluating the active force E_A (fig. 4, plate VII-7), the frictional force F_A is based on the submerged weight of the rock fill and filter (W_{A1} and W_{A2}) below the maximum pool level and the moist weight of the rock fill and filter (W_{A3}) above this level. During sudden drawdown, the upstream shell above the low pool level changes in weight from submerged to moist. It is assumed that this added increment of weight induces pore pressure, but does not cause any immediate gain of shear strength in the core. The induced pore pressure force created by the difference between the moist and submerged weights is represented in the force polygon in figure 4 by U_A This force need not be explicitly computed, as can be seen from the force polygon. Figure 4 shows that the resultant of U_A and the change in weight of the shell (492 kips) contribute a major portion of E_A

(3) Curves of E_P and E_A for various trial factors of safety are presented in figure 5, plate VII-7. A condition of equality between E_P and E_A for the sliding surface analyzed exists for a factor of safety equal to 1.23 in the case illustrated.

(4) If the shell is stronger than the foundation, the passive sliding plane will be in the foundation and full drawdown should be considered. If high

tailwater conditions will exist during spillway operations, a check of the downstream toe for sudden drawdown should be made.

6. Partial Pool, Upstream Slope--Case IV. A static reservoir reduces the stability of the upstream slope because of reduction in weight and resistance of the passive wedge due to buoyancy. In many cases, a pool elevation above conservation pool elevation is critical; this critical elevation must be determined by trial. Basic assumptions and shear strengths for this case are described in paragraph 11c of the main text.

a. Embankment with Central Core. The procedure used is similar to that discussed in paragraph 4a of this appendix, except that a horizontal saturation line is assumed within the embankment at the trial level of the pool. Either the S or $\frac{R+S}{2}$ shear strength of the core is used, depending on the magnitude of the effective normal stress.

b. Embankment with Inclined Core. (1) A stability analysis for an embankment with an inclined core on a strong foundation is shown in plate VII-8. The embankment section is shown in figure 1 of the plate. The inclination of the passive sliding plane θ_P and the passive earth force E_P for a trial factor of safety of 1.5 are determined as shown in figure 2. As in the sudden drawdown case, the most critical condition for each trial factor of safety is obtained with the passive wedge completely submerged, and thus the lowered pool level for each trial factor of safety should be located to intersect the upstream slope at the top of the vertical boundary between the active and passive wedges. Submerged weights are used below the partial pool elevation and moist unit weights above.

(2) Computations to the right of figure 1, plate VII-8, illustrate a simplified procedure for computing normal stresses on the trial failure planes for determining use of S or $\frac{R+S}{2}$ strengths. Composite strength envelopes are shown in figure 3.

(3) The value of E_A is determined from a force polygon as shown in figure 4, plate VII-8. The comparison of E_A and E_P versus trial factor of safety, shown in figure 5, indicates that the factor of safety for the sliding

surfaces analyzed is 1.51.

(4) This case should also be analyzed assuming the active sliding plane at the downstream face of the core with the pool level at several locations to check for a more critical condition. The analyses should assume that the core is consolidated under the overlying weights corresponding to the critical pool elevation.

(5) If the foundation is weaker than the shell, the passive sliding plane will be in the foundation, and the passive resistance is determined using a central block in a manner similar to that shown in plate VII-6.

7. Steady Seepage with Maximum Storage Pool--Case V. Steady seepage reduces the weight of the soil mass below the saturation line by hydrostatic uplift, and thus frictional shearing resistance is reduced. At the same time, the water forces of the reservoir pool act horizontally against the impervious core in the downstream direction. Basic criteria and shear strength to use are discussed in paragraph 11d of the main text.

a. Embankment with Central Core. (1) If the core is narrow with steep slopes and the embankment rests on a strong foundation, only the stability of the downstream shell need be examined. If the shell material is cohesionless and free draining, the critical sliding surface is the slope of the outer shell, and the factor of safety can be expressed as

$$F.S. = b \tan \phi$$

where

b = cotangent of the downstream embankment slope

ϕ = angle of internal friction of the shell material

Where cores are wide or foundations are weaker than the shell, the most critical sliding surfaces may pass through these zones and must be found by trial. Where the shear strength of the foundation is less than that of the shell material, the weakest horizontal sliding surface may be either in the shell just above the foundation, slightly within the foundation layer, or at the

bottom of the foundation layer, depending upon the normal loads and shear strengths. An example is given in plate VII-9. The active wedge and central block are divided into intermediate sections at boundaries where the shear strength parameters change. Composite strength diagrams are shown in figure 2, and computations to determine where the S or $\frac{R + S}{2}$ strength should be used are given.

(2) Since the active wedge portion A1, located in the cohesionless shell, is not entirely submerged, the maximum value of the active resultant force E_{A1} must be determined graphically (fig. 3, plate VII-9) based on the weight W_{A1} and direction of F_{A1} for each trial factor of safety. Values of θ_{A1} can be determined from plate VII-11 or by trial. However, θ_{A1} varies only slightly for the trial factors of safety used in the example, and a value of 65 deg is used for all trial factors of safety. When that portion of the active wedge in cohesionless material is completely submerged (or completely above the seepage line) E_{A1} can be computed using the chart in plate VII-12. The determination of the hydrostatic forces is shown in figure 1, and the values of E_A (for θ_{A2} = 50 deg) and E_P are shown in figures 4 and 5, respectively, of plate VII-9.

(3) The magnitude of E_A for each trial safety factor varies with the assumed inclination of the base of the active wedge θ_{A2} which must be varied to obtain the maximum value of E_A. A plot of E_A and E_P versus trial factors of safety is shown in figure 6, plate VII-9. It should be noted from figure 6 that θ_{A2} for the lowest factor of safety is 60 deg.

b. Embankment with Inclined Cores. The steady seepage case is not critical for an embankment with an inclined upstream core on a strong foundation. Conditions existing either at the end of construction or sudden drawdown are usually the critical cases for such a design.

8. Steady Seepage with Surcharge Pool--Case VI. This case applies after a condition of steady seepage has been established at a given pool level, the reservoir pool quickly rises to the surcharge pool level, and no appreciable change in the seepage pattern takes place because of the short duration at the

higher level. This analysis is especially applicable to rock-fill dams having narrow central cores. The procedure of analysis and shear strength criteria used for this case are identical to those given for Case V; the only difference in the two analyses is that in Case VI the horizontal thrust from the surcharge pool is added to the active wedge force polygon and the unit weight of that portion of the pervious upstream zone between the surcharge pool and the storage pool becomes submerged instead of moist. An example of this analysis is given in plate VII-10 where a surcharge pool has been applied to the steady seepage example shown in plate VII-9.

9. Earthquake. As discussed in paragraph 11f of the main text, it is assumed that the earthquake imparts an additional horizontal force F_h acting in the direction of sliding of the potential failure mass. This force is equal to the total weight of the sliding soil mass W times the seismic coefficient ψ. The weight W is based on the saturated unit weight below and moist unit weight above the saturation line, but does not include the weight of water above the embankment slope. In the wedge analysis, horizontal seismic forces are computed individually for the active wedge, the passive wedge, and the central block, and included in the respective force polygons.

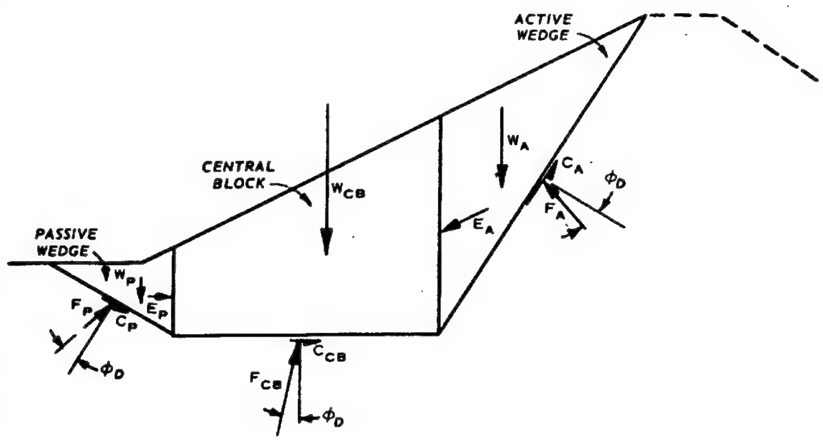

FIGURE 1. EMBANKMENT SECTION

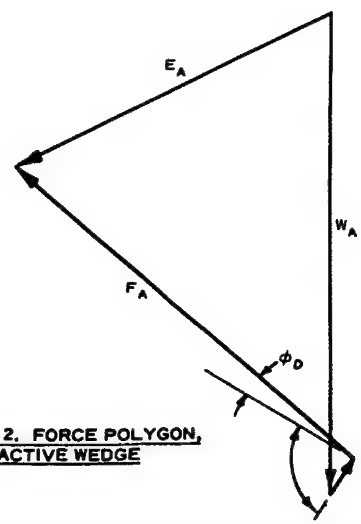

FIGURE 2. FORCE POLYGON, ACTIVE WEDGE

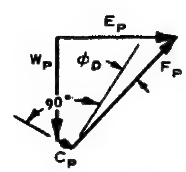

FIGURE 3. FORCE POLYGON, PASSIVE WEDGE

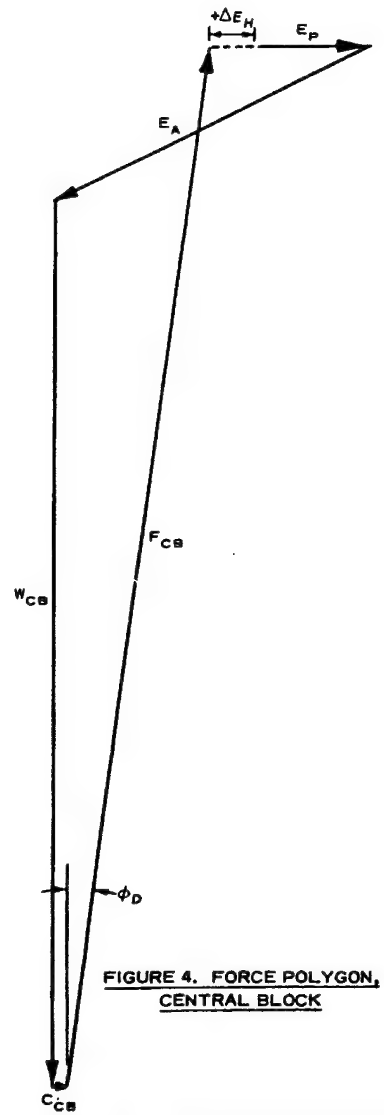

FIGURE 4. FORCE POLYGON, CENTRAL BLOCK

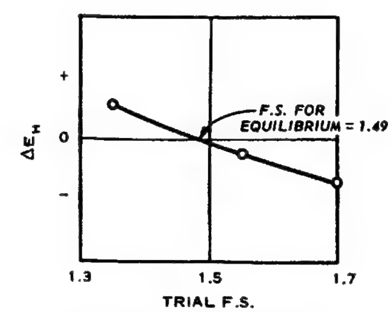

FIGURE 5. TRIAL FACTOR OF SAFETY VS ΔE

STABILITY ANALYSIS
WEDGE METHOD

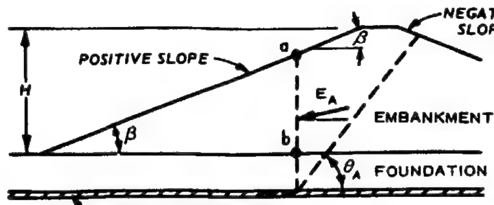

(a) ACTIVE WEDGE IN COHESIVE MATERIAL OR PARTIALLY UNDER CREST IN COHESIONLESS MATERIAL. (SOLVE FOR E_A USING FORCE POLYGON.)

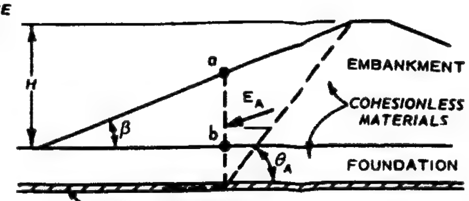

(b) ACTIVE WEDGE IN COHESIONLESS MATERIAL AND ENTIRELY UNDER SLOPE. (SOLVE FOR E_A USING CONJUGATE STRESS ANALYSIS.)

INCLINATION OF E_A FOR ALL CASES (POSITIVE SLOPE*)		
	ANGLE OF E_A WITH HORIZONTAL	
HEIGHT, $\overline{ab}$	SANDS AND SILTS	CLAYS
$ab < 5/8H$	β	$\beta/2$
$5/8H \le ab \le 7/8H$	$\beta/2$	$\beta/2$
$ab > 7/8H$	0	0

* E_A HORIZONTAL FOR SEGMENT UNDER NEGATIVE SLOPE

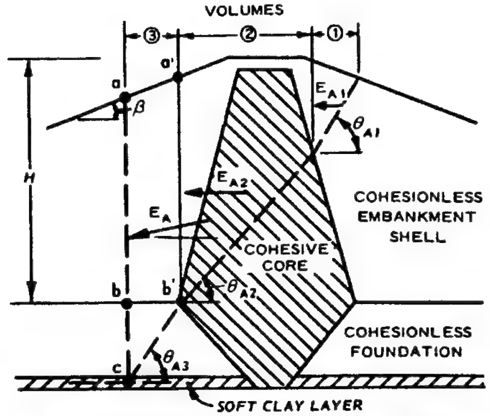

(c) ACTIVE WEDGE INCLUDES DIFFERENT MATERIALS. (SOLVE FOR E_A USING FORCE POLYGON.)

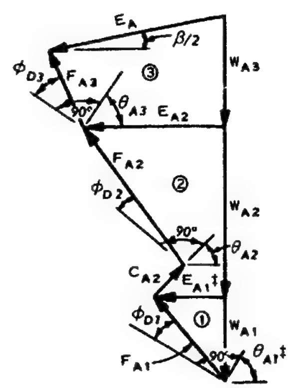

FIGURE 1. ACTIVE WEDGES

‡ FOR HOMOGENEOUS SANDS AND SILTS, E_{A1} AND θ_{A1} CAN BE DETERMINED DIRECTLY FROM PLATES VII-11 AND VII-12.

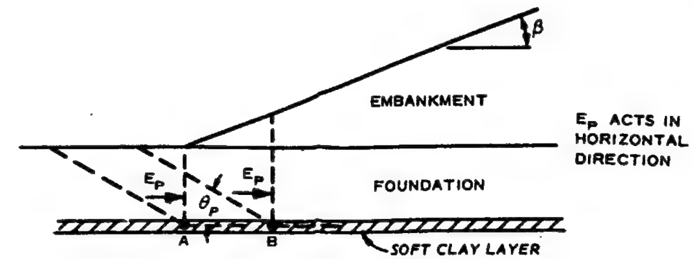

(a) SLIDING IN FOUNDATION

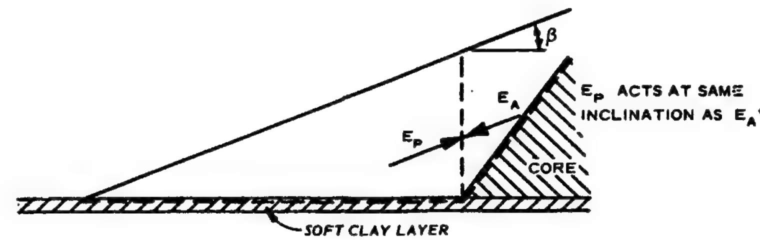

(b) SLIDING AT GROUND SURFACE

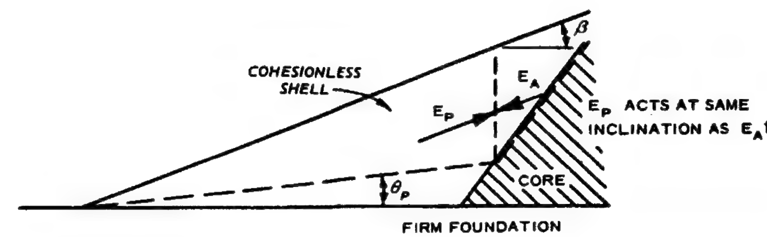

(c) SLIDING IN EMBANKMENT

FIGURE 2. PASSIVE WEDGES

† HOWEVER IF THERE IS A CENTRAL BLOCK, E_P ACTS PARALLEL TO THE OUTER SLOPE.

DIRECTION OF RESULTANT EARTH FORCES AND ACTIVE AND PASSIVE SLIDING PLANES, WEDGE METHOD

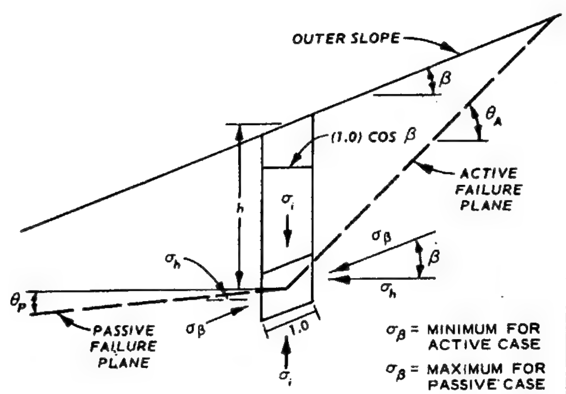

FIGURE 1. CONJUGATE STRESSES, COHESIONLESS EMBANKMENT, NO SEEPAGE FORCES

σ_i = VERTICAL STRESS ON PLANE PARALLEL TO OUTER SLOPE = $\gamma_h \cos\beta$ (WHERE γ_h = VERTICAL STRESS ON HORIZONTAL PLANE AT DEPTH h)

σ_h = HORIZONTAL STRESS ON VERTICAL PLANE = $\sigma_\beta \cos\beta$

K = EARTH PRESSURE COEFFICIENT = $\dfrac{\sigma_h}{\sigma_i} = \dfrac{\sigma_\beta \cos\beta}{\gamma_h \cos\beta}$

SINCE σ_β AND σ_i ARE EACH PARALLEL TO THE PLANE OF THE OTHER, THEY ARE CONJUGATE STRESSES. AN INFINITE SLOPE IS ASSUMED, AND σ_i IS CONSTANT AT DEPTH h ALONG THE SLOPE.

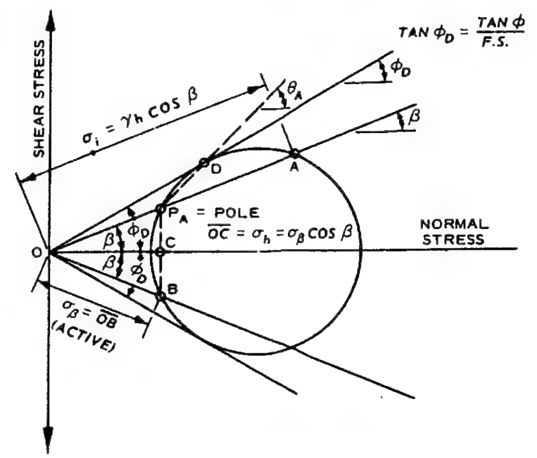

FIGURE 2. PROCEDURE FOR DETERMINING K_A & θ_A, ACTIVE CASE (σ_β = MINIMUM)

1. CONSTRUCT LINES AT ANGLES ϕ_D AND β.
2. CONSTRUCT CIRCLE OF CONVENIENT SIZE TANGENT TO LINE AT ANGLE ϕ_D. (IN THE EXAMPLE SHOWN THE SCALE IS SUCH THAT $\overline{OA} = \sigma_i = \gamma_h \cos\beta$, BUT THIS IS NOT ESSENTIAL TO DETERMINATION OF K_A*.)
3. CONSTRUCT VERTICAL LINE FROM THE POLE P_A TO INTERSECT THE CIRCLE AT B.
4. THE DISTANCE $\overline{OB}$ IN THE EXAMPLE EQUALS $\sigma_{\beta MIN}$ AND $\overline{OC} = (\sigma_{\beta MIN}) \cos\beta = \sigma_h$

   THEN $K_A = \dfrac{\sigma_h}{\sigma_i} = \dfrac{\overline{OC}}{\overline{OA}}$
5. THE ANGLE θ_A, WHICH DEFINES THE DIRECTION OF THE ACTIVE FAILURE PLANE, IS THE ANGLE FORMED WITH THE HORIZONTAL BY A LINE FROM THE POLE THROUGH THE POINT OF TANGENCY BETWEEN THE ϕ_D LINE AND THE CIRCLE (POINT D).
6. THE ACTIVE FORCE E_A ACTING ON THE VERTICAL BOUNDARY HAVING DEPTH h BELOW THE SLOPE IS $E_A = \dfrac{\gamma h^2}{2} K_A$

---

* IT IS APPARENT THAT THE RATIO $\dfrac{\overline{OC}}{\overline{OA}}$ IS INDEPENDENT OF THE SCALE USED IN CONSTRUCTING THE CIRCLE.

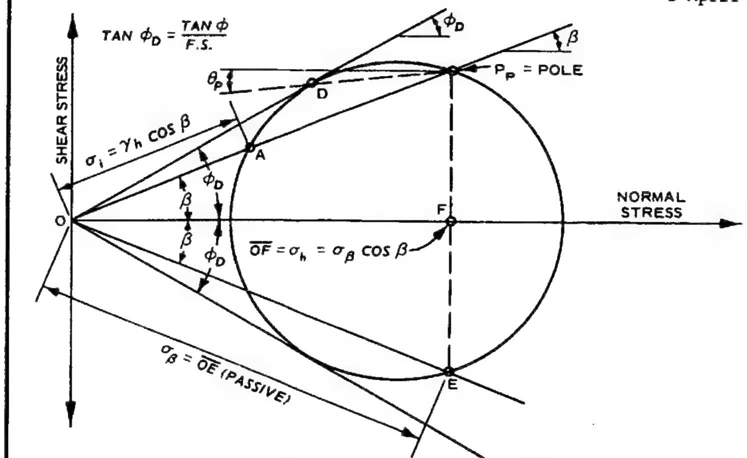

FIGURE 3. PROCEDURE FOR DETERMINING K_P & θ_P, PASSIVE CASE (σ_β = MAXIMUM)

1. CONSTRUCT LINES AT ANGLES ϕ_D AND β.
2. CONSTRUCT CIRCLE OF CONVENIENT SIZE TANGENT TO LINE AT ANGLE ϕ_D. (IN THE EXAMPLE SHOWN, THE SCALE CHOSEN IS SUCH THAT $\overline{OA} = \sigma_i = \gamma_h \cos\beta$, BUT THIS IS NOT ESSENTIAL TO DETERMINATION OF K_P.*)
3. CONSTRUCT VERTICAL LINE FROM POLE P_P TO INTERSECT CIRCLE AT E.
4. THE DISTANCE $\overline{OE}$ IN THE EXAMPLE EQUALS $\sigma_{\beta MAX}$ AND $\overline{OF} = (\sigma_{\beta MAX}) \cos\beta = \sigma_h$.

   THEN $K_P = \dfrac{\sigma_h}{\sigma_i} = \dfrac{\overline{OF}}{\overline{OA}}$
5. THE ANGLE θ_P, WHICH DEFINES THE DISTANCE OF THE PASSIVE FAILURE PLANE IS THAT ANGLE FORMED WITH THE HORIZONTAL BY A LINE FROM THE POLE P_P THROUGH THE POINT OF TANGENCY BETWEEN THE ϕ_D LINE AND THE CIRCLE (POINT D).
6. THE PASSIVE FORCE E_P ACTING ON THE VERTICAL BOUNDARY HAVING DEPTH h BELOW THE SLOPE IS $E_P = \dfrac{\gamma h^2}{2} K_P$.

---

* IT IS APPARENT THAT THE RATIO $\dfrac{\overline{OF}}{\overline{OA}}$ IS INDEPENDENT OF THE SCALE USED IN CONSTRUCTING THE CIRCLE.

USE OF CONJUGATE STRESSES

ADOPTED DESIGN DATA						
MATERIAL	UNIT WT LB/CU FT		ϕ DEG		c KIPS/SQ FT	
	γ_m	γ'	R*	S	R	S
COHESIONLESS EMBANKMENT SHELL AND FOUNDATION	130	77	—	35	—	0
SOFT CLAY FOUNDATION*	—	—	14	—	0.3	—

* ASSUMED FULLY CONSOLIDATED UNDER EMBANKMENT, THUS Q STRENGTH NOT APPLICABLE.

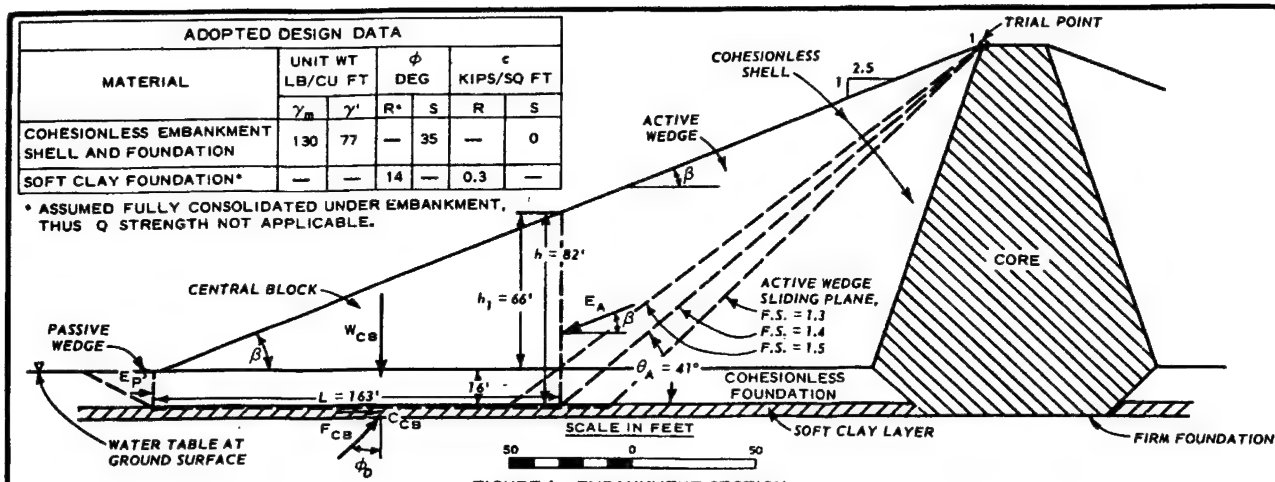

FIGURE 1. EMBANKMENT SECTION

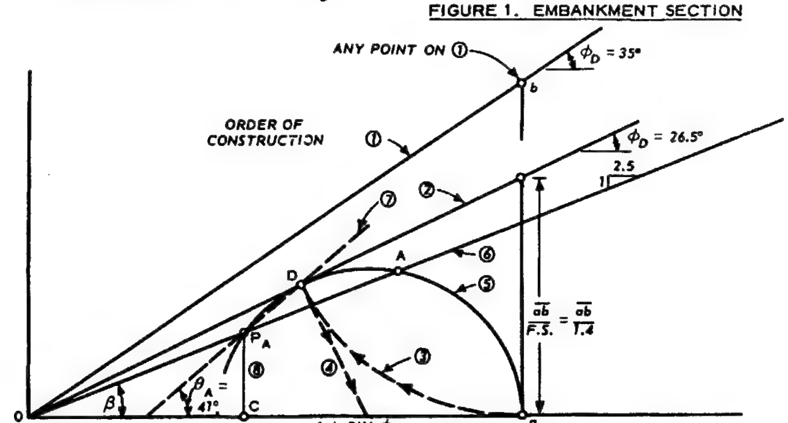

$K_A = \frac{\overline{OC}}{\overline{OA}} = 0.538$

$E_A = \left(\frac{\gamma_m h^2}{2}\right)^* K_A$

$E_A = \left(\frac{0.13(82)^2}{2}\right)0.538$

$E_A = 235$ KIPS

$K_P = \frac{1 + \sin\phi_D}{1 - \sin\phi_D} = \frac{1.446}{0.554} = 2.61$

$E_P = \frac{\gamma' h_2^2}{2} K_P = \frac{0.077(16)^2}{2} \times 2.61$

$E_P = 26$ KIPS

FIGURE 2. DETERMINATION OF E_A & E_P, TRIAL F.S. = 1.4

* THE EFFECT OF SUBMERGENCE OF THE LOWER PORTION OF THE ACTIVE WEDGE IN THIS CASE IS INSIGNIFICANT AND IGNORED HERE. IF AN APPRECIABLE PORTION OF THE ACTIVE WEDGE IS SUBMERGED AS IN CASE IV, PARTIAL POOL, IT IS EASIER TO DETERMINE E_A BY CONSTRUCTING A FORCE POLYGON.

$W_{CB} = \frac{h_1 \times L}{2}\gamma_m + h_2 L \gamma'$

$= \left(\frac{56 \times 163}{2} \times 0.13\right) + (16 \times 163 \times 0.077)$

$= 901$ KIPS

$C_{CB} = C_D \times L = \frac{0.3}{1.4} \times 163 = 35$ KIPS

ϕ_D (CLAY) = ARC TAN $\frac{0.249}{1.4} = 10.1°$

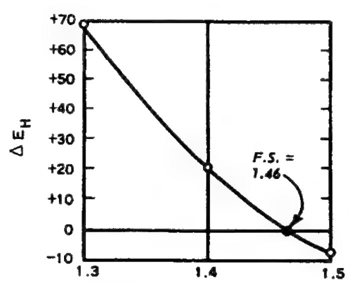

FIGURE 4. TRIAL F.S. VS ΔE

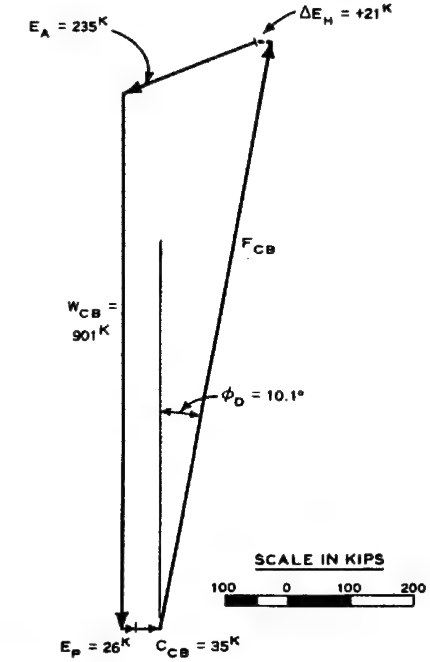

FIGURE 3. FORCE POLYGON, CENTRAL BLOCK TRIAL F.S. = 1.4

STABILITY ANALYSIS OF EMBANKMENT WITH CENTRAL CORE, CASE I - END OF CONSTRUCTION, WEDGE METHOD

MATERIAL	UNIT WT LB/CU FT	ADOPTED DESIGN DATA ϕ DEG		c. KIPS/SQ FT	
	γ_m	Q	S	Q	S.
ROCKFILL	116	—	40	—	0
GRAVEL FILTER	133*	—	35*	—	0
CORE	146	17	—	0.7	—

* ASSUMED SAME AS ROCKFILL IN DETERMINING E_p.

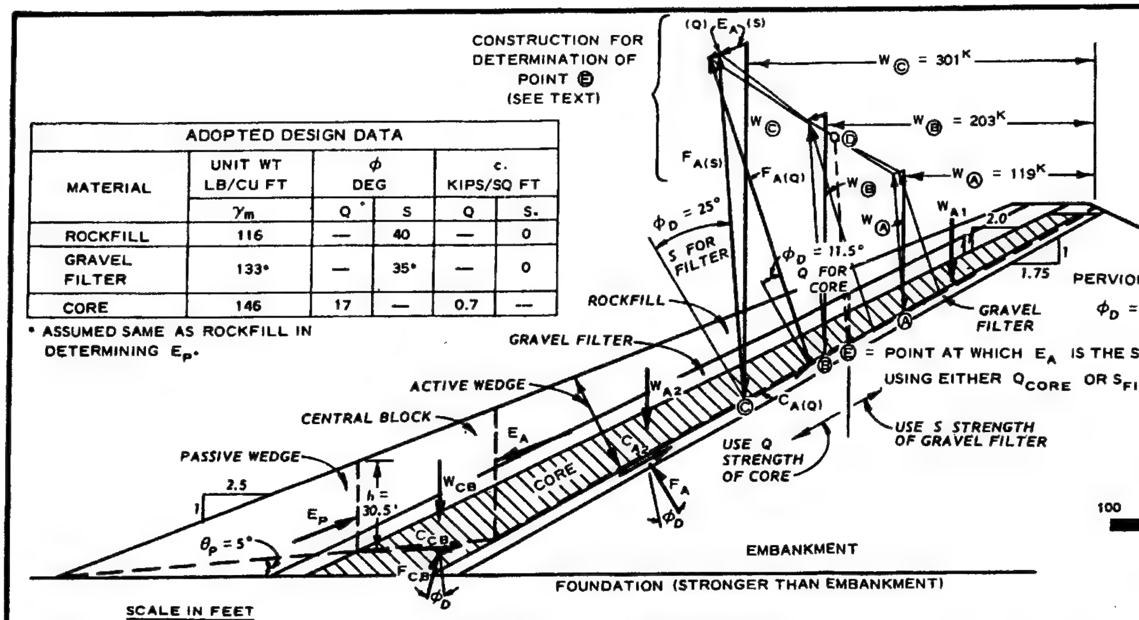

FIGURE 1. EMBANKMENT SECTION

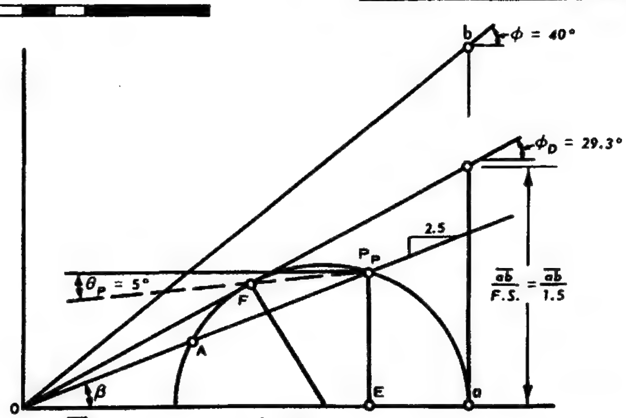

$K_p = \frac{\overline{OE}}{\overline{OA}} = 1.92$ $\qquad E_p = \frac{1}{2}\gamma_m h^2 K_p = \frac{1}{2}(0.116)(30.5)^2(1.92) = 104$ KIPS

FIGURE 2. DETERMINATION OF E_p & θ_p, TRIAL F.S. = 1.5

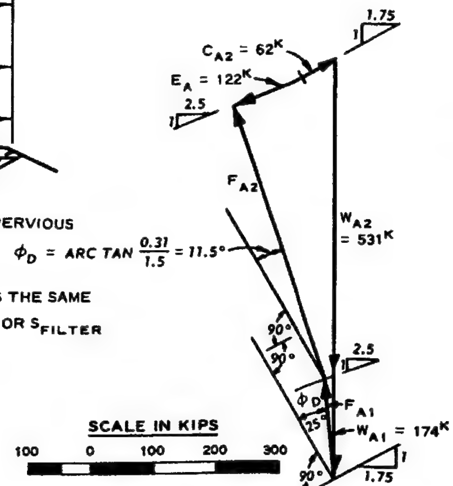

FIGURE 3. FORCE POLYGON ACTIVE WEDGE, TRIAL F.S. = 1.5

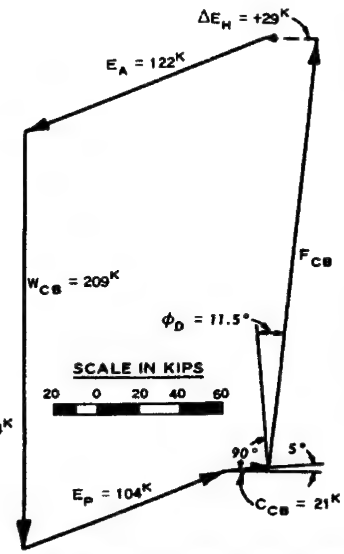

FIGURE 4. FORCE POLYGON, CENTRAL BLOCK, TRIAL F.S. = 1.5

DETERMINATION OF W_{A1} & W_{A2}

	VOL A1 FT^3	VOL A2 FT^3	γ_m KCF	W_{A1} KIPS	W_{A2} KIPS
ROCKFILL	334	1682	0.116	38.8	195.2
FILTER	346	633	0.133	46.0	84.2
CORE	610	1720	0.146	89.0	252.0
			TOTAL:	173.8^K	531.4^K

DETERMINATION OF W_{CB}

ROCKFILL	1002 FT^3 × 0.116 KCF = 116.3^K
FILTER	245 FT^3 × 0.133 KCF = 32.6
CORE	412 FT^3 × 0.146 KCF = 60.1
	TOTAL = 209.0^K

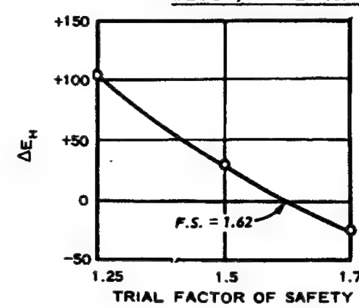

FIGURE 5. TRIAL F.S. VS ΔE

STABILITY ANALYSIS OF EMBANKMENT WITH INCLINED CORE, CASE I - END OF CONSTRUCTION, WEDGE METHOD

ADOPTED DESIGN DATA						
MATERIAL	UNIT WT LB/CU FT		TAN ϕ		c KIPS/SQ FT	
	γ_{SAT}	γ'	R	S	R	S
SHELL AND COHESIONLESS FOUNDATION	140	78	0.466	0.700	1.0	0
CLAY FOUNDATION	---	---	0.344	0.577	0.7	0

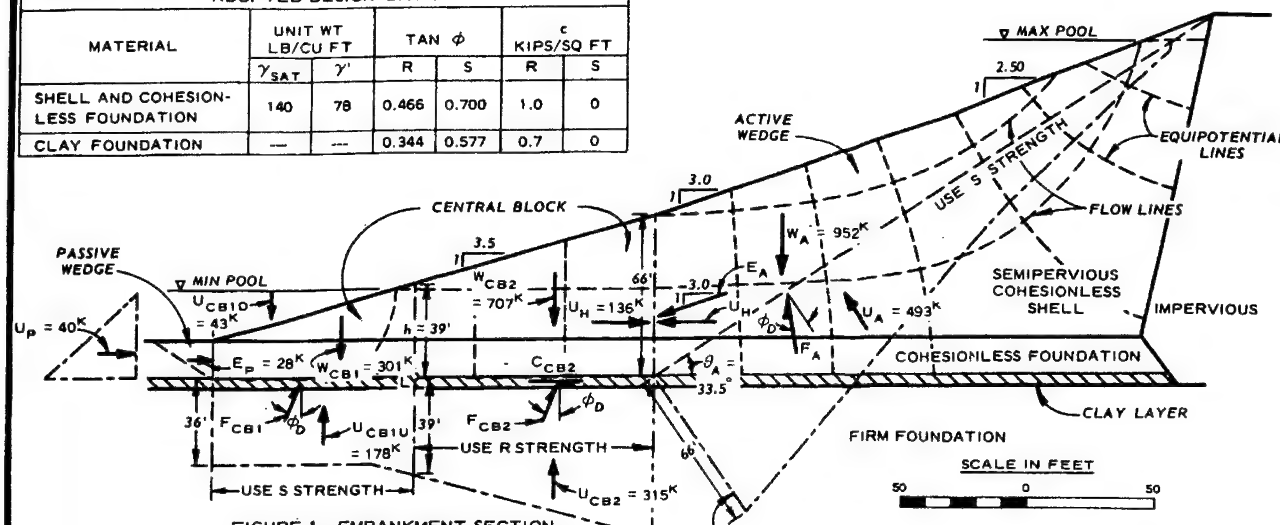

FIGURE 1. EMBANKMENT SECTION (WITH FLOW NET) (TRIAL F.S. = 1.3)

PIEZOMETRIC PRESSURES IN FT OF WATER ALONG TRIAL FAILURE PLANE (FOR GUIDANCE IN DETERMINING UPLIFT PRESSURES FROM A FLOW NET, REFER TO EM 1110-2-1901)

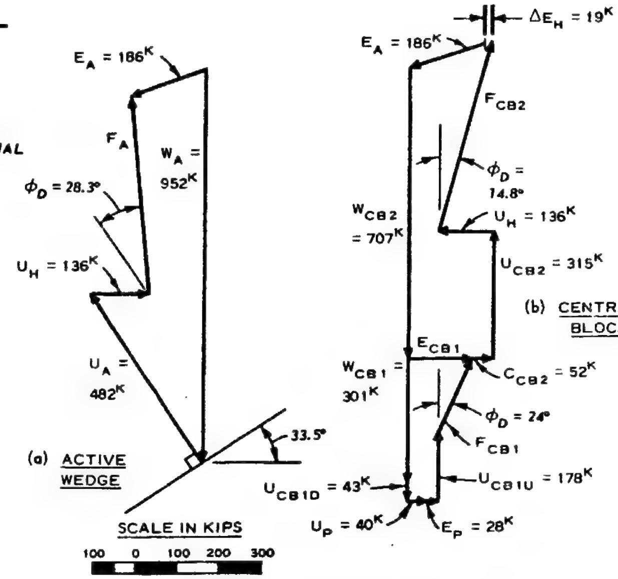

FIGURE 3. ACTIVE WEDGE AND CENTRAL BLOCK FORCE POLYGONS, TRIAL F.S. = 1.3

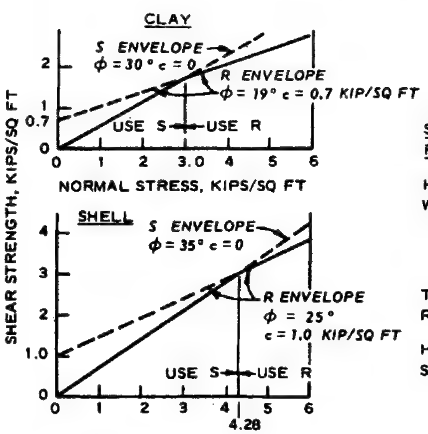

FIGURE 2. COMPOSITE STRENGTH ENVELOPES

$$E_P = \frac{1}{2}\gamma' h^2 K_P = \frac{(0.078)(16)^2}{2}\left[\frac{1 + \sin\left(\text{ARC TAN } \frac{0.70}{1.3}\right)}{1 - \sin\left(\text{ARC TAN } \frac{0.70}{1.3}\right)}\right] = 28 \text{ KIPS}$$

SHEAR STRENGTHS ALONG CENTRAL BLOCK AND ACTIVE WEDGE TRIAL FAILURE PLANES:

HEIGHT h AT LOCATION ALONG CENTRAL BLOCK SLIDING PLANE WHERE EFFECTIVE STRESS IS 3.0 KIPS/SQ FT IS

$$h = \frac{3.0}{\gamma'} = \frac{3.0 \text{ KIPS/SQ FT}}{0.078 \text{ KIP/CU FT}} = 39 \text{ FT}$$

THEREFORE USE S STRENGTH TO LEFT OF L (WHERE h = 39 FT) AND R STRENGTH TO RIGHT OF L.

HEIGHT h ALONG ACTIVE WEDGE SLIDING PLANE WHERE EFFECTIVE STRESS IS 4.28 KIPS/SQ FT IS

$$h = \frac{4.28 \text{ KIPS/SQ FT}}{\gamma' \times \cos\theta_A} = \frac{4.28 \text{ KIPS/SQ FT}}{0.078 \text{ KIP/CU FT} \times \cos 33.5°}$$

= 65.8 FT SINCE MAXIMUM HEIGHT IS 66 FT, USE S STRENGTH ALONG ENTIRE PLANE.

NOTE: THE COMPUTATIONS ABOVE ARE BASED ON VERTICAL EQUIPOTENTIAL LINES FOR SIMPLICITY.

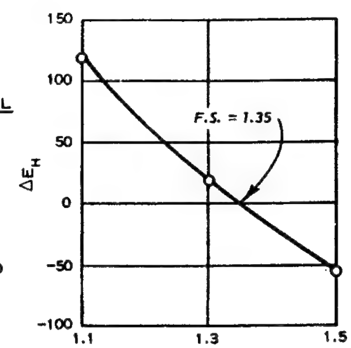

FIGURE 4. TRIAL F.S. VS ΔE_H

NOTE: W_A, W_{CB1}, AND W_{CB2} ARE BASED ON SATURATED WEIGHTS.

STABILITY ANALYSIS, EMBANKMENT WITH CENTRAL CORE AND SEMIPERVIOUS SHELL, CASE II - SUDDEN DRAWDOWN. WEDGE METHOD

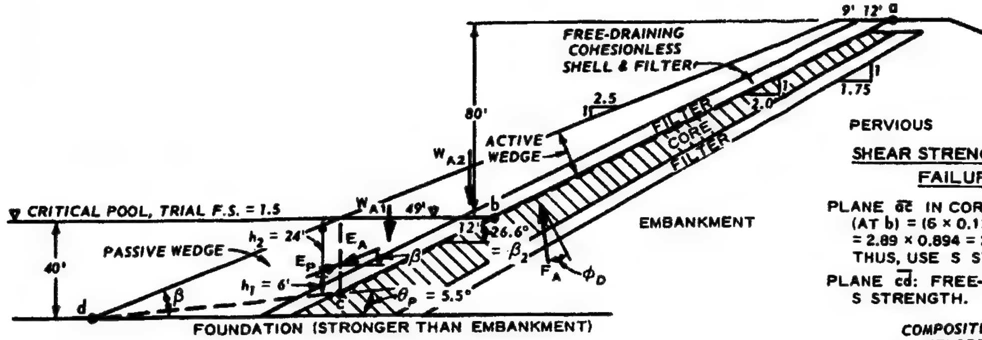

FIGURE 1. EMBANKMENT SECTION

SCALE IN FEET

50 0 50

PERVIOUS

SHEAR STRENGTH ALONG TRIAL FAILURE PLANES:

PLANE $\overline{ac}$ IN CORE: MAX NORMAL STRESS (AT b) = (6 × 0.133 + 18 × 0.116) COS 26.6° = 2.89 × 0.894 = 2.59 KIPS/SQ FT < 2.83 THUS, USE S STRENGTH.

PLANE $\overline{cd}$: FREE-DRAINING SHELL, USE S STRENGTH.

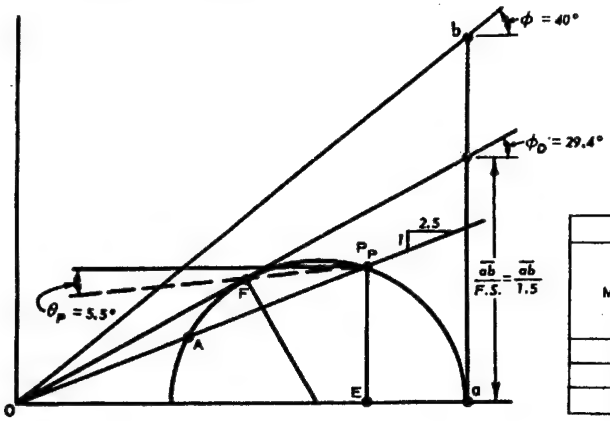

$K_p = \frac{\overline{OE}}{\overline{OA}} = 1.90$

$$E_p = \left[\frac{\gamma_2'(h_2)^2}{2} + h_1\gamma_2'h_2 + \frac{\gamma_1'(h_1)^2}{2}\right]K_p$$

$$E_p = \left[\frac{0.073}{2} \times (24)^2 + 6(0.073)(24) + \frac{0.079(6)^2}{2}\right] \times 1.90 = 62^K$$

FIGURE 2. DETERMINATION OF E_p & θ_p, TRIAL F.S. = 1.5

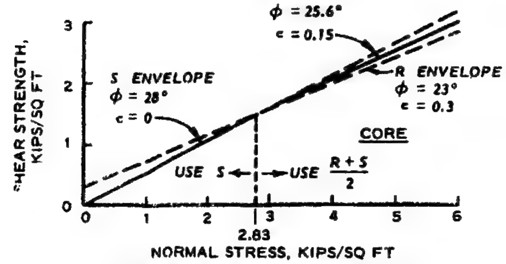

FIGURE 3. COMPOSITE STRENGTH ENVELOPE, CORE

ADOPTED DESIGN VALUES								
MATERIAL	UNIT WT LB/CU FT		TAN ϕ			c KIPS/SQ FT		
	γ_m	γ'	R	S	$\frac{R+S}{2}$	R	S	$\frac{R+S}{2}$
SHELL	116	73	—	0.839	—	—	0	—
CORE	146	87	0.424	0.532	0.478	0.3	0	0.15
FILTER	133	79	SAME AS SHELL					

DETERMINATION OF WEIGHTS, ACTIVE WEDGE

$$W_{A1} = \frac{1}{2} \times 24 \times 49 \times 0.073 + \left(\frac{1}{2} \times 30 \times 61 - \frac{1}{2} \times 24 \times 49\right) 0.079 = 69^K$$

$$W_{A2} = \frac{49+9}{2} \times 80 \times 0.116 + 12 \times 80 \times 0.133 = 397^K$$

$$W_A = 466^K$$

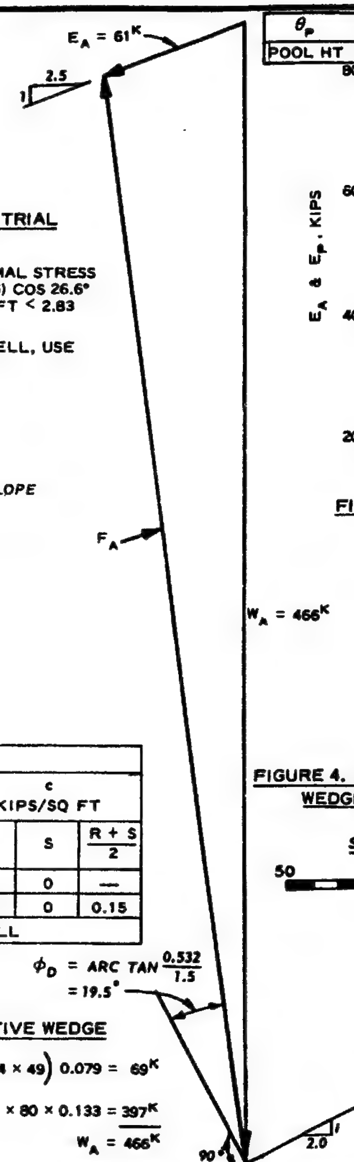

FIGURE 4. FORCE POLYGON, ACTIVE WEDGE FOR TRIAL F.S. = 1.5

SCALE IN KIPS

50 0 50

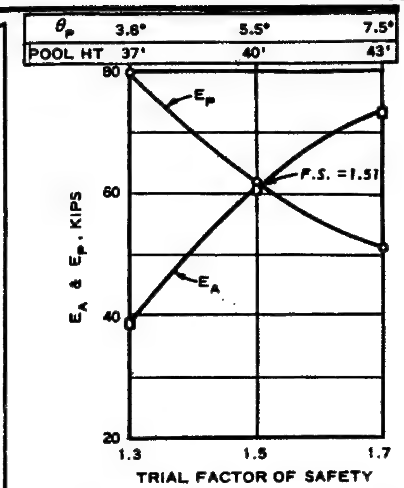

FIGURE 5. TRIAL FACTOR OF SAFETY VS E_A & E_p

STABILITY ANALYSIS, EMBANKMENT WITH INCLINED CORE AND FREE-DRAINING SHELL, CASE IV-PARTIAL POOL, WEDGE METHOD

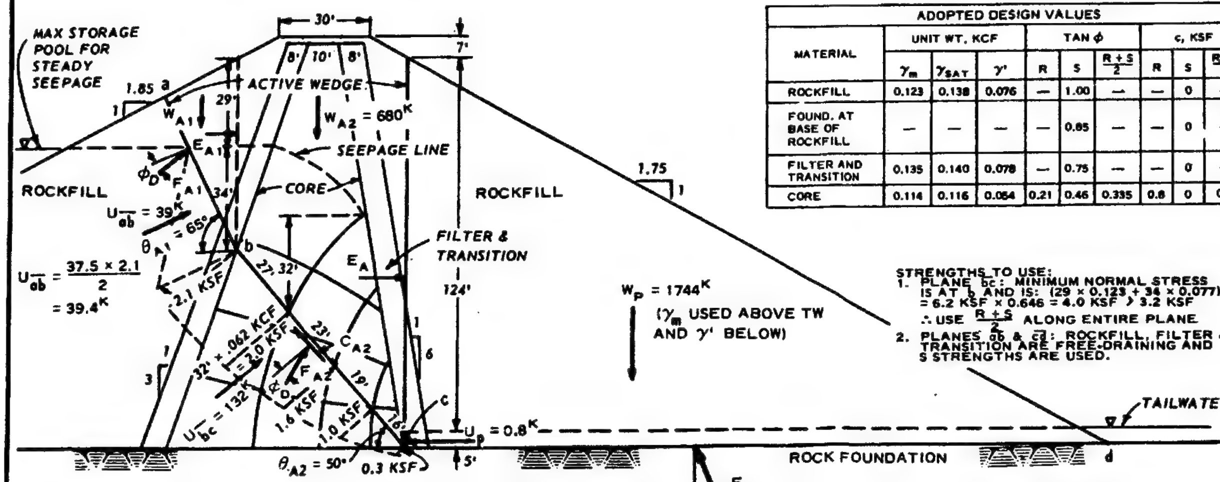

MATERIAL	UNIT WT, KCF			TAN ϕ			c, KSF		
	γ_m	γ_{SAT}	γ'	R	S	$\frac{R+S}{2}$	R	S	$\frac{R+S}{2}$
ROCKFILL	0.123	0.138	0.076	—	1.00	—	—	0	—
FOUND. AT BASE OF ROCKFILL	—	—	—	—	0.85	—	—	0	—
FILTER AND TRANSITION	0.135	0.140	0.078	—	0.75	—	—	0	—
CORE	0.114	0.116	0.054	0.21	0.46	0.335	0.8	0	0.4

ADOPTED DESIGN VALUES

STRENGTHS TO USE:

1. PLANE $\overline{bc}$: MINIMUM NORMAL STRESS IS AT b AND IS: $(29 \times 0.123 + 34 \times 0.077) \cos 50° = 6.2$ KSF $\times 0.646 = 4.0$ KSF > 3.2 KSF
   ∴ USE $\frac{R+S}{2}$ ALONG ENTIRE PLANE.
2. PLANES $\overline{ab}$ & $\overline{cd}$: ROCKFILL, FILTER AND TRANSITION ARE FREE-DRAINING AND S STRENGTHS ARE USED.

NOTE:
1. θ_{A1} FROM PLATE VII-12; FOR TRIAL F.S. = 2.0, ϕ_D ARC TAN $\frac{1.00}{F.S. = 2.0} = 26.6°$, $\theta_{A1} = 65°$
2. θ_{A2} ASSUMED = 50° FOR FIRST TRIAL
3. W_{A1} AND W_{A2} CALCULATED USING γ_m ABOVE SEEPAGE LINE AND γ_{SAT} BELOW

FIGURE 1. EMBANKMENT SECTION

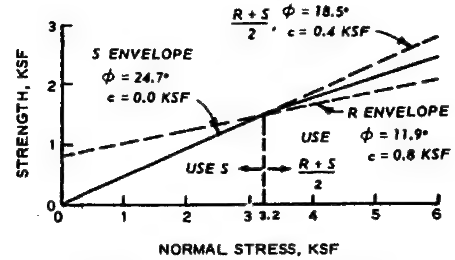

FIGURE 2. COMPOSITE STRENGTH ENVELOPE, CORE

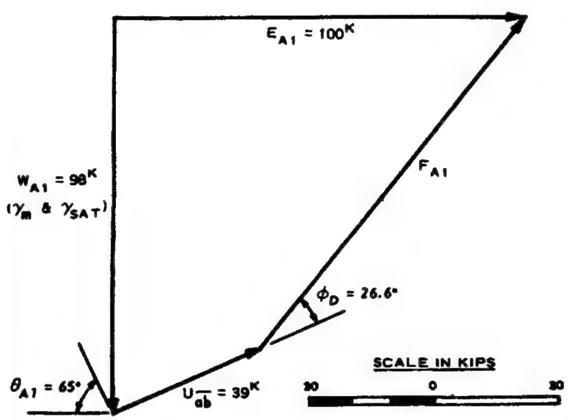

FIGURE 3. DETERMINATION OF E_{A1}, $\theta_{A2} = 50°$, F.S. = 2.0

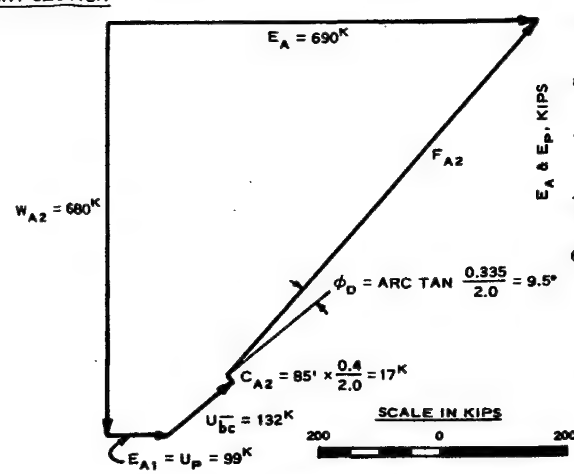

FIGURE 4. DETERMINATION OF E_A, TRIAL F.S. = 2.0

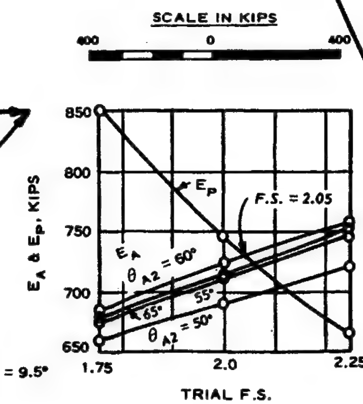

FIGURE 6. E_A & E_P VERSUS TRIAL F.S. AND θ_{A2}

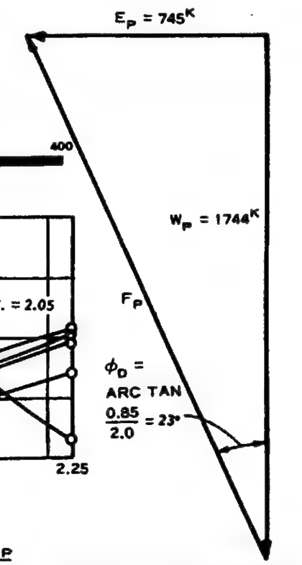

FIGURE 5. DETERMINATION OF E_p, F.S. = 2.0

STABILITY ANALYSIS, EMBANKMENT WITH CENTRAL CORE, CASE V-STEADY SEEPAGE, WEDGE METHOD

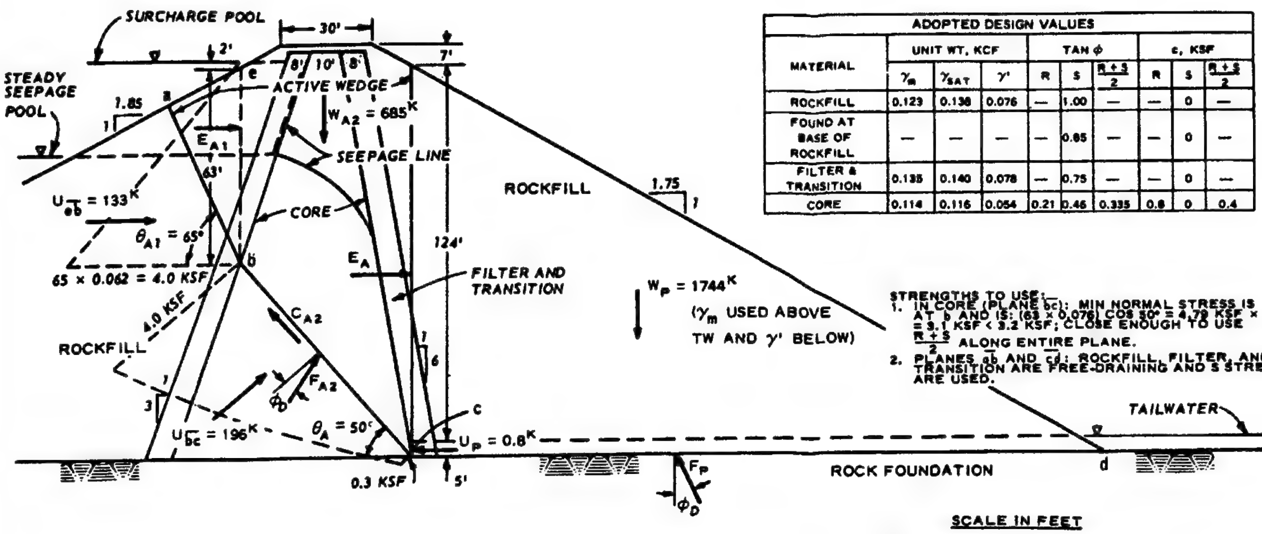

MATERIAL	UNIT WT, KCF			TAN ϕ			c, KSF		
	γ_m	γ_{SAT}	γ'	R	S	$\frac{R+S}{2}$	R	S	$\frac{R+S}{2}$
ROCKFILL	0.123	0.138	0.076	—	1.00	—	—	0	—
FOUND AT BASE OF ROCKFILL	—	—	—	—	0.85	—	—	0	—
FILTER & TRANSITION	0.135	0.140	0.078	—	0.75	—	—	0	—
CORE	0.114	0.116	0.054	0.21	0.46	0.335	0.8	0	0.4

ADOPTED DESIGN VALUES

STRENGTHS TO USE:—
1. IN CORE (PLANE $\overline{bc}$): MIN NORMAL STRESS IS AT b AND IS: (63 × 0.076) COS 50° = 4.79 KSF × 0.646 = 3.1 KSF < 3.2 KSF; CLOSE ENOUGH TO USE $\frac{R+S}{2}$ ALONG ENTIRE PLANE.
2. PLANES $\overline{ab}$ AND $\overline{cd}$: ROCKFILL, FILTER, AND TRANSITION ARE FREE-DRAINING AND S STRENGTHS ARE USED.

FIGURE 1. EMBANKMENT SECTION

NOTE: 1. θ_{A1} FROM PLATE VII-11; FOR TRIAL F.S. = 2.0, ϕ_D ARC TAN $\frac{1.00}{2.0}$ = 26.6°, θ_{A1} = 65°

2. θ_{A2} ASSUMED AS 50° FOR FIRST TRIAL

3. W_{A2} CALCULATED USING γ_m ABOVE THE SEEPAGE LINE AND γ_{SAT} BELOW

$E_{A1} = \frac{1}{2}\gamma' h^2 K_A$

FOR TRIAL F.S. = 2.0, ϕ_D = ARC TAN $\frac{1.00}{2}$ = 26.6°

K_A FROM PLATE VII-12 = 0.297

$E_{A1} = \frac{1}{2} \times 0.076 \times 63^2 \times 0.297 = 45^K$

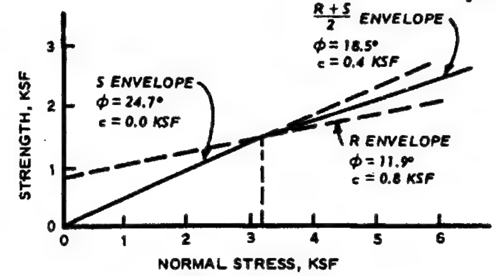

FIGURE 2. COMPOSITE STRENGTH ENVELOPE, CORE

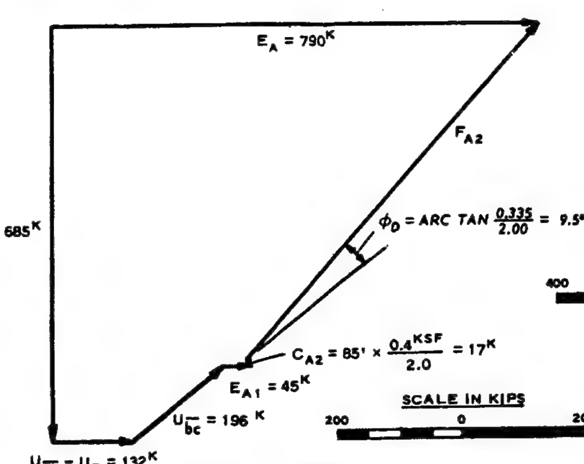

FIGURE 3. DETERMINATION OF E_A, TRIAL F.S. = 2.0

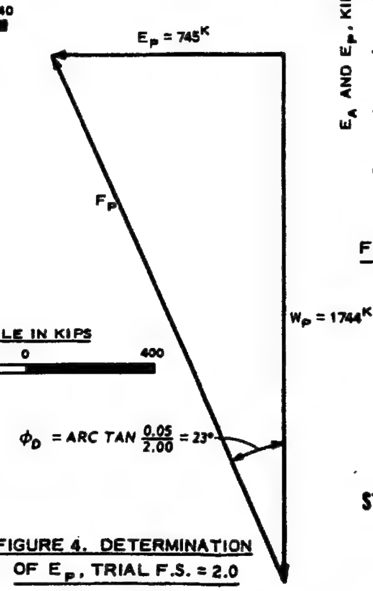

FIGURE 4. DETERMINATION OF E_p, TRIAL F.S. = 2.0

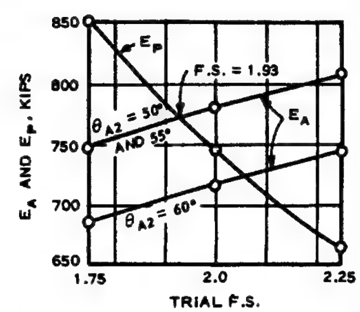

FIGURE 5. E_A AND E_p VERSUS TRIAL F.S. AND θ_{A2}

STABILITY ANALYSIS EMBANKMENT WITH CENTRAL CORE, CASE VI-SURCHARGE POOL, WEDGE METHOD

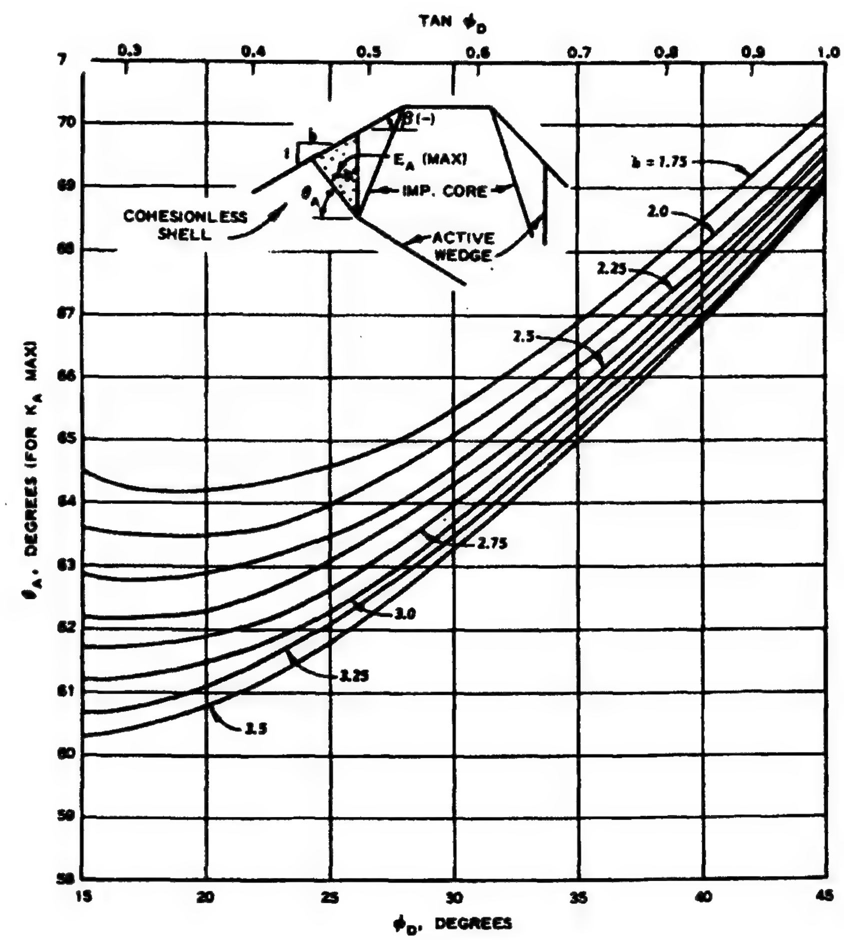

$$\theta_A = \phi_D + \text{ARC TAN} \left(- \text{TAN} (\phi_D + \beta) + \sqrt{\text{TAN} (\phi_D + \beta) \left[\text{TAN} (\phi_D + \beta) + \text{COT} \phi_D \right]} \right) \dagger$$

† FROM TABLE A-73, JUMIKIS EARTH PRESSURE COEFFICIENT TABLES (1962).[14]

θ_A VS ϕ_D FOR COHESIONLESS SOIL, COULOMB ACTIVE SLIDING PLANE FOR ACTIVE WEDGE BENEATH NEGATIVE SLOPE

Plate VII-11

APPENDIX VIII

Evaluation of Embankment Stability During Construction

1. Basic Considerations. Embankment stability during construction is affected primarily by pore water pressures induced by the weight of fill placed. When induced pore water pressures are low, stability during construction is generally not a problem. If pore water pressures measured in either the embankment or foundation are high, additional analyses of embankment stability during the construction period should be made, and it may be necessary to: (a) provide berms or flatten slopes, (b) decrease the rate of fill placement, or (c) temporarily discontinue fill operations. Emergency drainage such as electroosmosis may also be considered. The interpretation of measured pore water pressure and evaluation of stability during construction should be regarded as an integral part of embankment design to assure that design expectations and assumptions are consistent with actual embankment and foundation properties.

2. Development of Pore Water Pressure During Construction.

a. General. The development of pore water pressures during construction in either the foundation or in the embankment depends upon the soil properties and the amount of drainage or consolidation occurring during construction. Piezometer observations made during construction should be compared with predicted magnitudes to assess in a general way stability during construction.

b. Embankment Pore Water Pressures. (1) Pore water pressures developed in partially saturated embankment materials during construction depend primarily on (a) fill characteristics such as water content, density, permeability, and compressibility, (b) embankment height, (c) size of core or impervious sections, (d) internal drainage provisions, (e) rate of construction, (f) number of construction seasons, and (g) climatic conditions. Factors involved in pore pressure development in embankments and means

for estimating construction pore water pressures are discussed in a recent Corps of Engineers report[15] and are reviewed briefly below.

(2) As additional fill is placed above partially saturated material, the following effects can be observed: (a) the air in the compacted soil is compressed, thereby reducing its volume; (b) the increased pore air pressure causes additional solution of air in the pore water, and an additional volume decrease; (c) pore water pressures are increased; and (d) intergranular stresses are increased by an amount corresponding to the volume decrease caused by compression and solution of air in the soil pore water. Thus, the weight of overlying fill is supported partially by effective stresses in the soil and partially by pore water and air pressures. It is generally assumed, for simplicity and conservatism, that pore air and water pressures are equal, although pore air pressures are actually somewhat higher than pore water pressures. If drainage during construction is ignored, pore air and water pressures estimated[16,17] from application of Boyle's and Henry's laws are conservative. The Brahtz-Hilf procedure for evaluating pore pressures caused by loading a partially saturated soil without drainage taking place is shown in plate VIII-1, together with an example.

(3) When embankments are constructed slowly, in stages, or in two or more construction seasons, significant drainage of pore water may occur and estimated pore pressures may be too high unless consolidation is taken into account. Where stability under stage construction conditions is being investigated, and the gain in shear strength from consolidation occurring between construction periods is taken into account, embankment pore pressures may be estimated from procedures originally developed by the Bureau of Reclamation[17] and extended by Bishop.[18] Dissipation of pore pressures during periods when no fill is placed results in a decrease in soil volume and an increase in effective stress. Bishop pointed out that this increases the stiffness of the soil (i.e. decreases the coefficient of compressibility) and when fill placement is resumed, the induced pore pressures are lower than those that otherwise would have developed. A procedure and an example are shown

in plate VIII-2 for evaluating pore pressures in partially saturated soils with complete dissipation of pore pressures between construction seasons and in plate VIII-3 for partial dissipation of pore pressures in this interval.

(4) The rate of consolidation of partially saturated soils is relatively large during the loading period, when air is compressed and forced into solution, and is relatively slow in later stages when pore pressures decrease and air comes out of solution. The coefficient of consolidation is, therefore, not constant as is often assumed. A "gas factor" to apply to the coefficient of consolidation to account for the change in rate of consolidation of partially saturated soils has been suggested by Gould.[19]

c. Foundation Pore Water Pressures. (1) Excess pore water pressures developed in foundation soils beneath embankments, assuming that significant consolidation does not occur as the fill is placed, can be estimated according to the following equation, developed by Skempton[20]

$$\Delta u = B[\Delta\sigma_3 + A(\Delta\sigma_1 - \Delta\sigma_3)]$$

where A and B are experimentally determined pore pressure coefficients, which are illustrated in plate VIII-4 for failure conditions. In general, foundations are assumed saturated and the value of B can be taken as one, so the ratio of induced pore water pressure to the increase in major principal stress becomes

$$\frac{\Delta u}{\Delta\sigma_1} = A + (1 - A)\frac{\Delta\sigma_3}{\Delta\sigma_1}$$

The value of A should correspond to the field value for $\frac{\Delta\sigma_3}{\Delta\sigma_1}$, the ratio of lateral to vertical total stresses, but this is seldom done. The value of $\Delta\sigma_1$ can be taken as approximately equal to the stress imposed by the weight of overlying fill since impervious materials are usually restricted to the central

part of embankments where this approximation is reasonably correct. The dependence of excess pore water pressures on the preconsolidation stress of the soil is illustrated by figure 1a, plate VIII-4, and plate VIII-5, assuming a B value of 1.0.

(2) A summary of pore pressures observed in foundations of earth dams is given in a recent Corps of Engineers report.[21] Data presented in it suggest that the approach given above may substantially underestimate pore water pressures developed in shale foundations, but suitable alternative procedures have not been developed. Consequently, recourse must be made to field tests and measurements at sites having such foundation materials. The extent to which this may also be true for hard or highly overconsolidated clays that are not classed as clay shales in unknown.

3. Installation and Uses of Piezometers. a. Piezometers provide the principal means for controlling embankment stability. Undisturbed samples of the soils in which the piezometer tips are installed should be taken large enough in diameter to permit triaxial compression testing of three or four specimens from a common depth. Additional soil samples at other elevations may also be desirable. Piezometer locations and depths should be selected to minimize extrapolation in using the piezometric data in stability analyses.

b. Piezometer observations also may be used to estimate field values for the coefficient of consolidation. These field values may be compared with values assumed in design if consolidation during construction was assumed, and their variation with loading studied as a basis for predicting consolidation under future fill loading. Procedures for estimating the field coefficient of consolidation for one-dimensional compression were developed by Gould[22] and were later extended for combined vertical and radial drainage.[19]

c. Plots of induced pore pressure versus fill load can be used for predicting pore pressure under increased fill heights. However, where soils are partially saturated, the ratio of induced pore pressure to applied load increases as loading continues until all pore air is dissolved; thereafter,

the additional pore water pressure approximately equals the added fill weight. Therefore, linear extrapolation of a few early piezometer observations would not account for this nonlinear relation prior to saturation and would be unconservative.

4. Evaluation of Embankment Stability. a. Basic Considerations. (1) The evaluation of embankment stability during construction should consider all relevant evidence including, in addition to piezometric pressures, such items as (a) movements of settlement plates, (b) horizontal movements of fill and foundation, such as those observed with slope indicators, (c) vertical and horizontal movements of ground at and beyond the embankment toes, (d) vertical and horizontal movements of joints in conduits embedded in the fill, and (e) horizontal and vertical movements of foundations of bridges leading to outlet control towers. Although specific criteria for identifying abnormal behavior cannot be given, repeated observations will show if continuing deformations or anomolous changes in behavior are occurring.

(2) The principal means for assessing embankment stability during construction consist of stability analyses that are directly or indirectly related to pore water pressures. There are various procedures for making such analyses, and it may be desirable to use more than one procedure where embankment stability is questionable. Therefore, several procedures in current use are described in the following paragraphs. All ignore important factors such as nonuniform strain along potential failure surfaces, ultimate strengths that are lower than peak values, redistribution of stresses from embankment loading, and similar aspects that make even the most detailed procedures only approximations to actual conditions.

b. Method A: In Situ Shear Strength Procedure. (1) In this procedure, undisturbed samples are obtained during construction and tested at natural moisture content and density under Q test conditions, without application of back pressure, to determine in situ shear strength. Samples need be obtained only from embankment zones and foundation strata in which high pore pressures have been measured. The shear strength envelope should be

determined from the test results in the manner shown in figure 2 of the main text. The undisturbed samples should be obtained at various depths in each soil zone. Each sample should be tested at a single confining pressure of 0.8 times the estimated vertical stress under the in situ condition, since its natural water content and density apply only to the depth at which the sample was obtained.

(2) Stability analyses are then made that are similar to those made in design for the construction condition, except that the shearing resistance along the trial sliding surface is based on the shear resistances determined according to the procedure described above. These analyses consider only the total weight of soil and water in each slice in computing the driving forces and the shear resistance along the sliding surfaces. Water forces on the sides of the slices need not be taken into account since they are internal forces.

(3) The analyses described above apply only to the embankment at the time the undisturbed samples were obtained. If analyses for an increased height of embankment are also desired, additional Q-type tests should be performed in which the confining pressures equal 0.8 times the overburden stresses at the higher fill height. This is conservative since any subsequent consolidation during the fill placement period is ignored.

c. Method B: Measured and Design Pore Pressures. (1) This procedure compares pore water pressures measured during construction with values implicit in the use of Q shear strengths for the construction condition design analyses. If measured pore pressures are less than those implicitly assumed, additional evaluation of embankment stability during construction is not required, unless other field evidence fails to support these observations.

(2) The use of Q-type test results for construction condition design implies that both negative and positive pore water pressures are developed in the embankment and foundation. The pore water pressures inherent in the Q-type laboratory tests can be approximated from Q and S envelopes

and plotted versus total normal stress on the failure plane, as shown in plate VIII-6. If such a plot is prepared, field measured pore water pressures can be simply compared with design expectations, provided piezometers are installed close to the location of the assumed critical failure plane for the design construction condition.

(3) As seen from plate VIII-6, negative pore water pressures must occur in areas of low normal stress if design expectations are to be realized. However, since conventional piezometers are unreliable for measuring negative pore pressures, satisfactory confirmation of design expectations may be impossible to obtain. If high pore pressures are measured in those portions of the embankment or foundation where Q shear strengths are higher than S shear strengths, more detailed methods, such as method A, should be used to check stability during construction.

(4) In lieu of computing pore pressures implied by use of Q test results, they can be measured directly in the laboratory by performing $\overline{Q}$ tests with pore pressure measurements. This requires that the tests be performed slowly so that pore pressures at the center and ends of the test specimen are equalized. Because the test procedures are more complicated and time consuming, $\overline{Q}$ tests for construction condition analyses are not often performed. The same type of porous stone should be used in both the laboratory $\overline{Q}$ tests and the field piezometers so that the pore pressures of low values will have comparable errors.

d. Method C: Modified Swedish or Wedge Method Considering Water Forces. (1) This method is based on procedures described in Appendixes VI and VII. It requires detailed analyses including earth and water forces on the sides and bottom of each slice or wedge segment and should be used only where field and laboratory investigations have been extensive and where embankment soils and foundation materials are not unusual. It should not generally be used for clay shale embankments or foundations.

(2) The water forces on the sides and bottom of each slice or wedge segment can be interpolated from the piezometer observations. For stable

embankments, the soil shearing resistance should be taken as the R strength corresponding to an effective normal stress, prior to start of undrained shear, which is equal to the effective normal stress on the base of each slice or wedge segment, as determined by the stability analysis. When the embankment section is considered to be near failure, the S strength may be used. A near failure condition might be defined by measured horizontal or vertical movements that do not show a decrease with time or by measured pore water pressures that are approaching the stress imposed by the overlying fill. The analysis is similar to that described in Appendixes VI and VII for stability of the downstream slope under a condition of steady seepage.

e. Method D: Modified Bureau of Reclamation Procedure. This procedure consists of comparing field pore water pressures with values predicted according to procedures discussed in paragraph 2 of this appendix and plates VIII-1 to -5. Where this method is used, it should be supplemented by at least one of the other evaluation methods. This method does not consider shear-induced pore pressures.

f. Method E: Modified Swedish or Wedge Method Considering $\bar{\sigma}_1$ and $\bar{\sigma}_3$ Stresses. This method is generally similar to Method C, except that the shear resistance of the soil is the undrained strength corresponding to effective stresses at the start of shear equal to those estimated for field conditions.[23] The following steps are involved:

(1) A plot of shear strength versus effective normal stress on the failure plane at the start of shear is prepared from $\bar{Q}$ or $\bar{R}$ triaxial compression tests. This is done by assuming (after Taylor) that any point in the shearing phase of a $\bar{Q}$ or $\bar{R}$ test corresponds to the start of another test; see plate VIII-7. Next, construct lines of undrained shear strength versus $\bar{\sigma}_{fc}$, the effective normal stress on the failure plane prior to start of undrained shear, for various values of $\bar{\sigma}_1/\bar{\sigma}_3$ as shown in plates VIII-7 and -8.

(2) Assume a trial value of $\left(\bar{\sigma}_1/\bar{\sigma}_3\right)_c$, such as 2, and determine corresponding shear strength parameters c and ϕ from plate VIII-8.

(3) Assume trial safety factors and obtain closure of force polygons for the modified Swedish method, using field measured pore water pressures on the sides and bottom of each slice.

(4) Determine shear stress and corresponding effective normal stress on the base of each slice. Plot as shown in plate VIII-8 to obtain $\bar{\sigma}_1$ and $\bar{\sigma}_3$, and compute $\bar{\sigma}_1/\bar{\sigma}_3$ for each slice.

(5) Compare $\bar{\sigma}_1/\bar{\sigma}_3$ for each slice with value assumed in Step 1. If necessary, revise value of $\left(\bar{\sigma}_1/\bar{\sigma}_3\right)_c$ assumed in Step 1 and repeat Steps 2 through 5.

LEGEND

G = SPECIFIC GRAVITY
n = POROSITY (DECIMAL UNITS)
S = DEGREE OF SATURATION (DECIMAL UNITS)
V = VOLUME
V_a = VOLUME OF AIR
V_s = VOLUME OF SOLIDS
V_v = VOLUME OF VOIDS
V_w = VOLUME OF WATER
w = WATER CONTENT (DECIMAL UNITS)
γ_d = DRY DENSITY
γ_w = UNIT WEIGHT OF WATER

GENERAL EQUATIONS RELATING TO FIELD SAMPLE

(1) $$S = \frac{w\gamma_d}{\gamma_w\left(1 - \frac{\gamma_d}{G\gamma_w}\right)} = \frac{w}{G\frac{\gamma_w}{\gamma_d} - 1}$$

(2) $$\frac{V_a}{V} = (1 - S)\frac{wG}{S + wG} = 1 - \frac{\gamma_d}{\gamma_w}\left(\frac{1}{G} + w\right)$$

(3) $$n = \frac{V_v}{V} = \frac{\frac{V_a}{V}}{1 - S} = 1 - \frac{\gamma_d}{G\gamma_w} = \frac{wG}{S + wG}$$

(4) $$\frac{V_w}{V} = S\frac{V_v}{V} = \frac{w\gamma_d}{\gamma_w}$$

(5) $$\frac{V_s}{V} = \frac{\gamma_d}{\gamma_w G}$$

(6) $$\frac{V_a}{V} + \frac{V_w}{V} + \frac{V_s}{V} = 1.00$$

(7) $$u = \frac{p_a \frac{\Delta H}{H_o}}{\frac{V_a}{V} + h\frac{V_w}{V} - \frac{\Delta H}{H_o}} = \frac{p_a \frac{\Delta H}{H_o}}{n_o\left(1 - S_o + hS_o\right) - \frac{\Delta H}{H_o}}$$

WHERE:

u = AIR AND PORE WATER PRESSURE (ASSUMED EQUAL) INDUCED BY A TOTAL σ_T, EXPRESSED AS GAGE PRESSURE, PSI.
p_a = ABSOLUTE PRESSURE OF AIR IN VOIDS PRIOR TO LOADING BY SUPERPOSED FILL; ASSUMED EQUAL TO ATMOSPHERIC PRESSURE, 14.7 PSI.
$\frac{\Delta H}{H_o}$ = STRAIN OR COMPRESSION OF SOIL PER UNIT VOLUME (ONE-DIMENSIONAL COMPRESSION) CAUSED BY A TOTAL LOAD σ_T
h = HENRY'S CONSTANT OF SOLUBILITY OF AIR IN WATER BY VOLUME (0.0198 AT 68°F)
n_o = INITIAL POROSITY, PRIOR TO LOADING
S_o = INITIAL DEGREE OF SATURATION, PRIOR TO LOADING

EQUATION 7 IS VALID ONLY FOR PARTIALLY SATURATED SOILS AND AT POINT WHEN SOIL BECOMES SATURATED; I.E. WHEN

$$\frac{\Delta H}{H_o} = \frac{V_a}{V}$$

THE INDUCED AIR AND PORE WATER PRESSURE WHEN SOIL BECOMES SATURATED IS

(8) $$u_s = \frac{p_a V_a/V}{h V_w/V} = \frac{p_a}{h} \times \frac{1 - S_o}{S_o} = 50.5\,p_a\frac{1 - S_o}{S_o}$$

u_s = GAGE PRESSURE OF AIR AND WATER IN VOIDS OF SOIL

PROCEDURE FOR COMPUTING PORE PRESSURES

1. COMPUTE EQUATIONS 1-5 AND CHECK RESULTS USING EQUATION 6.
2. PLOT CONSOLIDATION TEST RESULTS AS $\frac{\Delta H}{H_o}$ VS $\bar{\sigma}$ (PLOT REQUIRED ONLY FOR VALUES OF $\frac{\Delta H}{H_o}$ FROM 0 TO $\frac{\Delta H}{H_o} = \frac{V_a}{V}$).
3. COMPUTE INDUCED PORE AND AIR PRESSURE CORRESPONDING TO SATURATION FROM EQUATION 8.
4. COMPUTE INDUCED PORE PRESSURE FROM EQUATION 7 FOR VARIOUS VALUES OF $\frac{\Delta H}{H_o}$ EQUAL TO AND LESS THAN $\frac{\Delta H}{H_o} = \frac{V_a}{V}$
5. OBTAIN $\bar{\sigma}$ CORRESPONDING TO VALUES OF $\frac{\Delta H}{H_o}$ USED IN STEP 4 FROM PLOT PREPARED IN STEP 2.
6. COMPUTE σ_T VALUES FOR EACH VALUE OF $\frac{\Delta H}{H_o}$; $\sigma_T = \bar{\sigma} + u$.
7. PLOT u VS σ_T; ALSO PLOT u VS $\frac{\Delta H}{H_o}$ AND $\bar{\sigma}$ VS $\frac{\Delta H}{H_o}$ AND σ_T VS $\frac{\Delta H}{H_o}$.

EXAMPLE
INITIAL CONDITION OF SOIL BEFORE LOADING

w = 17.1% = 0.171
γ_d = 108.2 PCF
G = 2.68

STEP 1:

EQ 1 $$S_o = \frac{wG}{G \times \frac{\gamma_w}{\gamma_d} - 1} = \frac{0.171 \times 2.68}{2.68 \times \frac{62.4}{108.2} - 1} = 0.864$$

EQ 2 $$\frac{V_a}{V} = 1 - \frac{\gamma_d}{\gamma_w}\left(\frac{1}{G} + w\right) = 1 - \frac{108.2}{62.4}\left(\frac{1}{2.68} + 0.171\right) = 0.048$$

EQ 3 $$n = \frac{V_v}{V} = 1 - \frac{108.2}{62.4 \times 2.68} = 1 - 0.653 = 0.347$$

EQ 4 $$\frac{V_w}{V} = 0.171 \times \frac{108.2}{62.4} = 0.299$$

EQ 5 $$\frac{V_s}{V} = \frac{108.2}{62.4 \times 2.68} = 0.653$$

EQ 6 $$\frac{V_a}{V} + \frac{V_w}{V} + \frac{V_s}{V} = 0.048 + 0.299 + 0.653 = 1.00 \quad \text{(CHECKS)}$$

STEP 2: CONSOLIDATION TEST RESULTS ARE PLOTTED IN FIG. 1 AS $\bar{\sigma}$ VS $\frac{\Delta H}{H_o}$

STEP 3: EQ 8 $$u_s = 50.5\ p_a\frac{1 - S_o}{S_o} = 50.5 \times 14.7 \times \frac{1 - 0.864}{0.864} = 116.6 \text{ PSI}$$

STEPS 4, 5, AND 6

EQ 7 $$u = \frac{p_a \frac{\Delta H}{H_o}}{n_o\left(1 - 0.98\,S_o\right) - \frac{\Delta H}{H_o}} = \frac{14.7 \times \frac{\Delta H}{H_o}}{0.347\,(1 - 0.98 \times 0.864) - \frac{\Delta H}{H_o}}$$

$$u = \frac{14.7 \times \frac{\Delta H}{H_o}}{0.0531 - \frac{\Delta H}{H_o}}$$

$\frac{\Delta H}{H_o}$	$\bar{\sigma}$ PSI	$0.0531 - \frac{\Delta H}{H_o}$	u PSI	$\sigma_T = \bar{\sigma} + u$
0.005	4.5	0.04	1.5	6.0
0.010	9.0	0.04	3.4	12.4
0.015	14.5	0.03	5.8	20.3
0.020	20.5	0.03	8.9	29.4
0.024	25.0	0.02	12.1	37.1
0.030	33.5	0.02	19.1	52.6
0.035	41.0	0.01	28.4	69.4
0.041	50.0	0.01	48.8	98.8
0.048*	57.0	0.005	138.4	195.4

*SATURATION, $\frac{\Delta H}{H_o} = \frac{V_a}{V}$

STEP 7: PLOT u VS $\frac{\Delta H}{H_o}$ AND σ_T VS $\frac{\Delta H}{H_o}$ IN FIG. 1 AND σ_T VS u IN FIG. 2.

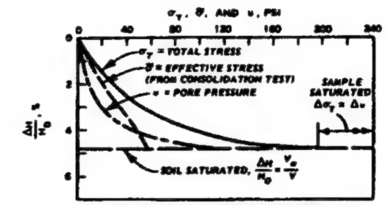

FIG. 1. TOTAL AND EFFECTIVE STRESSES AND PORE PRESSURE VS DEFORMATION

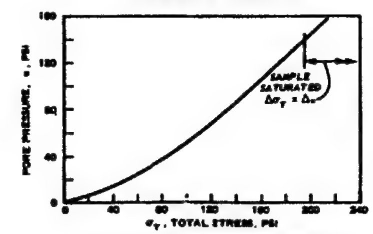

FIG. 2. TOTAL STRESS VS PORE PRESSURE

PORE PRESSURES IN PARTIALLY SATURATED SOILS
NO DRAINAGE DURING LOADING

Plate VIII-1

PORE PRESSURES INDUCED BY ADDITIONAL LOADING WITHOUT DRAINAGE, FOLLOWING AN INTERVAL IN WHICH NO FILL WAS PLACED AND DURING WHICH COMPLETE DISSIPATION OF PORE PRESSURES OCCURRED

AT THE END OF FIRST CONSTRUCTION SEASON

TOTAL FILL LOAD $= \sigma_{T_1}$

PORE PRESSURE $= u_1$

EFFECTIVE STRESS $= \bar{\sigma}_1$

VOLUME DECREASE $= \frac{\Delta H_1}{H_o}$

AT START OF SECOND CONSTRUCTION SEASON

TOTAL FILL LOAD $= \sigma_{T_1}$

PORE PRESSURE $= u_2 = 0$

EFFECTIVE STRESS $= \bar{\sigma}_{T_1} = \sigma_{T_1}$

VOLUME DECREASE $= \frac{\Delta H_2}{H_o}$

AT THE START OF SECOND CONSTRUCTION SEASON, POROSITY $= n_2$

(9) $$n_2 = n_o - \frac{\Delta H_2}{H_o}$$

DURING SECOND CONSTRUCTION SEASON, INDUCED PORE PRESSURE IS GIVEN BY

(10) $$u = \frac{P_o \frac{\Delta H'}{H_o}}{n_2(1 - S_o + hS_o) - \frac{\Delta H'}{H_o}}$$

WHERE

$\frac{\Delta H'}{H_o}$ = ADDITIONAL VOLUME CHANGE, MEASURED FROM $\frac{\Delta H_2}{H_o}$

S_o = DEGREE OF SATURATION PRIOR TO LOADING (AT START OF SECOND CONSTRUCTION SEASON, ASSUMED EQUAL TO S_o AT START OF FIRST CONSTRUCTION SEASON).

NOTE: SEE PLATE VIII-1 FOR BASIC DEFINITION OF TERMS.

ASSUMPTIONS: AT END OF FIRST CONSTRUCTION SEASON

TOTAL FILL LOAD $= \sigma_{T_1} = 37.8$ PSI

PORE PRESSURE $= u = 12.8$ PSI

EFFECTIVE STRESS $= \bar{\sigma}_1 = 25.0$ PSI

VOLUME DECREASE $= \frac{\Delta H_1}{H_o} = 0.024$ OR 2.4%

ASSUME THAT PORE PRESSURE DISSIPATES 100% DURING INTERVAL BETWEEN FIRST AND SECOND CONSTRUCTION SEASONS.

AT START OF SECOND CONSTRUCTION SEASON

PORE PRESSURE $= u_2 = 0$

EFFECTIVE STRESS $= \bar{\sigma}_{T_1} = 37.8$ PSI

VOLUME DECREASE $= \frac{\Delta H_2}{H_o} = 0.033$ OR 3.3%

COMPUTATIONS: AT START OF SECOND CONSTRUCTION SEASON

EQ 9 POROSITY $= n_2 = n_o - \frac{\Delta H_2}{H_o} = 0.345 - 0.033 = 0.312$

DURING SECOND CONSTRUCTION SEASON

EQ 10 $$u = \frac{P_o \frac{\Delta H'}{H_o}}{n_2(1 - 0.98 S_o) - \frac{\Delta H'}{H_o}} = \frac{14.7 \times \frac{\Delta H'}{H_o}}{0.312(1 - 0.98 \times 0.864) - \frac{\Delta H'}{H_o}}$$

$$u = \frac{14.7 \times \frac{\Delta H'}{H_o}}{0.0477 - \frac{\Delta H'}{H_o}}$$

$\frac{\Delta H'}{H_o}$	$\frac{\Delta H}{H_o}$	$0.0477 - \frac{\Delta H'}{H_o}$	u PSI	$\bar{\sigma}$ PSI	$\sigma_T = \bar{\sigma} + u$ PSI
0	0.033	0.0477	0	37.8	37.8
0.002	0.035	0.0457	0.6	41.0	41.6
0.008	0.041	0.0397	3.0	50.0	53.0
0.0126	0.0456	0.0351	5.3	57.0	62.3

PLOT $\bar{\sigma}$, u, AND σ_T VS $\frac{\Delta H}{H_o}$ IN FIG. 1.

PLOT σ_T VS u IN FIG. 2.

EXAMPLE

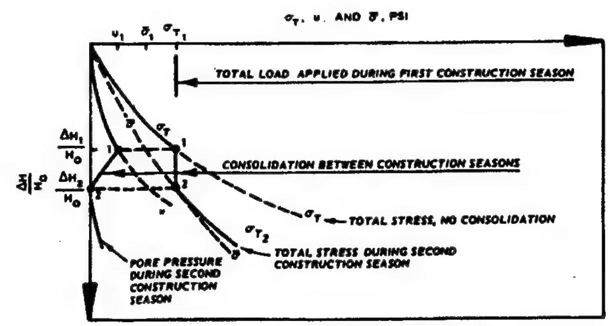

FIG. 1. TOTAL AND EFFECTIVE STRESSES AND PORE PRESSURE VS DEFORMATION

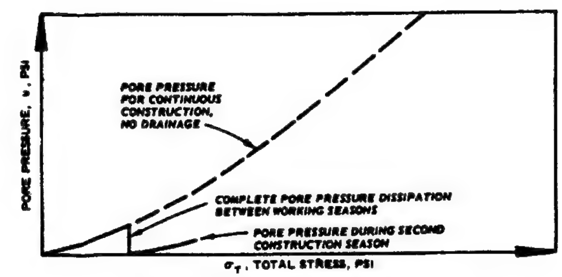

FIG. 2. TOTAL STRESS VS PORE PRESSURE

PORE PRESSURES IN PARTIALLY SATURATED SOILS

EFFECT OF COMPLETE DISSIPATION OF PORE PRESSURE BETWEEN CONSTRUCTION SEASONS

PORE PRESSURES INDUCED BY ADDITIONAL LOADING AFTER AN INTERVAL IN WHICH NO FILL WAS PLACED AND DURING WHICH PARTIAL DISSIPATION OF PORE PRESSURE OCCURRED

AT THE END OF FIRST CONSTRUCTION SEASON

TOTAL FILL LOAD $= \sigma_{T_1}$

PORE PRESSURE $= u_1$

EFFECTIVE STRESS $= \bar{\sigma}_1$

VOLUME DECREASE (STRAIN) $= \frac{\Delta H_1}{H_o}$

AT START OF SECOND CONSTRUCTION SEASON

TOTAL FILL LOAD $= \sigma_{T_1}$

PORE PRESSURE $= u_2$

EFFECTIVE STRESS $= \bar{\sigma}_2$

VOLUME DECREASE $= \frac{\Delta H_2}{H_o}$

AT START OF SECOND CONSTRUCTION SEASON

(9) POROSITY $= n_2 = n_o - \frac{\Delta H_2}{H_o}$

(11) DEGREE OF SATURATION $= S_2 = \dfrac{S_o\left(1 + \frac{u_2}{P_a}\right)}{1 + \frac{u_2}{P_a}(1 - h)\,S_o}$

DURING SECOND CONSTRUCTION SEASON, INDUCED PORE PRESSURE IS GIVEN BY

$$(12)\quad \Delta u = \frac{(P_a + u_2)\,\frac{\Delta H'}{H_o}}{n_2\,(1 - S_2 + hS_2) - \frac{\Delta H'}{H_o}}$$

WHERE Δu = ADDITIONAL PORE PRESSURE CAUSED BY LOADING DURING SECOND CONSTRUCTION SEASON.

P_a = ATMOSPHERIC PRESSURE, 14.7 PSI

u_2 = PORE PRESSURE AT START OF SECOND CONSTRUCTION SEASON.

$\frac{\Delta H'}{H_o}$ = ADDITIONAL VOLUME CHANGE, MEASURED FROM $\frac{\Delta H_2}{H_o}$

n_2 = POROSITY AT START OF SECOND CONSTRUCTION SEASON

S_2 = DEGREE OF SATURATION AT START OF SECOND CONSTRUCTION SEASON.

NOTE: SEE PLATE VIII-1 FOR BASIC DEFINITION OF TERMS.

ASSUME: AT END OF FIRST CONSTRUCTION SEASON

$\sigma_{T_1} = 37.8$ PSI

$u = 12.8$ PSI

$\bar{\sigma} = 25.0$ PSI

$\frac{\Delta H}{H_o} =$ 0.025 OR 2.4%

ASSUME THAT PORE PRESSURE DISSIPATES 50% DURING INTERVAL BETWEEN FIRST AND SECOND CONSTRUCTION SEASONS

AT START OF SECOND CONSTRUCTION SEASON

$u_2 = 6.4$ PSI

$\bar{\sigma} = 31.4$ PSI

$\frac{\Delta H_2}{H_o} =$ 0.0285 OR 2.85%

COMPUTATIONS: AT START OF SECOND CONSTRUCTION SEASON

$$(9)\quad n_2 = n_o - \frac{\Delta H_2}{H_o} = 0.345 - 0.0285 = 0.3165$$

$$(11)\quad S_2 = \frac{S_o\left(1 + \frac{u_2}{P_a}\right)}{1 + \frac{u_2}{P_a}(1 - h)\,S_o} = \frac{0.864\left(1 + \frac{6.4}{14.7}\right)}{1 + \frac{6.4}{14.7} \times 0.98 \times 0.864} = 0.906$$

DURING SECOND CONSTRUCTION SEASON

$$(12)\quad \Delta u = \frac{(P_a + u_2)\,\frac{\Delta H'}{H_o}}{n_2\,(1 - 0.98S_2) - \frac{\Delta H'}{H_o}} = \frac{(14.7 + 6.4)\,\frac{\Delta H'}{H_o}}{0.3165\,(1 - 0.98 \times 0.906) - \frac{\Delta H'}{H_o}}$$

$$\Delta u = \frac{21.1 \times \frac{\Delta H'}{H_o}}{0.0345 - \frac{\Delta H'}{H_o}}$$

$\frac{\Delta H'}{H_o}$	$\frac{\Delta H}{H_o}$	$0.0345 - \frac{\Delta H'}{H_o}$	Δu PSI	$u = \Delta u + u_2$ PSI	$\bar{\sigma}$ PSI	$\sigma_T = \bar{\sigma} + u$ PSI
0	0.0285	0.0345	0	6.4	31.4	37.8
0.0015	0.030	0.0330	1.0	7.4	33.5	40.9
0.0065	0.035	0.0280	4.9	11.3	41.0	52.3
0.0125	0.041	0.0220	12.0	18.4	50.0	68.4
0.0171	0.0456	0.0174	20.7	27.1	57.0	84.1

PLOT $\bar{\sigma}$, u, AND σ_T VS $\frac{\Delta H}{H_o}$ IN FIG. 1.

PLOT σ_T VS u IN FIG. 2.

EXAMPLE

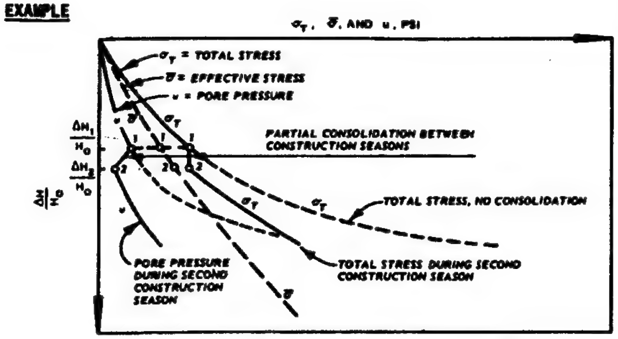

FIG. 1. TOTAL AND EFFECTIVE STRESSES AND PORE PRESSURE VS DEFORMATION

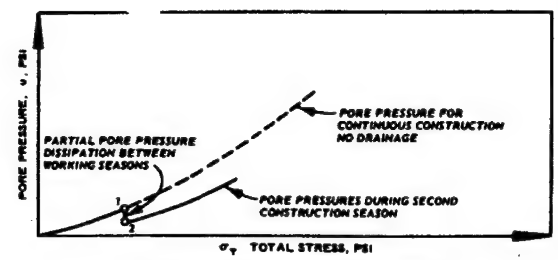

FIG. 2. TOTAL STRESS VS PORE PRESSURE

PORE PRESSURES IN PARTIALLY SATURATED SOILS

EFFECT OF PARTIAL DISSIPATION OF PORE PRESSURE BETWEEN CONSTRUCTION SEASONS

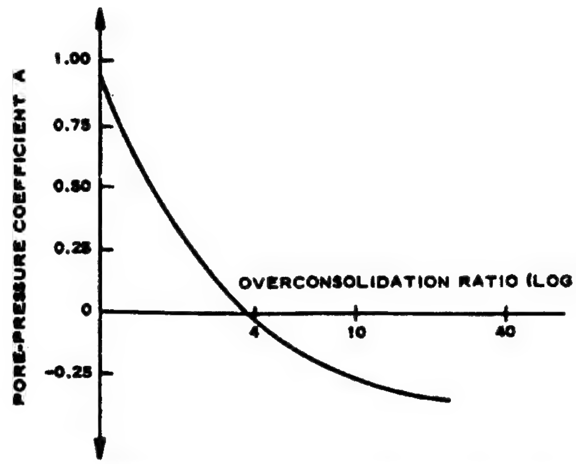

a. PORE-PRESSURE COEFFICIENT A VERSUS OVERCONSOLIDATION RATIO; COEFFICIENT MEASURED AT FAILURE, STRESS INCREASING

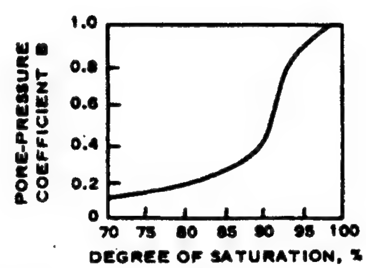

b. PORE-PRESSURE COEFFICIENT B VERSUS DEGREE OF SATURATION; COEFFICIENT MEASURED AT FAILURE, STRESS INCREASING. CURVE APPLIES TO ONE SOIL ONLY, UNDER PARTICULAR CONDITIONS OF TEST

PORE PRESSURE
COEFFICIENTS A AND B

$\Delta u = B\,[\Delta\sigma_3 + A\,(\Delta\sigma_1 - \Delta\sigma_3)]$ (PER SKEMPTON)

WHERE Δu = INCREASED PORE WATER PRESSURE

$\Delta\sigma_3$ = INCREASE IN MINOR PRINCIPAL STRESS

$\Delta\sigma_1$ = INCREASE IN MAJOR PRINCIPAL STRESS

B = 1.0 FOR SATURATED SOILS

A = FACTOR DEPENDENT ON OVERCONSOLIDATION RATIO

THEN $$\frac{\Delta u}{\Delta\sigma_1} = A + (1 - A)\frac{\Delta\sigma_3}{\Delta\sigma_1}$$

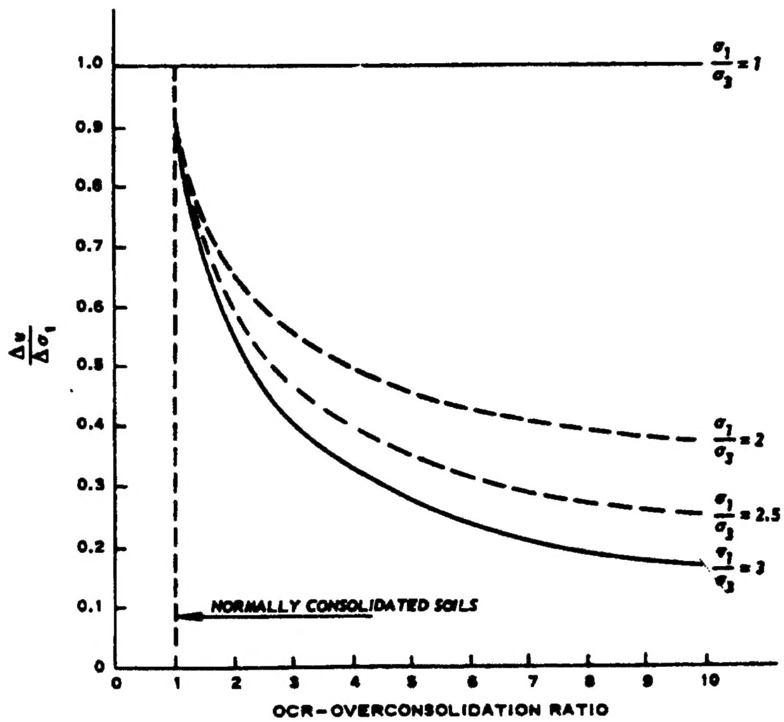

DEVELOPMENT OF EXCESS
PORE WATER PRESSURES

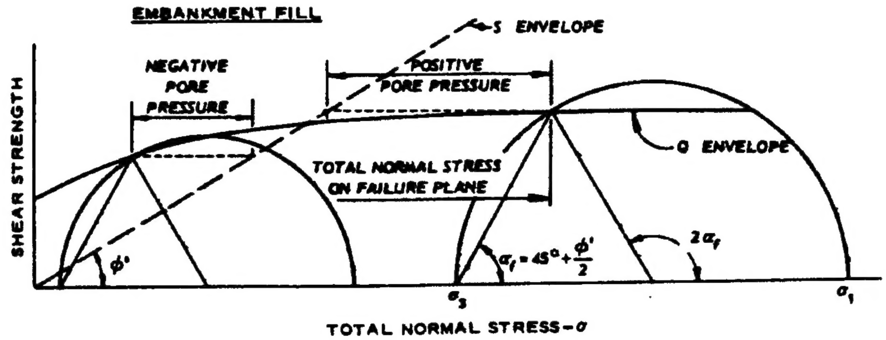

PORE PRESSURES IMPLIED WHEN Q SHEAR STRENGTHS ARE USED FOR CONSTRUCTION CONDITION DESIGN

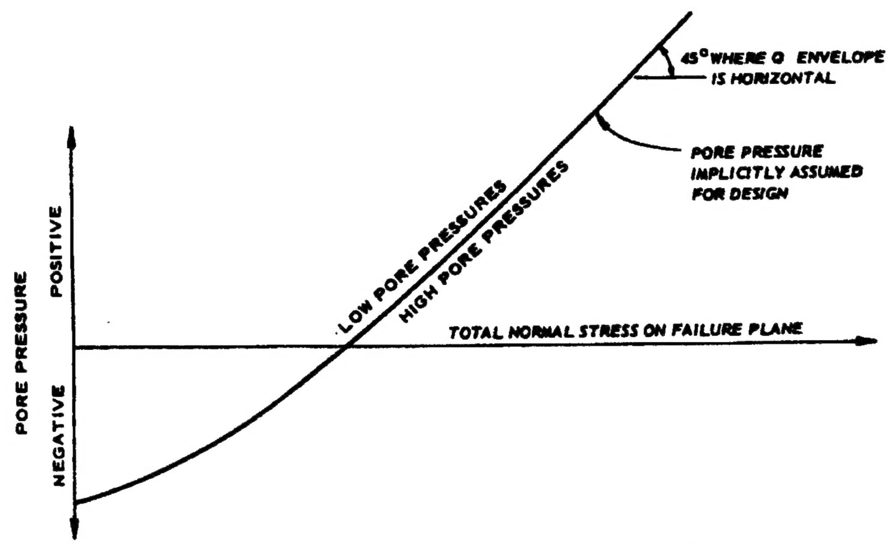

PORE PRESSURE VS TOTAL NORMAL STRESS ON FAILURE PLANE

DATA FOR ESTIMATING PORE PRESSURES IN Q TEST

Plate VIII-6

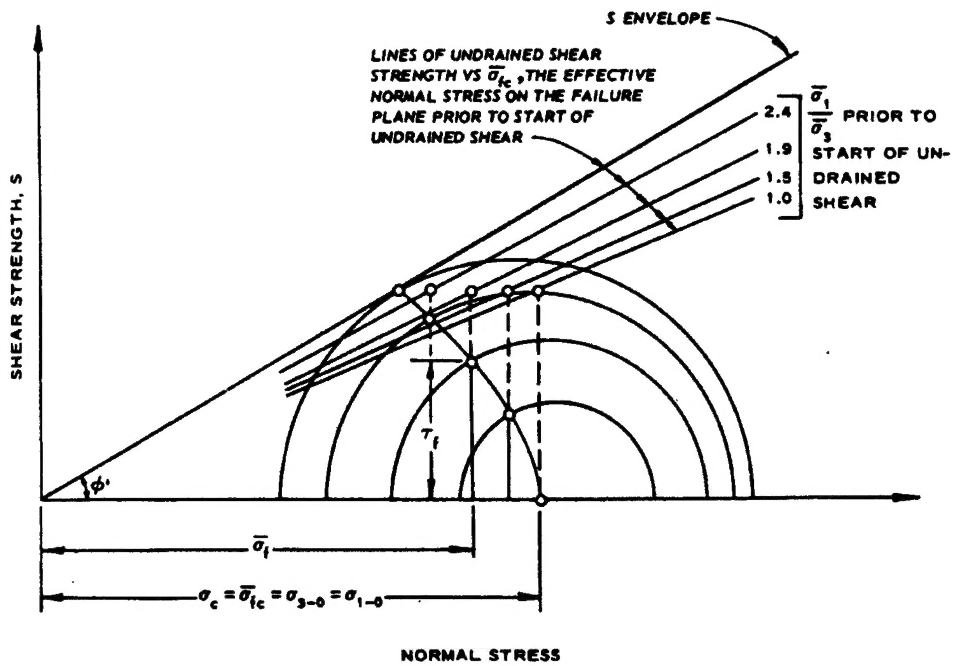

UNDRAINED SHEAR STRENGTH
FOR VARIOUS RATIOS OF $\bar{\sigma}_1/\bar{\sigma}_3$
AT START OF SHEAR

Plate VIII-7

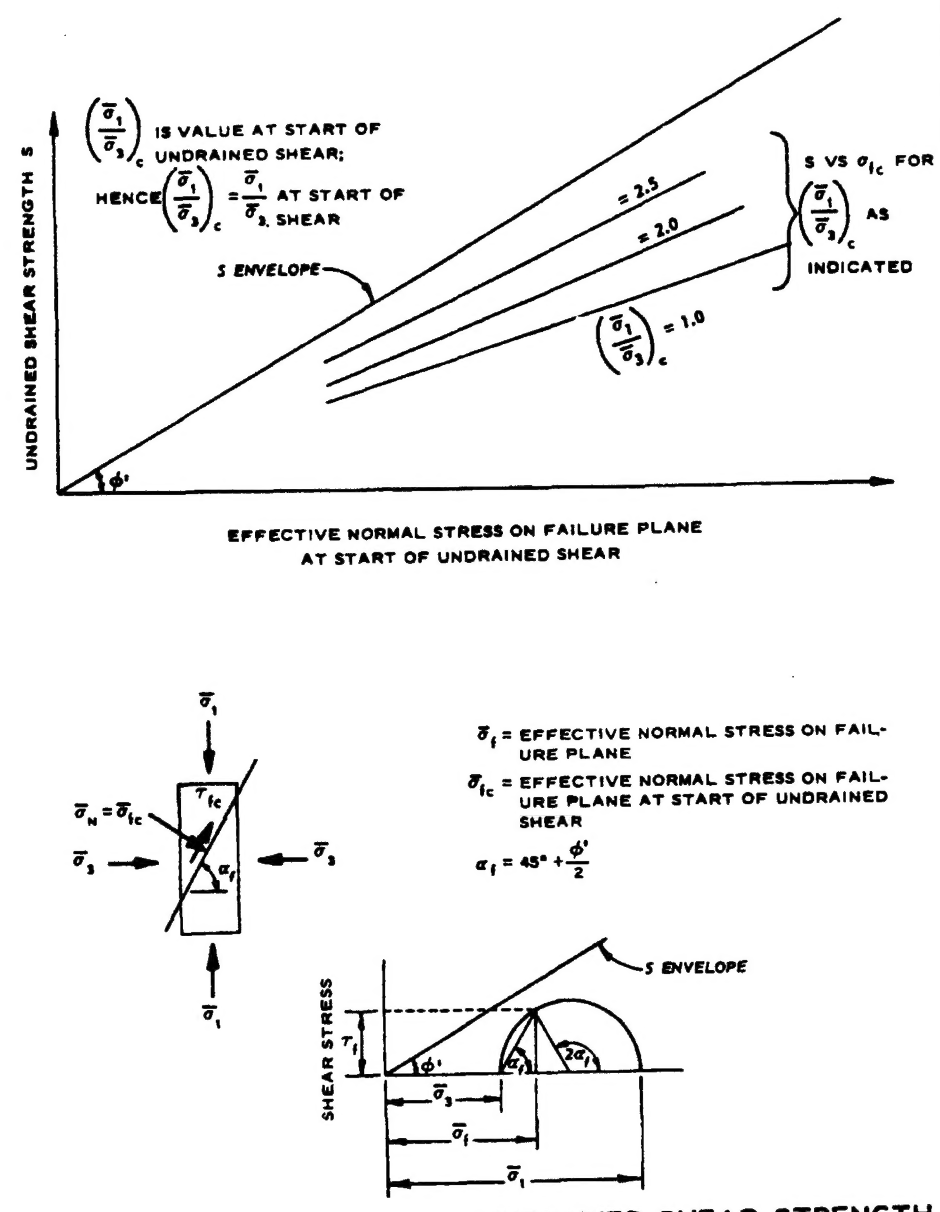

UNDRAINED SHEAR STRENGTH FOR FIELD STRESS CONDITIONS

Plate VIII-8

☆U.S. GOVERNMENT PRINTING OFFICE: 1994 - 521-947/81206